MOLECULAR MODELLING OF SOME EXPLOSIVES AND PROPELLANTS

A THESIS SUBMITTED TO
THE GRADUATE SCHOOL OF NATURAL AND APPLIED SCIENCES
OF
MIDDLE EAST TECHNICAL UNIVERSITY

BY

SERHAT VARIŞ

IN PARTIAL FULFILLMENT OF THE REQUIREMENTS
FOR
THE DEGREE OF DOCTOR OF PHILOSOPHY
IN
CHEMISTRY

AUGUST 2013

Approval of the thesis:

MOLECULAR MODELLING OF SOME EXPLOSIVES AND PROPELLANTS

submitted by **SERHAT VARIŞ** in partial fulfillment of the requirements for the degree of **Doctor of Philosophy in Chemistry Department, Middle East Technical University** by

Prof. Dr. Canan Özgen
Dean, Graduate School of **Natural and Applied Sciences** ____________________

Prof. Dr. İlker Özkan
Head of Department, **Chemistry** ____________________

Prof. Dr. Lemi Türker
Supervisor, **Chemistry Department, METU** ____________________

Examining Committee Members

Prof. Dr. Şakir Erkoç
Physics Department, METU ____________________

Prof. Dr. Lemi Türker
Chemistry Department, METU ____________________

Prof. Dr. Fatma Sevin Düz
Chemistry Department, Hacettepe University ____________________

Assoc. Prof. Dr. M. Fatih Danışman
Chemistry Department, METU ____________________

Assoc. Prof. Dr. Okan Esentürk
Chemistry Department, METU ____________________

Date: August 27th, 2013

I hereby declare that all information in this document has been obtained and presented in accordance with academic rules and ethical conduct. I also declare that, as required by these rules and conduct, I have fully cited and referenced all material and results that are not original to this work.

Name, Last name : Serhat VARIŞ

Signature :

ABSTRACT

MOLECULAR MODELLING OF SOME EXPLOSIVES AND PROPELLANTS

VARIŞ, Serhat
Ph.D., Department of Chemistry
Supervisor: Prof. Dr. Lemi TÜRKER

August 2013, 147 pages

Explosive is an energetic material, which may be initiated by friction, impact, shock, spark, flame, heating, or any simple submission of an energy pulse, that either is chemically or else energetically unstable or yields a rapid expansion of the material usually accompanied by the production of heat and large changes in pressure. Due to many tragic explosions resulting from unintended initiation of munitions by human body electrostatic discharge, impact or shock, theoretical and computational studies that clarify their various explosive properties and some other features became hot subject in energetic materials science. Detonation velocity and detonation pressure are the significant ballistic parameters to estimate the explosive performances of energetic materials. The detonation properties have been evaluated by the Kamlet-Jacobs equations, based on the quantum chemically calculated densities and heat of formation values. The explosives in the present study have been investigated with Density Functional Theory at B3LYP/6-31G(d,p) level by SPARTAN Package Program. It has been found that there might be some candidates of relatively insensitive and high energy density materials among the considered molecules so far not mentioned in the literature. The thesis also concentrates on liquid aviation fuels (jet propellants, *JP*) that are employed in aircrafts, namely JP-10 and JP-900. The oxidation of the fuels through hydroperoxidation and decomposition of the formed hydroperoxides are considered. Feasible decomposition products are determined for both JP-10 and JP-900 hydroperoxides.

Keywords: Explosives, Kamlet-Jacobs equations, detonation parameters, aviation fuel, hydroperoxidation.

ÖZ

BAZI PATLAYICI VE YAKITLARIN MOLEKÜLER MODELLENMESİ

VARIŞ, Serhat
Doktora, Kimya Bölümü
Tez Yöneticisi: Prof. Dr. Lemi TÜRKER

Ağustos 2013, 147 sayfa

Patlayıcılar, darbe, şok, kıvılcım, alev, ısı, ya da kimyasal ya da herhangi basit bir enerji kaynağı ile aktive olan, kimyasal ya da enerjik olarak kararsız maddelerdir. Patlama sonrasında ani bir genleşme olur ve bu da genellikle ısı ve basınçta büyük değişikliklerin olmasına neden olur. İnsan vücudu elektrostatik boşalması, darbe veya şok gibi nedenlerle mühimmatların kasıtsız aktive olmasından kaynaklanan ve felaketle sonuçlanan patlamalardan dolayı, patlayıcı özelliklerini aydınlatan teorik ve hesaplama çalışmaları, enerjik malzeme biliminde popüler bir konu olmuştur. Patlama hızı ve patlama basıncı, enerjik malzeme patlayıcı performanslarının değerlendirilmesini sağlayan önemli balistik parametrelerdir. Patlama özellikleri, kuantum kimyasal hesaplamalarla belirlenen yoğunluk ve oluşum ısısı parametrelerine dayalı Kamlet-Jacobs denklemlerini kullanılarak değerlendirilmiştir. Bu çalışmadaki patlayıcılar, SPARTAN paket program kullanılarak yoğunluk fonksiyonel teorisiyle B3LYP/6-31G (d,p) düzeyinde incelenmiştir. Yapılan çalışmalar sonucunda, şimdiye kadar literatürde yer almayan moleküller dizayn edilmiştir. Bu moleküller arasında nispeten duyarsız ve yüksek enerji yoğunluklu malzemelere aday moleküller olduğu gösterilmiştir. Bu tez, ayrıca uçaklarda kullanılan sıvı yakıtları (JP-10 ve JP-900) da incelemektedir. Yakıtların hidroperoksit yoluyla yükseltgenmesi ve yükseltgenen yakıtların bozunmalarını göz önünde bulundurulmuştur. Hem JP-10 hem de JP-900 için en olası bozunma ürünleri de belirlenmiştir.

Anahtar Kelimeler: Patlayıcılar, Kamlet-Jacobs Denklemleri, Patlama Parametreleri, Jet yakıtları, Hidroperoksidasyon.

To my wife

ACKNOWLEDGMENTS

It is a great pleasure to thank my supervisor Prof. Dr. Lemi TÜRKER for his invaluable guidance, support, suggestions and inspiring advice for the completion of my thesis. I have gained a different viewpoint to science under his supervision.

I would like to thank Scientific and Technological Research Council of Turkey- Defense Industries Research and Development Institute, TÜBİTAK-SAGE, for their permission and support to complete my Ph.D. thesis.

I also wish to express my profound thanks to my thesis progress committee members Prof. Dr. Fatma SEVİN DÜZ and Assoc. Prof. Dr. Fatih DANIŞMAN for their guidance and kind contributions to my thesis.

It was great to have the chance to work with Dr. Çağlar ÇELİK BAYAR. I would like to thank for her endless help in addition to her kind friendship.

I would like to express my special thanks to my family for their support and encouragement.

Words fail to express my gratefulness to my wife Ayşe Gül VARIŞ her patience, understanding, and support throughout my entire Ph.D. thesis work.

TABLE OF CONTENTS

ABSTRACT v

ÖZ…..... vi

ACKNOWLEDGMENTS viii

TABLE OF CONTENTS ix

LIST OF FIGURES xii

LIST OF TABLES xiv

ABBREVIATIONS xvii

CHAPTERS 1

1. INTRODUCTION 1

1.1. The History of Explosives 1
1.2. The Explosives 3
1.2.1. The Categorization of Explosives 4
1.2.2. Properties of explosive materials 6
1.2.2.1. Decomposition, Detonation and Deflagration 6
1.2.2.2. Detonation Velocity and Pressure 7
1.2.2.3. Oxygen Balance (Ω) 8
1.2.2.4. Detonation Products 9
1.2.2.5. Explosive Power and Power Index 10
1.2.2.6. Heat of Detonation 10
1.2.2.7. Density 11
1.2.2.8. The Calculation of Detonation Pressure and Velocity using Detonation Parameters 12
1.2.2.9. Sensitivity of Explosives 13
1.3. Introduction for Molecular Modeling 15
1.3.1. Molecular Mechanics 17
1.3.2. Semiemprical Methods 17
1.3.2.1. Parameterization Method 3 (PM3) 18
1.3.3. Ab initio Methods 18
1.3.3.1. The Hartree-Fock Theory 18
1.3.4. Utilization of Computational Chemistry in Energetic Materials Field 20
1.3.5. Methods of calculation 20
1.4. Objectives of the Study 21
2. A THEORETICAL STUDY OF JP-10 HYDROPEROXIDATION 23

2.1. Introduction 23
2.2. Results and Discussion 25
2.2.1. The Formation Tendencies of JP-10 Radicals and Hydroperoxides 25
2.2.2. Decomposition of JP-10 Hydroperoxides 29

2.3. Conclusion 33
3. JP-900 HYDROPEROXIDATION and DECOMPOSITION 35
3.1. Introduction 35
3.2. Results and Discussion 36
3.2.1. The Formation Tendencies of JP-900 Radicals and Hydroperoxides 36
3.2.2. Decomposition of JP-900 Hydroperoxides 40
3.3. Conclusion 43
4. DESENSITIZATION of TNAZ via STRUCTURAL MOLECULAR MODIFICATION and EXPLOSIVE PROPERTIES- A DFT STUDY 45
4.1. Introduction 45
4.2. Results and Discussion 46
4.2.1. The Geometries 46
4.2.2. Relative Total Energies 49
4.2.3. Bond Dissociation Energies (BDE) 50
4.2.4. The Frontier Molecular Orbitals 52
4.2.5. Explosive Properties 53
4.2.6. Detonation Products 54
4.2.7. Explosive Power and Power Index 57
4.3. Conclusion 58
5. PREDICTION of EXPLOSIVE PERFORMANCE PROPERTIES OF z-DBBD and ITS ISOMERS by QUANTUM CHEMICAL COMPUTATIONS - A DFT STUDY 59
5.1. Introduction 59
5.2. Results and Discussion 60
5.2.1. The Geometries 60
5.2.2. Relative Total Energies 64
5.2.3. Bond Dissociation Energies (BDE) 64
5.2.4. The Frontier Molecular Orbitals 65
5.2.5. Explosive Properties 66
5.2.6. Detonation Products 68
5.2.7. Explosive Power and Power Index 68
5.3. Conclusion 69
6. EFFECTS of EPOXIDATION AND NITRATION ON BALLISTIC PROPERTIES of FOX-7 – A DFT STUDY 71
6.1. Introduction 71
6.2. Results and Discussion 72
6.2.1. The Geometries 72
6.2.2. Relative Total Energies 73
6.2.3. Bond Dissociation Energies (BDE) 74
6.2.4. The Frontier Molecular Orbitals 75
6.2.5. Explosive Properties 76
6.2.6. Detonation Products 78
6.2.7. Explosive Power and Power Index 78

6.3. Conclusion 79
7. NITRO DERIVATIVES OF PARABANIC ACID AS POTENTIAL EXPLOSIVES—A DFT STUDY 81
7.1. Introduction 81
7.2. Results and Discussion 82
7.2.1. The Geometries 82
7.2.2. Relative Total Energies 84
7.2.3. Explosive Properties 85
7.2.4. Detonation Products 87
7.2.5. Explosive Power and index 88
7.2.6. Conclusion 89
8. CONCLUSION 91
REFERENCES 95
APPENDICES 106
A.THE CARTESIAN COORDINATES OF THE STRUCTURES CONSIDERED IN CHAPTER-2 107
B.THE CARTESIAN COORDINATES OF THE STRUCTURES CONSIDERED IN CHAPTER-3 117
C.THE CARTESIAN COORDINATES OF THE STRUCTURES CONSIDERED IN CHAPTER-4 127
D.THE CARTESIAN COORDINATES OF THE STRUCTURES CONSIDERED IN CHAPTER-5 133
E.THE CARTESIAN COORDINATES OF THE STRUCTURES CONSIDERED IN CHAPTER-6 137
F.THE CARTESIAN COORDINATES OF THE STRUCTURES CONSIDERED IN CHAPTER-7 141
CURRICULUM VITAE 147

LIST OF FIGURES

FIGURES

Figure 1-1. The chemical structure of nitroglycerine.......1

Figure 1-2. The chemical structure of nitrocellulose (guncotton)........2

Figure 1-3. The chemical structure of Picric Acid, Tetryl, TNT, PETN, RDX and HMX. 3

Figure 1-4. A diagram for the reaction profile of chemical explosives [1]........4

Figure 1-5. Classification of explosives on the basis of structure........5

Figure 1-6. The schematic show of triggering sequence [19]........7

Figure 1-7. Experimental setup for impact sensitivity........14

Figure 1-8. A simplified PES in three dimensions, Reprinted from reference [71]........16

Figure 1-9. Pople diagram showing the dependence of the performance of an *ab initio* method on the basis set and the amount of electron correlation. Reprinted from reference [76]........19

Figure 2-1. Synthetic Route to JP-10. 24

Figure 2-2. Numberings of hydrogen and carbon atoms of JP-10........25

Figure 2-3. A suggested hydroperoxide formation route. 27

Figure 2-4. The carboxylic acid (ester)–alkane mechanism for the decomposition........29

Figure 2-5. The alcohol–aldehyde mechanism for the decomposition........30

Figure 2-6. The alcohol–ketone mechanism for the decomposition........30

Figure 2-7. Decomposition of JP-10 Hydroperoxide labeled as “I”. Products 1-3 belong to the alcohol-ketone mechanism whereas products 4 and 5 to the carboxylic acid (ester)-alkane mechanism........32

Figure 2-8. Decomposition of JP-10 Hydroperoxide labeled as “A”. Products 6-8 belong to the alcohol-ketone mechanism whereas products 9 and 10 to the carboxylic acid (ester)-alkane mechanism. 33

Figure 3-1. The structures of *cis*- *trans*-Decalin 35

Figure 3-2. Numberings of hydrogen and carbon atoms of JP-900 36

Figure 3-3. A suggested hydroperoxide formation route 38

Figure 3-4. a)Decomposition of JP-900 “hydroperoxide-C’’. Products 1 and 2 belong to the carboxylic acid (ester)-alkane mechanism whereas products 3 and 4 belong to the alcohol–aldehyde mechanism. b) Decomposition of JP-900 “hydroperoxide-K’’. Products 5 and 6 belong to the carboxylic acid (ester)-alkane mechanism whereas products 7 and 8 belong to the alcohol–aldehyde mechanism. c) Decomposition of JP-900 "hydroperoxide-I’’. Products 9 and 10 belong to the ketone – alcohol mechanism. 41

Figure 4-1. The Structures of TNAZ (1) and some azetidine derivatives 47

Figure 4-2. The numbering manner of TNAZ and azetidine derivatives 47

Figure 5-1. The geometry optimized structures of TACOT, z-DBBD and its three isomers. 60

Figure 6-1. The Structures of FOX-7 (1) and other derivatives in the presently considered. 72

Figure 6-2. The numbering manner of the present structures 73

Figure 7-1. The structures of PA and other derivatives 82

Figure 7-2. The numbering manner of the present structures 83

Figure 8-1. Examples of Sensitive Explosives 92

Figure 8-2. Examples of explosives with high detonation velocity and pressure 93

Figure 8-3. Examples of explosives with high power index values 94

Figure 8-4. Examples of explosives with high BDE values 94

LIST OF TABLES

TABLES

Table 1-1. Detonation velocity values of some common explosives (Picric Acid, Tetryl, TNT, PETN, RDX and HMX) 8

Table 1-2. The Kistiakowsky–Wilson Rules 9

Table 1-3. Density values of Picric Acid, Tetryl, TNT, PETN, RDX and HMX [21] 11

Table 1-4. Stoichiometric relations for the calculations of the N, M_{ave} and Q parameters of $C_aH_bO_cN_d$ type explosives [49]. 12

Table 2-1. Labelings of the radicals and hydroperoxides originated from JP-10. 26

Table 2-2. Total and relative electronic energy values of radicals and hydroperoxides originated from JP-10 (from the lowest to the highest). 27

Table 2-3. ΔG^o_{rxn} values of the formation of radicals from JP-10 from the lowest to the highest (UB3LYP/6-31G(d,p)). 28

Table 2-4. The total and the relative electronic energy values (UB3LYP/6-31G(d,p)) of “Hydroperoxide I and A” and their decomposition products and ΔG^o_{rxn} values (from the lowest to the highest). 31

Table 3-1. Labelings of the radicals and hydroperoxides originated from JP-900. 37

Table 3-2. Total and relative electronic energy values of radicals and hydroperoxides originated from JP-900 (from the lowest to the highest). 38

Table 3-3. ΔG^o_{rxn} values of the formation of radicals from JP-900 from the lowest to the highest (UB3LYP/6-31G(d,p)). 39

Table 3-4. The total and the relative electronic energy values of ‘‘Hydroperoxide-C, K and I’’ and their decomposition products and ΔG_{rxn} values (from the lowest to the highest). 42

Table 4-1. The bond lengths (Å) of the geometry optimized TNAZ and azetidine derivatives calculated at the theoretical level of (DFT) B3LYP/6–31G(d.p) 48

Table 4-2. The calculated (corrected) absolute and relative total energies of TNAZ and azetidine derivatives at (DFT) B3LYP/6–31G(d,p) theoretical level. 49

Table 4-3. The homolytic bond dissociation energies (BDE) of C−NO_2 and N−NO_2 bonds of TNAZ and azetidine derivatives calculated at (DFT) UB3LYP/6–31G(d.p) theoretical level. 51

Table 4-4. The HOMO, LUMO, Δε energies (Δε = ε_{LUMO} – ε_{HOMO}), Mulliken electronegativities (χ_M) and chemical hardnesses (η) values of TNAZ and azetidine derivatives calculated at HF/6–31G(d.p)//B3LYP/6–31G(d.p) theoretical level. 53

Table 4-5. Predicted densities and detonation properties of TNAZ and azetidine derivatives at the theoretical level of B3LYP/6–31G(d,p). 55

Table 4-6. Gaseous decomposition products of TNAZ and other azetidine derivatives using the Kistiakowsky and Wilson Rules 56

Table 4-7. The power index values of TNAZ, azetidine derivatives, Picric Acid, TNT, RDX and HMX 57

Table 5-1. The bond lengths (Å) of the geometry optimized TACOT, z-DBBD and its three isomers calculated at the theoretical level of B3LYP/6–31G(d,p) 62

Table 5-2. Calculated ZPE and total energies (zero point corrected) of z-DBBD and its three isomers at (DFT) B3LYP/6–31G(d,p) theoretical level (Energies in kJ/mol). 64

Table 5-3. The homolytic bond dissociation energies (BDE) of C−NO_2 bond of TACOT, z-DBBD and its three isomers at (DFT) UB3LYP/6–31G(d,p) theoretical level. 65

Table 5-4. The HOMO, LUMO, Δε energies (Δε = ε_{LUMO} – ε_{HOMO}), Mulliken electronegativities (χ_M) and chemical hardnesses (η) values of TACOT, *z*-DBBD and its three isomers calculated at HF/6–31G(d,p)//B3LYP/6-31G(d,p) theoretical level. 66

Table 5-5. Predicted densities and detonation properties of molecules at the theoretical level of B3LYP/6–31G(d,p). 67

Table 5-6. The comparative power index values of TACOT, *z*-DBBD and its three isomers. 69

Table 6-1. The bond lengths (Å) of the geometry optimized FOX-7 and its derivatives calculated at the theoretical level of (DFT) B3LYP/6–31G(d,p) 73

Table 6-2. The calculated corrected total electronic energies of FOX-7 and derivatives at (DFT) B3LYP/6–31G(d,p) theoretical level. 74

Table 6-3. The homolytic bond dissociation energies (BDE) of C−NO_2 and N−NO_2 bonds of FOX-7 and derivatives calculated at (DFT) UB3LYP/6–31G(d.p) theoretical level. 74

Table 6-4. The HOMO, LUMO, Δε energies (Δε = $\varepsilon_{LUMO} - \varepsilon_{HOMO}$), Mulliken electronegativities (χ_M) and chemical hardnesses (η) values of FOX-7 and its derivatives calculated at HF/6–31G(d.p)//B3LYP/6–31G(d.p) theoretical level..................................... 75

Table 6-5. Predicted densities and detonation properties of FOX-7 and its derivatives at the theoretical level of B3LYP/6–31G(d,p). 77

Table 6-6. The identity and quantity of the decomposition products of the compounds 1-6. 78

Table 6-7. The power index values of FOX-7, derivatives, Picric Acid, RDX and HMX..... 79

Table 7-1. The bond lengths (Å) of the geometry optimized parabanic acid and its nitro derivatives (compounds 1-8) calculated at the theoretical level of B3LYP/6–31G(d,p). 84

Table 7-2. The calculated corrected total electronic energies of PA and derivatives at (DFT) B3LYP/6–31G(d,p) theoretical level... 85

Table 7-3. Predicted densities and detonation properties of PA and its derivatives at the theoretical level of B3LYP/6–31G(d,p). 86

Table 7-4. The identity and the quantity of the decomposition products of the compounds 1-8. 88

Table 7-5. The power index values of the compounds 1-8 and Picric Acid.......................... 89

ABBREVIATIONS

Å	Angstrom
AO	Atomic Orbital
ANFO	Ammonium Nitrate and Fuel Oil
AM1	Austin Model 1
B3LYP	Becke's three parameter exchange hybrid functional with Lee, Yang, Parr (LYP) correlation functional
BDE	Bond Dissociation Energy
CBS	Complete Basis Set
DFT	Density Functional Theory
FOX-7	1,1-Diamino-2,2-Dintro Ethylene
HEDM	High Energy Density Material
HF	Hartree-Fock Theory
HMX	High Melting Explosive, Octogen
HOF	Heat of Formation
HOMO	Highest Occupied Molecular Orbital
JP	Jet Propellant
LDA	Local Density Approximation
LDSA	Local Density-Spin Approximation
LSDA	Local Spin-Density Approximation
LUMO	Lowest Unoccupied Molecular Orbital
MM	Molecular Mechanics
MNDO	Modified Neglect of Diatomic Overlap
MO	Molecular Orbital
PA	Parabanic Acid
PBX	Polymer Bonded Explosive
PES	Potential Energy Surfaces
PETN	Pentaerythritol Tetranitrate
PM3	Parameterization Method 3
RDX	Research and Development Explosive, Hexogen
RHF	Restricted Hartree-Fock Theory
SCF	Self-Consistent Field
STO	Slater Type Orbital
TACOT	2, 4, 8, 10-tetranitrobenzotriazolo [2, 1-a] benzotriazol-6-ium inner salt
TNAZ	1,3,3-Trinitro Azetidine
TNT	1,3,5-Trinitro Toluene
UHF	Unrestricted Hartree-Fock
z-DBBD	4,11-dinitro[1,2,5]- oxadiazolo[3,4-e] [1,2,5]oxadiazolo[3’,4’:4,5] benzotriazolo- [2,1-a] benzotriazol-6-ium inner salt 1,8-dioxide
ZPVE	Zero point vibrational energy

CHAPTER-1

INTRODUCTION

1.1. The History of Explosives

The Black powder, also acknowledged as gunpowder, was the first explosive composition consisting of charcoal and sulfur as fuel and potassium nitrate as oxidizer. In 220 BC, Chinese alchemists accidentally discovered the black powder. At the end of the 13th century, the black powder became widespread among many countries as a military utility to crack the walls of castles and cities.

In the middle of the 19th century, black powder was appeared to be inadequate. Tough mining and tunneling processes necessitated a ‘superior’ explosive. In 1846, Professor Ascanio Sobrero discovered liquid nitroglycerine (See Figure 1-1) [1] in Italy. Nitroglycerine is a very significant advancement in energetic materials science, it can be considered as the first modern explosive as it contains both oxidizer and fuel in the same molecule. After a few years Immanuel Nobel, industrialized a process for the production of nitroglycerine, and in 1863 he established a production plant near Stockholm. The son Nobel, Alfred focused on the safety problems of transportation of nitroglycerine due to the catastrophic explosion in 1866 which completely destroyed the nitroglycerine factory. He mixed nitroglycerine with absorbent clay, ‘Kieselguhr’ in order to decrease the sensitivity of nitroglycerine. This mixture was named as ghur dynamite and patented in 1867 [2].

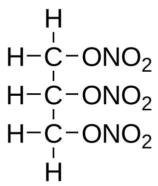

Figure 1-1. The chemical structure of nitroglycerine

Schönbein at Basel and Böttger at Frankfurt-am-Main worked on the nitration of cellulose to obtain nitrocellulose (guncotton) (see Figure 1-2) in 1845, at the same time as nitroglycerine was being prepared [3].

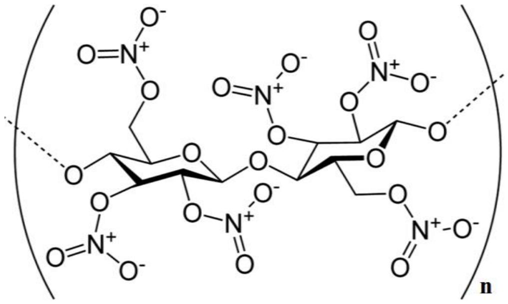

Figure 1-2. The chemical structure of nitrocellulose (guncotton).

Alfred Nobel found that a gel was formed by mixing nitrocellulose and nitroglycerine in 1875. This gel was advanced to create blasting gelatin, gelatin dynamite and later in 1888, ballistite, the first smokeless powder [4]. It was a combination of nitrocellulose, nitroglycerine, benzene and camphor. In 1867, the Swedish chemists Ohlsson and Norrbin discovered that the explosive characteristic of dynamites was improved by the addition of ammonium nitrate (NH_4NO_3).

In 1950, explosive manufacturers began to develop waterproof explosives which contained less hazardous ammonium nitrate. The most noteworthy composition was ANFO. The acronym “ANFO” is an ammonium nitrate and fuel oil mixture (commonly 94% ammonium nitrate (AN), 6% fuel oil). Ammonium nitrate cannot be considered as an explosive, but can be induced to detonate if used with other explosives [5].

Picric acid [(trinitrophenol) ($C_6H_3N_3O_7$)] was found to be an appropriate substitute for black powder in 1885 by Turpin, and in 1888 black powder was replaced by picric acid in British ammunitions as “Liddite” [6]. Tetryl was also being synthesized at the same time as picric acid. Tetryl was first obtained in 1877 by Mertens [7]. In 1902, the Germans and British had worked with trinitrotoluene [(TNT) ($C_7H_5N_3O_6$)], first prepared by Wilbrand in 1863 [8]. Pentaerythritol Tetranitrate (PETN) was first obtained in 1894 by nitration of pentaerythritol. Manufacture of PETN could not be accomplished until formaldehyde and acetaldehyde required in the synthesis of pentaerythritol became readily obtainable about a decade prior to World War II. Research and Development Explosive (RDX) was first prepared in 1899 by the Georg Friedrich Henning for medicinal use. Its value as an explosive was not acknowledged until 1920 by Herz [9]. In 1940, Bachmann industrialized a production process for RDX (1.5) from hexamine with successful yield [10]. Research and development sustained during World War II to develop original and more influential explosives and explosive compositions. Torpex (TNT/RDX/aluminum) and cyclotetramethylene tetranitramine, known as Octogen [(HMX) ($C_4H_8N_8O_8$)], became available at the end of World War II [11] (see Figure 1-3 for the structures).

In order to decrease the sensitivity of the explosives, polymer bonded explosives (PBXs) were developed. The explosive crystals are embedded in a polyurethane medium. Since 1952, Lawrence Livermore Laboratories, the US Navy and various other groups have developed a series of PBX formulations, such as PBX-109, PBX-110 [11].

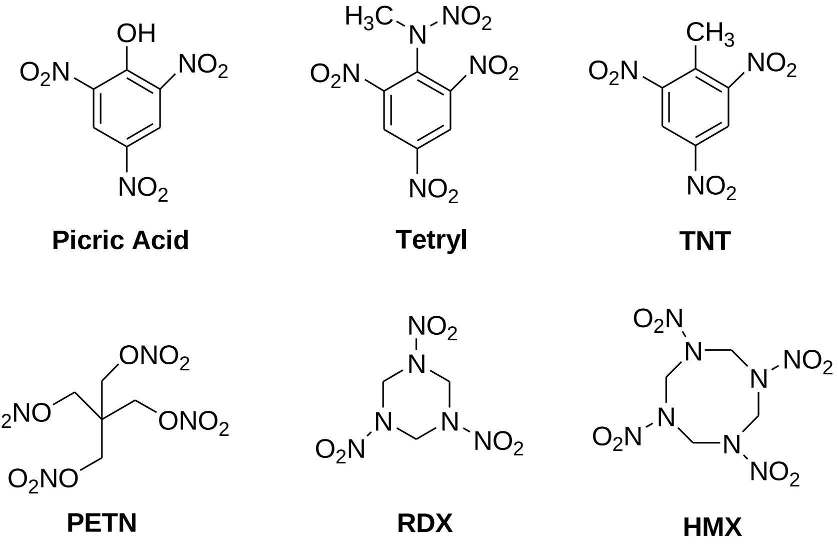

Picric Acid **Tetryl** **TNT**

PETN **RDX** **HMX**

Figure 1-3. The chemical structure of Picric Acid, Tetryl, TNT, PETN, RDX and HMX.

1.2. The Explosives

An explosive can be described as energetic liquid or solid or a mixture, which can be detonated by any energy pulse. It produces an explosion by its own energy without the contribution of exterior reactants like atmospheric oxygen [12]. Explosion results in instantaneous yield of heat and gas. Generally, an explosive has three basic features:

1. It is an energetically unstable chemical substance or mixture ignited by detonation, friction, heat, impact, shock, or a combination of these conditions.

2. Upon ignition, it decomposes very rapidly in a detonation (contrasted with a deflagration, which is a slower decomposition as in the example of ignition of gunpowder).

3. Upon detonation, there is a prompt release of heat and large amounts of pressurized hot gases, which expand rapidly with adequate force to overcome narrowing forces, e.g., the confining forces of surrounding rock formation.

An unstable energetic molecule, inherently consisting of fuel and oxidizer, can be called explosive if it participates in a chemical explosion. For instance, although wood has greater energy content than most energetic materials, it cannot be taken into account as an explosive due to its high energy of activation. Its energy is released in an extended period (See Figure 1-4).

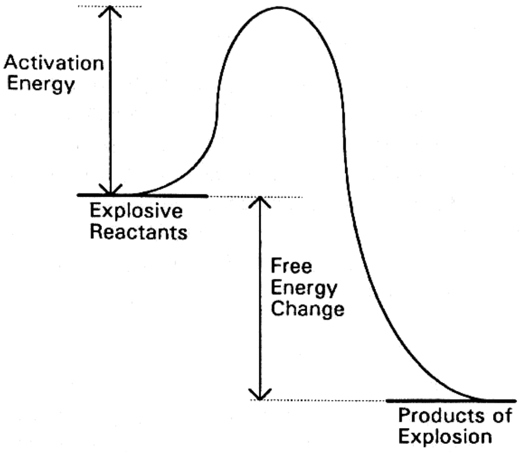

Figure 1-4. A diagram for the reaction profile of chemical explosives [1]

1.2.1. The Categorization of Explosives

The categorization of explosive materials can be made according to several properties, for example their rates of decomposition, chemical structure and their employment objective etc.

Figure 1-5 shows the classification of explosives according to the chemical structures. Explosives are separated into two base groups; organic and inorganic based explosives. Lead azide, silver azide, mercury fulminate and ammonium nitrate are examples of inorganic explosives. The organic ones are subdivided into aromatic and aliphatic explosives. Aromatic explosives contain aromatic rings; the well-known examples are TNT, tetryl and picric acid (See Figure 1-3). The aliphatic ones contain either carbon chains or cyclic carbon structures; the examples are RDX, HMX or PETN [13].

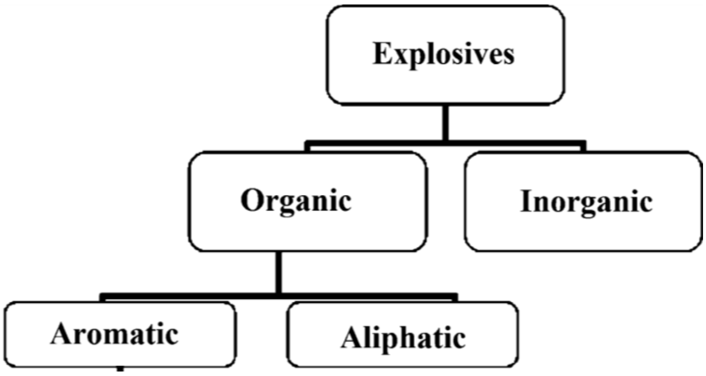

Figure 1-5. Classification of explosives on the basis of structure

Pletz [14] classified the explosives on the basis of the functional groups they have. He projected the theory of "explosophores" and "auxoploses" similar to Witt's proposal of chromophores and auxochromes in the dyes, and Ehrlich's toxophores and autotoxes in chemotherapeutics [14]. He proposed that explosive properties of any energetic materials vary with the functional groups they possess. These groups are called explosophores. The auxoploses groups strengthen those properties conferred by the explosophore. Pletz classified the explosives in eight groups that possess the subsequent functional groups as explosophores:

(i) $–NO_2$ and $–ONO_2$ in both organic and inorganic substances
(ii) –N=N- and -N=N=N- in inorganic and organic azides
(iii) –N=C in fulminates
(iv) $–NX_3$, for example in NCl_3 (X: a halogen)
(v) –O-O- and –O-O-O- in inorganic and organic peroxides and ozonides
(vi) $–OClO_2$ and $–OClO_3$ in inorganic and organic chlorates and perchlorates
(vii) -C≡C- in acetylene and metal acetylides
(viii) M-C metal bonded with carbon in some organometallic compounds.

Even though this categorization is principally appropriate, the difference between the terms "explosophore" and "auxoplose" is not clear. Lothrop and Handrick [15] classified all the data on the performance of explosives and related it to four parameters: the oxygen balance, "plosophoric" groups, "auxoplosive" groups and heat of explosion. A plosophore was assigned as a functional group of atoms that is able to create an explosive when introduced to a hydrocarbon. They divided plosophores into 2 groups as "primary" and "secondary" plosophores. The primary plosophores contain aromatic and aliphatic nitro groups, nitrate esters, and the nitramine group; whereas the secondary plosophores contain groups such as azo, azide, nitroso, peroxide, ozonide, perchlorate, etc. They defined auxoplosives as groups that do not provide the molecule with explosive properties, but affect them physically (changes the color intensity and shade of a dye). Examples of auxoplosives are hydroxyl, carboxyl, chlorine, sulfur, ether, oxygen, amine, etc. This classification by Lothrop and Handrick has taken some criticism [16, 17] due to the oxygen present (for example, in carbonyl or hydroxyl groups) has slight influence on the performance of an explosive.

The explosives can be classified according to their employment. They are divided into 3 parts:

i) Primary explosives or initiators
ii) High explosives
iii) Propellants (low explosives).

The primary explosives are very sensitive to energy pulse. A very small amount of energy is enough for initiation. They are used in detonators and filling ignition caps. High explosives are explosives that actually detonate at a supersonic speed. Their detonation velocity values vary from 3 to 9 km/s. Low explosives are compounds that detonate with velocity less than the speed of sound. It is a mixture of fuel and oxidizer that reacts rapidly. They are usually employed as propellants [18].

1.2.2. Properties of explosive materials

The physical properties of explosives should be identified in order to determine the appropriateness for a specific use. The utility of an explosive can only be appreciated when the properties and the parameters affecting them are fully comprehensible. Some of the most significant characteristics are explained in the following sections.

1.2.2.1. Decomposition, Detonation and Deflagration

The chemical decomposition of energetic materials may endure a second, hours, days, or years. The slow decomposition may occur during storage conditions. The prompt decomposition processes include deflagration and detonation.

“Detonation” is a term used to explain the explosion actuality. It is an exothermic process that spreads through the reaction zone at a supersonic velocity resulting in a shock wave. Ordinarily a detonation is achieved by shock wave moving at supersonic velocity through material. This shock wave firstly compresses the material, heats it and induces the explosive to break down into its constituent molecules. Detonation results in the formation of hot gases. Figure 1-6 shows the picture of a triggering sequence, also entitled as explosive train. It is a sequence of events that concludes in the detonation of explosives. A primary explosive of greater sensitivity is employed to trigger the main body of the explosive. It is activated by shock, impact, friction or spark. It then proceeds into the microscopic level involving the crystal lattice characteristics plus energy behavior of the energetic material. Next, the initiation event moves into the molecular level where chemical reactions generated by rapid thermochemical decomposition occur; and finally, it proceeds into the atomic level where atomized species form and recombine into the final small gaseous molecules detected as detonation products [19] (Figure 1-6).

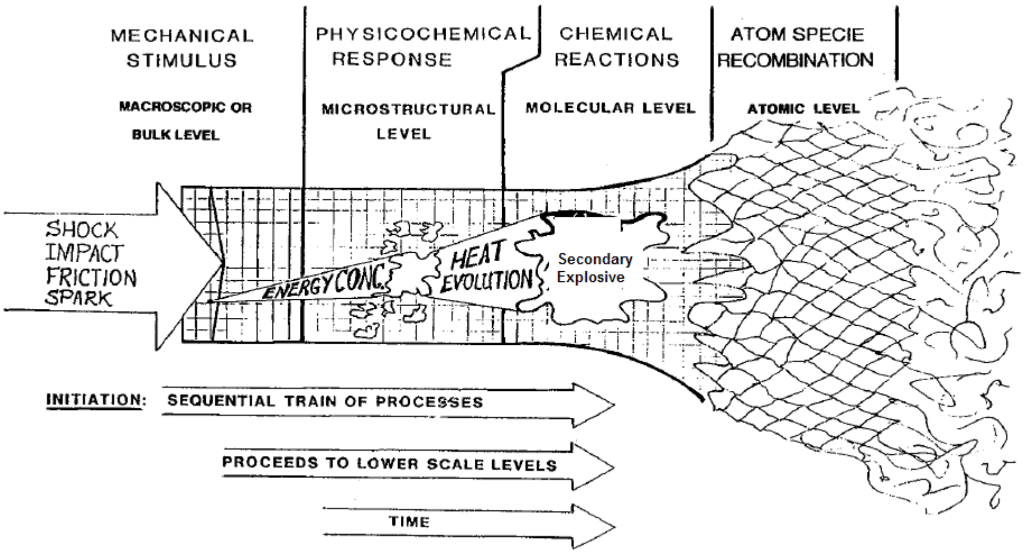

Figure 1-6. The schematic show of triggering sequence [19]

Deflagration means "to burn down" in Latin language. It is a phenomenon that propagates through heat transfer at a subsonic velocity. The burning hot particles heat the other part of cold material and ignite it. Unlike deflagration, detonation propagates through shock at supersonic velocity [12]. Commonly, primary and secondary explosives detonate whereas low explosives deflagrate. Deflagrating explosives burn vigorously than usual inflammable materials do. They burn with a flame or sparks, or whistling. Detonation velocity values vary from roughly 1500 to 9000 m.s^{-1}; whereas deflagration velocity is lower than that of detonation velocity.

1.2.2.2. Detonation Velocity and Pressure

There are two vital parameters to evaluate the explosive performance of an energetic material. One is detonation velocity and the other is detonation pressure.

The term “velocity of detonation” or “detonation velocity” is the rate of detonation waving through a high explosive. The term “velocity of detonation” is used solely for high explosives whereas “velocity of explosion” is used for both high and low explosives. Primary explosives detonate at a velocity of approximately 3500-5500 m.s^{-1}; whereas, secondary explosives detonate at a velocity of around 5500 $m.s^{-1}$ and above [20]. Table 1-1 shows detonation velocity values of some of the well-known explosives [21].

Table 1-1. Detonation velocity values of some common explosives (Picric Acid, Tetryl, TNT, PETN, RDX and HMX)

Explosive	Detonation Velocity (m/s)
Nitroglycerin	7700
Picric Acid	7350
Tetryl	7570
TNT	6900
PETN	7720
RDX	8750
HMX	9100

The detonation of an explosive is the consequence of a complex interaction between chemistry and hydrodynamics. Detonation creates a great pressure and temperature instantaneously behind the detonation wave. Chapman-Jouguet (C-J) thermodynamic detonation theory is conventionally used to understand detonation of explosives [22-28]. The release of detonation energy occurs in the form of kinetic energy and heat in a short period, i.e. microseconds. During the detonation of an explosive, a supersonic wave is created near the initiation point and propagates through the explosive, resulting in the exothermic decomposition of the explosive. The detonation wave passes into the surrounding medium, and exerts an impulsive, intense pressure, equal to a violent mechanical blow. When the medium is a solid, for instance rock or stone, this mechanical blow will create numerous cracks in the rock. This consequence is acknowledged as ‘brisance’ which is directly associated to the detonation pressure in the shockwave front. After the shockwave has gone away from the explosive, the gaseous products start to expand due to high temperature of the medium and do work on the surrounding medium. The intensity of the gaseous expansion creates the detonation pressure.

1.2.2.3. Oxygen Balance (Ω)

Oxygen balance (Ω) is the degree of oxidation of an explosive. It is the ratio of the “present oxygen” in the molecule to “the oxygen required for the complete oxidation” of the molecule. If an explosive molecule possesses sufficient oxygen (O) to convert its all carbon atoms to carbon dioxide (CO_2), all of its hydrogen (H) to water (H_2O), and all of its nitrogen (N) atoms to Nitrogen (N_2), the molecule is said to have a zero oxygen balance. The molecule is said to be overoxidized, if it contains more oxygen than needed and said to be underoxidized, if it contains less oxygen than needed. The sensitivity, strength, and brisance of an energetic material depend on oxygen balance and incline to its best as the oxygen balance approaches zero [22].

Oxygen balance can be calculated simply by the following formula for a $C_aH_bO_cN_d$ type explosive, where MW_{O2} is the molecular weight of O_2, $MW_{explosive}$ is the molecular weight of explosive [22].

$$\%\Omega = \frac{MW_{O2}}{MW_{Explosive}}\left(c - 2a + \frac{b}{2}\right)x100 \qquad \textbf{(1)}$$

For example, trinitrotriazine (C_3N_6O6) has an oxygen balance of zero. Examples of materials with negative oxygen balance are e.g. trinitrotoluene (-74%), aluminum powder (-89%), sulfur (-100%), or carbon (-266.7%). Examples of materials with positive oxygen balance are e.g. ammonium nitrate (+20%), ammonium perchlorate (+34%), potassium chlorate (+39.2%), sodium chlorate (+45%), sodium nitrate (+47%), tetranitromethane (+49%), lithium perchlorate (+60%), or nitroglycerine (+3.5%).

1.2.2.4. Detonation Products

The high amount of energy deposited in the explosive shows itself by a rapid expansion of hot gases upon detonation, creating a shock wave at ultrasonic velocity. The quantity and identity of the so called gaseous products should be enlightened to evaluate the detonation parameters. A set of rules (displayed in Table 1-2) was established by Kistiakowsky and Wilson to predict the decomposition products in an explosive reaction [29-30].

Table 1-2. The Kistiakowsky–Wilson Rules

Order	Condition	Reaction
1	Oxygen atoms oxidize ‘H’ atoms to H_2O molecules	$2H + O \rightarrow H_2O$ (gas)
2	Remaining ‘O’ atoms oxidize all ‘C’ atoms to CO molecules.	$C + O \rightarrow CO$ (gas)
3	Remaining ‘O’ atoms oxidize all ‘CO’ molecules to CO_2 molecules	$CO + O \rightarrow CO_2$ (gas)
4	Excess of O, H and N atoms are converted to O_2, H_2 and N_2. Any excess C stays as C_{solid}.	$2H \rightarrow H_2$ (gas) $2N \rightarrow N_2$ (gas) $2O \rightarrow O_2$ (gas)

1.2.2.5. Explosive Power and Power Index

Heat and hot gases are the products of an explosive reaction. The volume of evolved gas provides information on how much work done by the explosive.

Standard conditions should be established in order to determine the volume of generated gas, because the volume of gas differs along with the temperature. The standard conditions (273 K, 1atm) also enable the scientist to make comparisons between various explosives. Division of the value of total volume of gas produced upon detonation by the molecular weight gives an idea of how much gas is released per gram of explosive [31-34].

The heat of explosion “Q” and the volume of produced gas “V” can be associated to obtain the value for the explosive power as shown in the following equation:

$$\text{Explosive Power} = Q.V \qquad \textbf{(2)}$$

The value for the explosive power is then compared with the explosive power of a standard explosive, namely Picric Acid, to obtain power index, as shown in the following equation:

$$\%PowerIndex = \frac{Q.V}{Q_{PA}.V_{PA}} x100 \qquad \textbf{(3)}$$

1.2.2.6. Heat of Detonation

The heat energy released in a detonation reaction is called heat of detonation. The heat of detonation is an important parameter as well as detonation pressure and detonation velocity required for the determination of performance of an explosive. Heat of detonation is a measurement of the energy available to do mechanical work and approximating potential damage to environments. This is the heat of reaction of the explosive itself going to the explosive products. It can be calculated taking the energy difference between the detonation products and reactant explosive [35]. The identity and the quantity of the explosive products have been revealed in Section 1.2.2.4.

$$\Delta H^{o}_{det} = \Sigma\ \Delta H^{o}_{f}\,(\text{detonation products}) - \Delta H^{o}_{f}\,(\text{explosive}) \quad \textbf{(4)}$$

where ΔH^{o}_{det} is heat of detonation, ΔH^{o}_{f} is standard heat of formation.

Heat of formation is another essential thermochemical property of an explosive since it is directly associated with detonation velocity and pressure. In an explosive reaction, energy is initially used to break the bonds of explosive into its constituent elements as shown in the following reaction 1.1 for HMX.

$$C_4H_8N_8O_8 \rightarrow 4C + 8H + 8N + 8O \qquad \textbf{(1.1)}$$

These elements rapidly compose new bonds releasing the excess energy as shown in Reaction 1.2.

$$4C + 8H + 8N + 8O \rightarrow 4CO + 4H_2O + 4N_2 \ \textbf{(1.2)}$$

The reaction may occur in a few steps involving complicated systems of reaction chains, etc. However, the energy released depends solely on the initial and final states and not on the intermediate ones. Once the reaction is completed, the net heat evolved is exactly the same as if the reactant molecules were first dissociated into their atoms, and then reacted directly to form the final products according to Hess Law [36-37].

1.2.2.7. Density

The energy released by the detonation wave depends on the mass of explosive traversed per unit area of the wave. However, detonation velocity seems to be directly proportional to loading density. The higher the loading density, the higher the detonation parameters. Therefore, density is considered as a significant feature to evaluate the performance of an explosive. The valuable studies by Kamlet and coworkers have related density with detonation velocity and pressure [38-43]. Thus, the design of a new explosive necessitates the density information. Table 1-3 shows density data of some well-known explosives.

Table 1-3. Density values of Picric Acid, Tetryl, TNT, PETN, RDX and HMX [21]

Explosive	Density (g/cm^3)
Nitroglycerin	1.60
TNT	1.65
Tetryl	1.73
Picric Acid	1.76
PETN	1.77
RDX	1.82
HMX	1.91

1.2.2.8. The Calculation of Detonation Pressure and Velocity using Detonation Parameters

An organic chemist dealing with the synthesis of novel explosives, should figure out detonation properties (i.e detonation energy, velocity, pressure) prior to synthesis. The computation of these properties allows one to choose the promising high energy density material (HEDM) candidates for laboratory synthesis and further considerations [44].

Detonation velocity (D), and detonation pressure (P) are the two most significant parameters to assess the explosive performances of energetic materials and can be calculated by the empirical Kamlet-Jacobs equations [38-43] below:

$$D = 1.01\,(N\,M_{ave}^{1/2}\,Q^{1/2})^{1/2}\,(1+1.30\,\rho) \qquad \textbf{(5)}$$

$$P = 1.558\,\rho^2\,N\,M_{ave}^{1/2}\,Q^{1/2} \qquad \textbf{(6)}$$

where each term in equations 5 and 6 is defined as follows: D, detonation velocity (km/s); P, detonation pressure (GPa); ρ, density of the compound (g/cm^3); N, moles of gaseous detonation products per gram of explosive; M_{ave}, average molecular weight of gaseous products; Q, chemical energy of detonation (kJ/g). The parameters N, M_{ave}, and Q are calculated according to the chemical composition of each explosive as listed in Table 1-4.

Table 1-4. Stoichiometric relations for the calculations of the N, M_{ave} and Q parameters of $C_aH_bO_cN_d$ type explosives [49].

	Stoichiometric Relations		
Parameter	**c ≥ 2a + b/2**	**2a + b/2 > c ≥ b/2**	**b/2 > c**
N	(b + 2c + 2d)/4M	(b + 2c + 2d)/4M	(b + d)/2M
M_{ave}	4M/(b + 2c + 2d)	(56d + 88c – 8b)/(b + 2c + 2d)	(2b + 28d + 32c)/(b + d)
$Qx10^{-3}$	(28.9b + 94.05a + 0.239ΔH°$_f$)/M	[28.9b + 94.05(c/2 – b/4) + 0.239ΔH°$_f$]/M	(57.8c + 0.239ΔH°$_f$)/M

In Table 1-4, $C_aH_bO_cN_d$ designates the empirical formula of the compound. ΔH°$_f$ is the standard heat of formation of the studied compound (in kJ/mol).

As seen from equations 5 and 6, the density should be considered as the key physical parameter in detonation performance, since detonation velocity increase proportionally with the packing density and detonation pressure of the explosives increase proportionally with square of packing density.

Besides experimental measurements of density, there are theoretical methods to determine. The “group volume additivity” method is one the oldest method. The molar volume is obtained by adding up the volume of the atoms or functional groups [45]. The disadvantage of this method is that it cannot estimate molecular conformation, isomerization and crystal packing efficiency. It gives the same density results for different isomers or conformations of the identical compounds or even for different compounds with the equivalent functional group composition, and disregards the density differences due to crystal polymorphism. So, it is not an effective way of prediction of the density of explosives.

Keshavarz *et. al.* [46] has proposed several simple equations for the calculation of density of explosives, but these equations are applicable only for some limited elements or functional groups such as acyclic and cyclic nitramines, nitrate esters etc.

Another method, which is also utilized in the present study, is based on quantum chemical calculations. The density of the molecule is calculated by the division of the molecular weight by molecular volume. The molecular volume of each molecule is obtained from the statistical average of 100 single-point molar volume calculations over optimized geometries. The molar volume was outlined inside a contour of 0.001 electrons/Bohr^3 density that was evaluated by using a Monte Carlo integration technique executed in the Gaussian’03 package program. This method is not limited for specific classes and applicable for almost all organic explosives. Although it is a time consuming method, the results are quite close to the experimental values. There are also invaluable studies in the literature that employ this method to predict the density of explosives accurately [47-52].

Another parameter for the calculation detonation parameters is the chemical energy of detonation, Q value, which requires the value of heat of formation (ΔH^o_f) of the explosive (See Table 1-4). According to the Kamlet -Jacob Equations (equations 5 and 6) [38-43], the heat of detonation, Q, has only a small effect on D and P. Accordingly, ΔH^o_f also has also a small influence on D and P. Therefore, approximate estimation of ΔH^o_f by the semiemprical molecular orbital method such as PM3 is admissible [53]. Because it is a semi empirical method and the parameters involved in it are fundamentally based on experimental values. The prior studies in the literature have reported that PM3 method provides very reasonable results which are compatible with the experimental data [54-56]. It is also quite fast method that does not require high computational cost as in the case of DFT and *ab initio* methods.

1.2.2.9. Sensitivity of Explosives

The field of sensitivity of explosives properly includes all effects of externally imposed physical conditions on the behavior of explosives and hence is of exceedingly large scope [57-59].

Sensitivity of explosives is defined as how easy an energetic material may explode by any energy pulse [60]. It may also be defined as 'propagating capability' [61]. There are principally five types of sensitivity: friction, shock, spark, heat and impact sensitivity. Friction sensitivity is the ease with which an explosive can be initiated by a blow friction and is stated in terms of what occurs when a pendulum of known weight scrapes across an explosive (ignites or explodes or snaps or crackles). Shock sensitivity is the ease with which an explosive can be set off by a blow shock from explosive charge. Spark sensitivity is the ease with which an explosive can be exploded by an electrostatic spark. Heat sensitivity is the ease with which an explosive can be set off by heat [62].

In the present thesis, we have investigated the "impact sensitivity" of the considered energetic materials. Impact sensitivity measurements of energetic compounds can be done experimentally by physical tests, especially drop height test [63]. Figure 1-7 shows the experimental setup for the impact sensitivity test. A known mass (m) is dropped from an assigned height (h) onto the energetic material each time; the sample is checked whether an explosion occurs. The energy is calculated by the E=mgh relation. The minimum energy at which explosion occurs is recorded as impact sensitivity of the explosive.

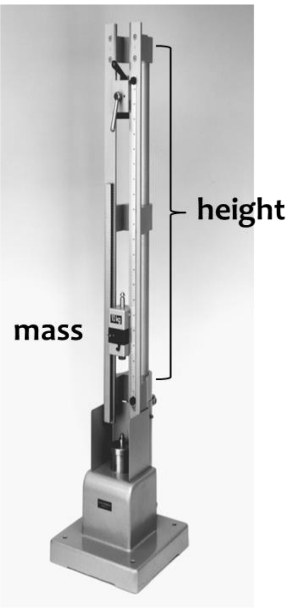

E=mgh

Figure 1-7. Experimental setup for impact sensitivity

Additionally, there are theoretical approaches for the computational determination of impact sensitivity. There are several valuable studies in the literature [64–66] on the homolytic bond dissociation energy (BDE) of the nitro compounds, which have proved that there is a parallel correlation between the BDE for the weakest R–NO_2 bond in the molecule and its sensitivity. The ordinary trend is that the greater the homolytic BDE value for scission of –O-NO_2, -N–NO_2 or -C–NO_2 bonds are, the lower the sensitivity is.

In nitroaliphatics, nitramines and nitrate esters, the attachment of nitro groups is comparatively weak, and therefore scission of that bond is a significant step in decomposition of these energetic materials. The homolytic bond dissociation energy (BDE) calculations for the removal of nitrogen dioxide moiety from the structures are achieved at UB3LYP/6-31G(d,p) level of theory for the determination of C-NO_2 and N–NO_2 bond strengths of the compounds. The expressions for the homolysis of R–NO_2 bond and for computing its homolytic BDE are shown as follows:

$$R\text{–}NO_2(g) \rightarrow R^{\cdot}(g) + NO_2^{\cdot}(g) \tag{7}$$

$$BDE(R\text{–}NO_2) = [E(R^{\cdot}) + E(NO_2^{\cdot})] - E(R\text{–}NO_2) \tag{8}$$

where R–NO_2 indicates the neutral molecule and $R^{\cdot}$ and $NO_2^{\cdot}$ indicate the originated radicals after the bond dissociation; BDE(R–NO_2) is the bond dissociation energy of the bond R–NO_2; E(R–NO_2), E($R^{\cdot}$), and E($NO_2^{\cdot}$) are the zero-point energy corrected total energies of the parent compound and the corresponding radicals, respectively [67-68]. Moreover, the basis set superposition error (BSSE) analyses are accomplished.

1.3. Introduction for Molecular Modeling

Molecular modeling in chemistry is a useful tool for the comprehension of chemistry. Models are essential. Molecular modeling makes it possible to do and explain chemistry better. It provides improved implements for investigation, interpretation or discovery of new phenomena. Nadendla [69] reported that it is a skill-demanding and must be learnt by applying and not just reading as in the case of experimental chemistry. Molecular modeling is easy to accomplish with presently accessible software, but the trouble is to determine the correct model and appropriate elucidation.

Computational chemistry is a set of techniques to investigate chemical problems on a PC. Inquiries commonly inspected computationally are:

- *Molecular geometry:* The shapes of molecules – bond lengths, angles, and dihedrals.
- *Energies of molecules and transition states:* It expresses which isomer is favored at equilibrium, and how fast a reaction should go.
- *Chemical reactivity:* It gives information on where the electrons are focused (nucleophilic sites) and where they want to attack (electrophilic sites).
- *IR, UV, and NMR spectra*: Theses spectra are easily obtained.

- *The interaction of a substrate with an enzyme:* It informs about how a molecule fits into the active site of an enzyme for drug design.
- *The physical properties of substances:* These properties depend on the characteristics of individual molecules and on how the molecules interact in the bulk material.

The principal attempt in molecular modeling is to consider not just one structure for a particular chemical formula, but all possible structures. Many features of chemistry can be limited to questions on potential energy surfaces (PES) [70]. A PES shows the energy of a molecule as a function of its geometry. It is similar to a hilly landscape, with valleys and mountain summits. Real PESs have several dimensions, but key feature can be represented by a 3 dimensional PES, as shown in Figure 1-8.

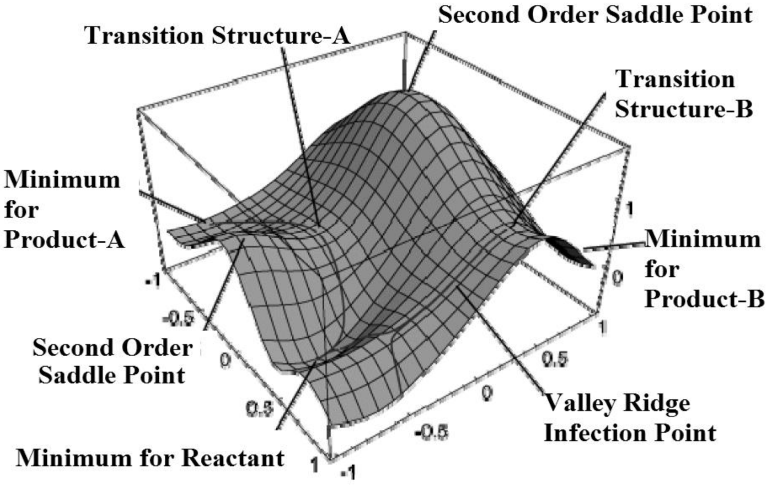

Figure 1-8. A simplified PES in three dimensions, Reprinted from reference [71]

The form of a PES for a particular number of nuclei and electrons can be calculated solving the Schrödinger equation for every possible set of atomic coordinates. The transition state of a reaction relates to a maximum in the reaction coordinate and a minimum in all other coordinates, i.e. the highest point on the lowest energy path being a first-order saddle point. A reaction path links reactants and products by a mountain pass. The energy of reactions can be determined from the individual energies or altitudes of the minima for reactants and products. The structure, energetics, properties, reactivity, spectra and dynamics of molecules can be easily interpreted considering potential energy surfaces.

Development of quantum chemistry makes it possible to practice chemical research by molecular modeling. First *ab initio* ("from the beginning", Latin) computations showed qualitative agreement between experiment and semi-empirical calculations. As the computer technology developed, applications to a larger portion of the chemist's interest extended. Computational chemistry can now be employed as an analytical tool like NMR or X-ray crystallography. It is a predictive tool to be considered prior to experiment. Currently the number and extent of theoretical/computational chemistry resources widely accessible are increasing continuously and reached a tremendous amount. Today, depending on the required accuracy, one can computationally obtain information from systems of several thousands of atoms by using supercomputers.

Some of the most frequently used computational methods are listed below:

- Molecular Mechanics
- Semiempirical (SE) methods
- *Ab initio* methods
- Density functional theory

1.3.1. Molecular Mechanics

Classical mechanics is used to model molecular systems in molecular mechanics. The potential energy of all systems in molecular mechanics is determined employing force fields. Molecular mechanics can be used to study small molecules as well as large biological systems or material assemblies with many thousands to millions of atoms.

All-atomistic molecular mechanics methods possess the characteristics shown below:

- Each atom is treated as a single particle.
- Each particle is assigned a radius (naturally the van der Waals radius), polarizability, and a constant net charge (commonly obtained from quantum calculations and/or experiment)
- Bonded interactions are treated as "springs" with an equilibrium distance equal to the experimental or calculated bond length [71].

1.3.2. Semiemprical Methods

Semi-empirical quantum chemistry methods are constructed on the Hartree–Fock formalism; however make many approximations and get some parameters from empirical data. They are very significant in computational chemistry for discussing large molecules where the full Hartree–Fock method without the approximations is too costly. The use of empirical parameters appears to allow some inclusion of electron correlation effects into the methods. Generally, the core electrons are not included in the calculation and only a minimal basis set is used. Furthermore, some of the two-electron integrals are omitted. In order to correct for the errors due to exclusion of the some calculation, the method is parameterized. Parameters to approximate the omitted values are achieved by fitting the results to experimental data or *ab initio* calculations. These parameters substitute some of the integrals which are excluded.

1.3.2.1. Parameterization Method 3 (PM3)

PM3, Parameterized Method-3, is a semi-empirical method for the quantum calculation of molecular electronic structure in computational chemistry. It neglects the Differential Diatomic Overlap integral approximation. PM3 [72] employs almost the same equations as the AM1 [73] method accompanied by an improved set of parameters. The PM3 is a popular method especially for organic systems. It is more accurate than AM1 for hydrogen bond angles; however AM1 is more accurate for hydrogen bond energies. The PM3 and AM1 methods are also more current than other semiempirical methods due to the available algorithms for including solvation effects in these calculations.

There are also some acknowledged limitations of PM3. PM3 inclines to guess that the barrier to rotation around the C-N bond in peptides is too low. Bonds between Si and the halide atoms are too short. PM3 also tends to predict incorrect electronic states for germanium compounds. It tends to predict sp^3 nitrogen as constantly being pyramidal. Some spurious minima are predicted. Proton affinities are not accurate. Some polycyclic rings are not flat. The predicted charge on nitrogen is incorrect. Nonbonded distances are too short. Hydrogen bonds are too short by about 0.1Å, but the orientation is usually correct. Averagely, PM3 calculates energies and bond lengths more precisely than AM1.

1.3.3. *Ab initio* Methods

Ab initio methods are the computations derived straight from theoretical principles without any experimental data. Several approximations are involved in *ab initio*. The approximations made are usually mathematical approximations, i.e. using a simpler functional form for a function or finding an approximate solution to a differential equation.

1.3.3.1. The Hartree-Fock Theory

The most common type of *ab initio* calculation is called a Hartree-Fock calculation (abbreviated HF) [74, 75], where the first approximation is the central field approximation. This means that the Coulombic electron-electron repulsion is taken into account by integrating the repulsion term. This gives the average influence of repulsion, but not the explicit repulsion interaction. This is a variational calculation, meaning that the approximate energies calculated are all equal to or greater than the exact energy. Because of the central field approximation, energies from HF calculations are always greater than the exact energy and tend to a limiting value called the Hartree-Fock limit as the basis set is improved (see Figure 1-9).

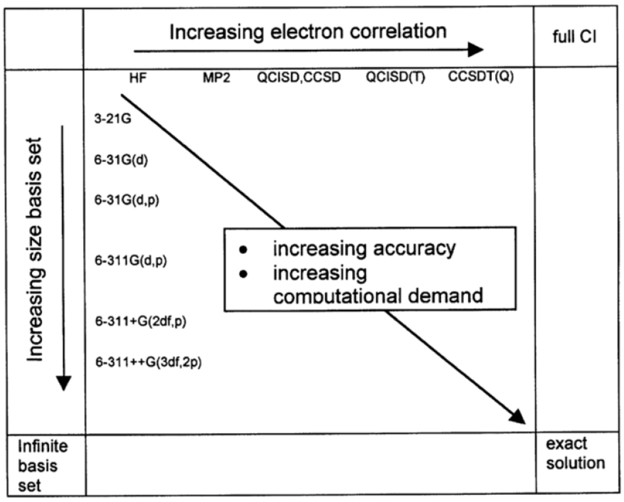

Figure 1-9. Pople diagram showing the dependence of the performance of an *ab initio* method on the basis set and the amount of electron correlation. Reprinted from reference [76].

It is an advantageous method that it breaks the many-electron Schrödinger equation [77] into many simpler one-electron equations. Each one electron equation is solved to produce a single-electron wave function, entitled as an orbital, and energy, entitled as orbital energy. The orbital defines the behavior of an electron in the net field of all the other electrons.

The so-called orbitals are then combined into a determinant. This is done to fulfill two necessities of quantum mechanics. One is that the electrons must be indistinguishable. Linear combination of orbitals enables each electron to appear in each orbital, one can say that an electron was put in a particular orbital but cannot say which electron it is. The second requirement says that the wave function for fermions (i.e. an electron is a fermion) must be anti-symmetric with respect to interchanging two particles. Consequently, if electron 1 and electron 2 are interchanged, the sign of the total wave function must change. This is fulfilled only by a determinant because switching two electrons is equivalent to interchanging two columns of the determinant, which changes its sign.

The stages in a Hartree-Fock calculation begin with an initial estimate for the orbital coefficients, generally using a semiempirical method. This function is used to determine energy and a new set of orbital coefficients, which can then be employed to get a new set, and so on. This procedure lasts iteratively until the energies and orbital coefficients stay constant from one iteration to the next. This is called having the calculation converge. There is no warranty the calculation will converge. If it does not, some technical skill is required to solve the problem. This iterative procedure is called a self-consistent field procedure (SCF). Some researchers refer to these as SCF calculations to differentiate them from the earlier method created by Hartree, but HF is used more widely.

A variation on the HF method is the way that orbitals are constructed to reflect paired or unpaired electrons. If the molecule has a singlet spin, then the same orbital spatial function can be used for both α and β spin electrons in each pair. This is called the restricted Hartree-Fock method (RHF) [78].

Two techniques are available for the construction of HF wave functions of molecules with unpaired electrons. One technique is to use two completely separate sets of orbitals for α and β electrons, called an unrestricted Hartree-Fock wave function (UHF) [79]. This means that paired electrons will not have the same spatial distribution. This introduces an error into the calculation, called spin contamination. Spin contamination might introduce an insignificant error or the error could be large enough to make the results unusable depending on the chemical system involved. UHF calculation is popular because they are easy to implement and run fairly efficiently.

1.3.4. Utilization of Computational Chemistry in Energetic Materials Field

Computational chemistry (molecular modeling) is a beneficial tool that gives information about chemical and physical properties of materials without doing a physical experiment. It has been widely utilized in energetic materials field. A more precise approach has been established with the fast development in computer technology and theoretical chemistry. Computational chemistry facilitates the prediction of performance of explosives prior to the synthesis [80-82]. Presently, the research on energetic materials is carried out using thermodynamics and molecular engineering approaches, which enable them to design effectual materials. In recent years, theoretical calculations for the determination of detonation behavior of explosives have attracted too many scientists all over the world [13, 14, 83, 84]. Computational chemistry enables one to make a distinction between promising explosive candidates and poor ones before synthesis. The most widely used thermochemical codes for the prediction of detonation properties are TIGER, CHEETAH, LOTUSES and EXPLO 5 [84-88]. These thermochemical codes are particular to explosives, and are very expensive as well. The calculations in the present thesis have been performed by using more academic package programs namely, Gaussian 03 [89], Spartan 06 [90], and Hyperchem 8.03 [91].

1.3.5. Methods of calculation

All the calculations in the present thesis have been done as explained in the following paragraph. The preliminary geometry optimizations resulting in energy minima have been completed employing MM2 followed by semi–empirical PM3 self–consistent fields molecular orbital (SCF–MO) methods [92] at the restricted level [93, 94]. Afterwards, further geometry optimizations have been achieved using STO and HF level of theory (6-31G(d,p)) and then within the framework of Density Functional Theory (DFT, B3LYP) [95, 96] at the restricted level [16] of 6–31G(d,p) basis set. The exchange term of B3LYP contains hybrid Hartree–Fock and local spin density (LSD) exchange functions with Becke's gradient correlation to LSD exchange. [96, 97] The correlation term of B3LYP consists of

Vosko, Wilk, Nusair (VWN3) local correlation functional [98] and Lee, Yang, Parr (LYP) correlation correction functional [99].

Vibrational analyses and the calculation of total electronic energies have been performed using B3LYP/6–31G(d,p) type calculations for closed–shell systems. The total electronic energies have been corrected for zero point vibrational energies (ZPE). The normal mode analysis for each compound has yielded no imaginary frequency which indicates each compound had at least a local minimum on the potential energy surface.

Moreover, the geometry optimizations and the single point calculations of all the structures have been performed at unrestricted (UB3LYP/6-31G(d,p)) theoretical level for bond dissociation energy (BDE) calculations. Note that in bond dissociation process open-shell systems are generated by the elimination of R radical via homolytic bond dissociation (radicalic dissociation process). The basis set superposition error (BSSE) analysis for bond dissociations have been carried out with the counterpoise method, introduced by Boys and Bernardi [100], at the same level of theory. BSSE analyses have been performed at the same theoretical levels (UB3LYP/6-31G(d,p)) by Gaussian 03 software package.

The spin states of the compounds investigated in the thesis were considered as singlet; whereas spin states of the examined radicals are considered as doublet.

Gas phase heat of formations of all the molecules have been calculated by a semi–empirical approach (PM3) over DFT (B3LYP/6–31G(d,p)) optimized geometries. The frontier molecular orbital energies have been obtained by HF/6-31G(d,p)//B3LYP/6-31G(d,p) method due to the absence of Hartree-Fock type orbital concept in DFT.

The density of the molecule is calculated by the division of the molecular weight by molecular volume. The molecular volume of each molecule is obtained from the statistical average of 100 single-point molar volume calculations over optimized geometries. The molar volume was outlined inside a contour of 0.001 electrons/Bohr^3 density that has been evaluated by using a Monte Carlo integration technique executed in the Gaussian’03 package program.

All the computations, except for molar volume and BSSE calculations, have been performed using Spartan 06 software [90]. The molar volume and BSSE calculations have been done by Gaussian’03 [89].

1.4. Objectives of the Study

Molecular modeling is a valuable tool that gives information about chemical and physical properties of materials without doing a physical experiment. It has been widely utilized in energetic materials field. In the present work, we have also performed molecular modeling on some fuels and explosives. The thesis consists of six chapters (excluding introduction, Chapter-1), which have their own literature surveys, methodologies and conclusions.

Chapter-II is about JP-10, an aviation fuel widely used in aircrafts. It is a bicyclic hydrocarbon based fuel. Fuel degradation may occur under long time, low-temperature storage conditions (storage stability) or under short time high-temperature stress (thermal oxidative stability). Oxidation through hydroperoxide formation has been considered. Also decomposition of the formed fuel hydroperoxide has been reviewed. The most probable decomposition products have been identified. Chapter-III is about another significant aviation fuel, JP-900. It has also been studied in this perspective.

Chapter-IV focuses on explosive, 1,3,3-trinitroazetidine, TNAZ. The explosive properties of TNAZ and its derivatives have been studied. A decrease in the sensitivity of TNAZ has been tried by making molecular level changes on the molecule. The nitro groups have been converted to nitroso and amino groups and their explosive properties have been examined.

Chapter-V is on explosive TACOT, and its four novel benzofuroxan derivatives. The explosive properties of both TACOT and four benzofuroxan isomers have been determined and compared with TACOT (an existing molecule).

Chapter-VI concerns an explosive, FOX-7, 1, 1-diamino-2,2-dinitroethylene. The effects of further nitration of the amino groups on the molecule and effects of epoxidation of the double bond in the middle of the molecule on the explosive performance have been investigated.

Chapter VII deals with the design of novel explosives based on parabanic acid structure. The great magnitudes of the calculated density of parabanic acid and its high nitrogen content have inspired us to investigate the parabanic acid frame. A series of molecules have been designed by nitration and imination and their explosive performances have been investigated.

CHAPTER 2

A THEORETICAL STUDY OF JP-10 HYDROPEROXIDATION

2.1. Introduction

A jet fuel is a type of aviation fuel designed for use in aircrafts powered by gas-turbine engines. Commonly, it is a combination of a large number of different hydrocarbons. The most common fuels are Jet A and Jet A-1 which are manufactured to a worldwide consistent set of qualifications. Another jet fuel that is frequently used in civilian turbine engine-powered aviation is entitled as Jet B. It is a naphtha-kerosene based fuel that is used for its improved cold-weather performance. However, Jet B's lighter composition makes it more hazardous to handle [101, 102].

Military establishments around the world use a different categorization system of JP numbers. The term JP is an acronym for Jet Propellant. Some are almost indistinguishable to their civilian counterparts and differ only by the quantities of a few additives; Jet A-1 is analogous to JP-8, Jet B is analogous to JP-4 [102, 103]. JP-8, a jet fuel, was specified in 1990 by the U.S. Government. It is kerosene-based and is a replacement for the JP-4 fuel. By the fall of 1996, the U.S. Air Force replaced JP-4 with JP-8 completely which is a less combustible and less dangerous fuel for better safety and combat survivability.

Other military fuels are highly particular products and are developed for very specific uses. JP-5 fuel is fairly common, and was introduced to decrease the risk of fire on aircraft transporters. Other fuels were particular to one type of aircraft. For example, JP-6 was developed specifically for the XB-70 Valkyrie and JP-7 for the SR-71 Blackbird. Both these fuels were planned to have a great flash point to better cope with the heat and stresses of high speed supersonic flight. One aircraft-specific jet fuel still in use by the United States Air Force is JPTS, which was developed in 1956 for the Lockheed U-2 spy plane [104].

Jet fuels are sometimes classified as kerosene- or naphtha-type. Kerosene-type fuels include Jet A, Jet A1, JP-5 and JP-8. Naphtha-type jet fuels, sometimes referred to as "wide-cut" jet fuels, include Jet B and JP-4 [101-104].

JP-8, a jet fuel, was identified in 1990 by the U.S. Government. It is kerosene-based and is an auxiliary for the JP-4 fuel. In 1996, the U.S. Air Force replaced JP-4 with JP-8 completely which is a less flammable and less dangerous fuel for better safety and combat survivability.

JP-10 ($C_{10}H_{16}$) is one of the cyclic, high-energy-density fuels being used in aircrafts [105, 106]. JP-10, also called exo-tetrahydrodicyclopentadiene, is a single-component hydrocarbon, produced synthetically by the hydrogenation of dicyclopentadiene (Figure 2-1)

[107]. It is a popular missile fuel because of its highly increased energy storage through its strained cyclic geometry [108] and is considered ideal for volume limited applications.

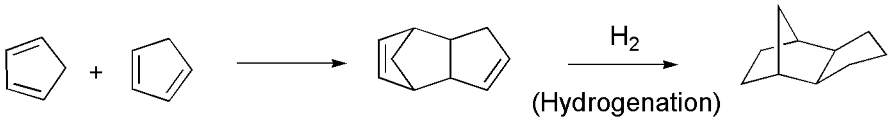

Figure 2-1. Synthetic Route to JP-10.

In recent years, the quality of petroleum feedstock used by refineries has decreased. This has required the utilization of more severe refinery processes in order to produce jet fuels of higher thermal stability and purity. Inspection of fuels refined by different processes has shown that there is a high concentration of peroxides in fuels which have been severely hydrotreated. It is acknowledged that hydrogenation is responsible for removing natural inhibitors, including sulfur compounds, to hydroperoxide formation [109].

Fuel instability is related to hydroperoxide concentration present in the fuel. Fuel degradation happens under long time, low-temperature storage conditions (storage stability) or under short time high-temperature stress (thermal oxidative stability). The latter situation becomes vital during flight conditions, where fuel serves as a coolant on its path to the combustion chamber. Minor thermal degradations take place in nonoxidizing atmospheres, but the presence of oxygen or active species such as hydroperoxides seriously accelerate the oxidative degradation causing undesirable deviations in fuel properties. The rates of reactions in autoxidation schemes depend on hydrocarbon structure, heteroatom concentration, oxygen concentration and temperature. In the presence of sufficient oxygen, the concentration of hydroperoxides formed reaches high levels. If the available oxygen is low, but the temperature is raised, the hydroperoxide concentration is limited by free-radical decomposition. Under these circumstances, fuel degradation can be associated with both hydroperoxide formation and decomposition [109].

Hydroperoxide formation causes elastomer failures in aircraft fuel systems. During the 1970s, hydroperoxide induced elastomer deterioration caused the loss of many aircrafts. Because of occurrence of these accidents, a cooperative program was initiated to develop a method to predict the hydroperoxide forming tendency of a jet fuel during storage [110].

The formation of hydroperoxide compounds in partial oxidations of hydrocarbons is a starting point for the comprehension of subsequent cracking mechanisms in organic materials [111, 112]. We have thought that JP-10 can also serve as a potential material to be susceptible to oxidation through hydroperoxide formation. This has encouraged us to study hydroperoxide formation of JP-10 theoretically.

2.2. Results and Discussion

All the calculations have been done as expressed in section 1.3.5.

2.2.1. The Formation Tendencies of JP-10 Radicals and Hydroperoxides

Numberings of the hydrogen and carbon atoms of JP-10 are shown in Figure 2-2. Numberings of the radicals and hydroperoxides have been done in the same manner. Table 2-1 shows the labeling of both the radicals and hydroperoxides originated from the corresponding atoms.

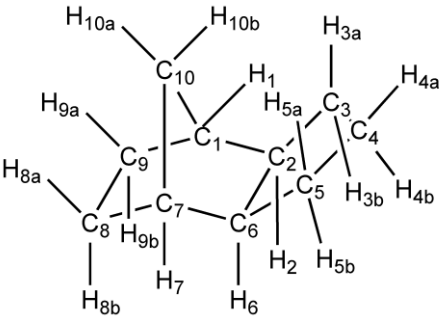

Figure 2-2. Numberings of hydrogen and carbon atoms of JP-10.

Table 2-1. Labelings of the radicals and hydroperoxides originated from JP-10.

The Atoms	Radical Label	The Atoms	Hydroperoxide Label
C_1-H_1	**a**	C_1-OOH_1	**A**
C_2-H_2	**b**	C_2-OOH_2	**B**
C_3-H_{3a}	**c**	C_3-OOH_{3a}	**C**
C_3-H_{3b}	**d**	C_3-OOH_{3b}	**D**
C_4-H_{4a}	**e**	C_4-OOH_{4a}	**E**
C_4-H_{4b}	**f**	C_4-OOH_{4b}	**F**
C_5-H_{5a}	**g**	C_5-OOH_{5a}	**G**
C_5-H_{5b}	**h**	C_5-OOH_{5b}	**H**
C_6-H_6	**i**	C_6-OOH_6	**I**
C_7-H_7	**j**	C_7-OOH_7	**J**
C_8-H_{8a}	**k**	C_8-OOH_{8a}	**K**
C_8-H_{8b}	**l**	C_8-OOH_{8b}	**L**
C_9-H_{9a}	**m**	C_9-OOH_{9a}	**M**
C_9-H_{9b}	**n**	C_9-OOH_{9b}	**N**
C_{10}-H_{10a}	**o**	C_{10}-OOH_{10a}	**O**
C_{10}-H_{10b}	**p**	C_{10}-OOH_{10b}	**P**

JP-10 molecule belongs to C_1 point group, which means that it has no symmetry plane and all the hydrogen atoms belonging to the molecule are different (16 different atoms). Therefore, in the present study, JP-10 itself, 16 different radicals and 16 different hydroperoxides originated from JP-10 have been investigated theoretically. A semi-empirical method, PM3, has been applied over DFT optimized geometry of JP-10 to calculate the heat of formation value at the standard state. The gas phase heat of formation value of JP-10 has been calculated as -78.39 $kJ.mol^{-1}$. JP-10 is assigned to be a nonpolar fuel [113]. We have calculated the dipole moment as 0.02 Debye, which supports its nonpolarity.

JP-10 is susceptible to oxidation through hydroperoxide formation like all hydrocarbons under storage conditions [114]. This has led us to study hydroperoxide formation of JP-10, theoretically. The following mechanism has been proposed: Firstly, homolytic H-abstraction from a specific site of JP-10 occurs. Then, $^{\cdot}OOH$ radical reacts with the carbon radical formed to produce the corresponding JP-10 hydroperoxide. Figure 2-3 shows one of the hydroperoxide formation routes. Also, the decomposition of hydroperoxide has been discussed in the following paragraphs.

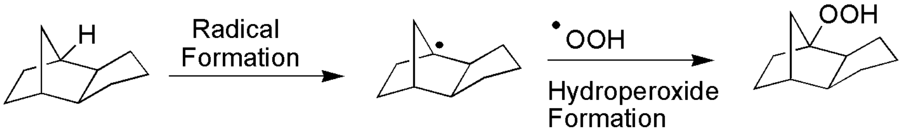

Figure 2-3. A suggested hydroperoxide formation route.

As indicated in Table 2-2, stabilities of the radicals are in the following manner: c > d = e = f = g = h >b=l = m = n > i = k > o = p > a = j. It is expected that the tertiary radicals (a, b, i and j) be far more stable than the others; however secondary radicals c, d, e, f, g and h showed better stability. We thought that this unexpected lesser stability of the tertiary radicals is due to the strained cyclic geometry of JP-10 molecule. The present tertiary radicals have to overcome certain strain to attain more or less a planar structure which is the expected geometry for acyclic carbon radicals; whereas the present secondary radicals can get almost-planar stable structures.

Table 2-2. Total and relative electronic energy values of radicals and hydroperoxides originated from JP-10 (from the lowest to the highest).

Radical Energies UB3LYP/6-31G(d,p)			**Hydroperoxide Energies** UB3LYP/6-31G(d,p)		
Label	**E_{total} (kJ/mol)**	**E_{rel} (kJ/mol)**	**Label**	**E_{total} (kJ/mol)**	**E_{rel} (kJ/mol)**
c	-1023502	0	**I**	-1419932	0
d	-1023501	1	**A**	-1419926	5
e	-1023501	1	**J**	-1419926	6
f	-1023501	1	**M**	-1419926	6
g	-1023501	1	**B**	-1419925	7
h	-1023501	1	**F**	-1419923	9
b	-1023497	5	**L**	-1419923	9
l	-1023497	5	**H**	-1419921	11
m	-1023497	5	**E**	-1419920	12
n	-1023497	5	**D**	-1419918	13
i	-1023496	6	**O**	-1419917	15
k	-1023496	6	**K**	-1419915	16
o	-1023474	28	**C**	-1419911	21
p	-1023474	28	**N**	-1419908	24
a	-1023461	41	**G**	-1419902	30
j	-1023461	41	**P**	-1419897	35

Table 2-3 shows the ΔG^o_{rxn} values of the formation of radicals from JP-10. ΔG^o_{rxn} has been calculated as the difference between the G^o values of the products and the reactants by means of UB3LYP/6-31G(d,p) type approach.

Table 2-3. ΔG^o_{rxn} values of the formation of radicals from JP-10 from the lowest to the highest (UB3LYP/6-31G(d,p)).

Radical Label	ΔG^o_{rxn} (kJ/mol)
e	1707
f	1707
c	1708
d	1708
h	1708
g	1709
b	1713
i	1714
k	1714
l	1714
m	1714
n	1714
o	1735
p	1736
a	1749
j	1750

When ΔG^o_{rxn} values in Table 2-3 are considered, it is obvious that the positions on the cyclopentane ring have similar tendencies for radical formation (c - h radicals). This easiness with respect to the tertiary ones has been thought to be due to the relatively unstrained geometries of the secondary radicals from cyclopentane moiety. The feasibility of formation of radicals b, i, k, l, m and n are analogous. According to the ΔG^o_{rxn} values indicated in Table 2-3, the formations of tertiary radicals b and i seem more probable when compared to bridgehead tertiary radicals a and j and bridge secondary radicals o and p.

The formations of bridgehead radicals are not feasible. For them, not only Gibbs free energy changes (endothermic) for the radical formations are quite large; but also radicals formed are high in relative electronic energies (see Table 2-2). They are the least stable radicals. This may arise from the increase in the strain of the bridgehead carbons radicals, C_1 and C_7 which cannot properly change from sp^3 to sp^2 hybridization [115].

Labeling of hydroperoxides has been achieved in the same way with radical labeling (Table 2-1). Stability sequence is in the following manner: I > A>J=M>B > F = L > H > E > D > O > K > C > N > G > P (Table 2-2). The structures having OOH group at the tertiary positions (A, B, I and J) are the most stable hydroperoxides. Thus, it appears that the tertiary radicals (a, b, i and j), which show poor stability; react with OOH radical to form hydroperoxides of good stability.

By comparing the total electronic energies of the hydroperoxide molecules we have also designated "the most feasible carbon centers". These are carbons which are potent sites to be oxidized through hydroperoxidation. Carbon centers C_1, C_2, C_6, C_7 and C_9 are very susceptible to oxidation through hydroperoxidation because the corresponding hydroperoxides A, B, I, J and M are very low in total electronic energies (Table 2-1 and Table 2-2). The carbon center C_{10} at the bridge position seems to be least feasible position for oxidation as a result of the highest total electronic energy of all.

2.2.2. Decomposition of JP-10 Hydroperoxides

The hydroperoxides formed may decompose to different products having less total electronic energies. In this part of the study, we have investigated the decomposition of the most stable hydroperoxides, namely "A" ($[1]^{1,7}$-bridgehead hydroperoxide)" and "I" ($[0]^{2,6}$-bridgehead hydroperoxide). The following decomposition mechanisms for hydroperoxides have been considered in this work; the carboxylic acid (ester)-alkane, alcohol-aldehyde and alcohol-ketone mechanisms. The choice of these mechanisms is based on analytic information as well as the distribution of products formed from the oxidative cracking of hydroperoxides [111, 112, 116].

The carboxylic acid (ester)–alkane mechanism (Figure 2-4) consists of the formation of carboxylic acids and alkane part via cracking of the alkane part by the recombination of the oxygen atoms of the hydroperoxide group. In the work of Hayashi et al. [114] the cracking reaction, forming acetic acid, is preceded by a transfer of one proton from the alkane. In the mechanisms investigated in reference [116], the formations of free radicals are not considered, i.e. only considered is the recombination of the atoms of the hydroperoxide groups.

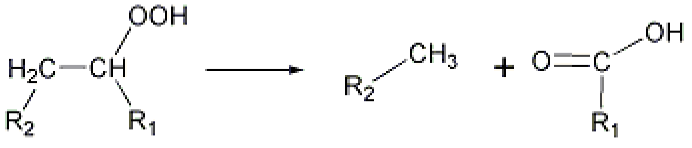

Figure 2-4. The carboxylic acid (ester)–alkane mechanism for the decomposition

In the alcohol–aldehyde mechanism (Figure 2-5), as the name indicates, there is the decomposition of the hydroperoxide group, forming alcohols and aldehyde. The presence of alkyl ramifications in the molecule leads to the alcohol–ketone mechanism (Figure 2-6) which is similar to the previous case, differing only by the formation of ketones instead of aldehyde. This mechanism occurs for the decomposition of tertiary peroxides forming, thus, ketones and alcohols.

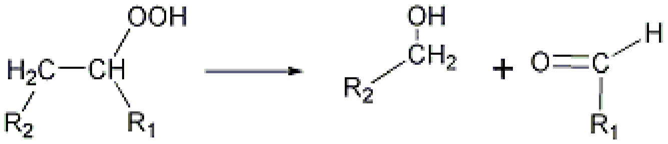

Figure 2-5. The alcohol–aldehyde mechanism for the decomposition

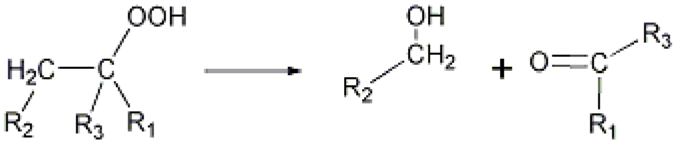

Figure 2-6. The alcohol–ketone mechanism for the decomposition

Presently, the decompositions of the most stable JP-10 hydroperoxides have been considered. High concentration of the most stable hydroperoxides affects the quality of fuel more than least stable ones do. Because the least stable hydroperoxides disappear promptly and only kinetically affect the quality of the fuel. Therefore, the most stable hydroperoxides labeled as “A” and “I”, have been investigated in the light of the suggested mechanisms mentioned above. As seen from Figure 2-7 and Figure 2-8, we have made total electronic energy calculations on these 10 different but isomeric products over DFT optimized structures (using UB3LYP method and 6-31G(d,p) basis set). The total electronic energies were corrected for zero point vibrational energies (ZPE).

The hydroperoxide labeled as “I” is the most stable hydroperoxide of all. Note that all the products are isomers. In Table 2-4, the total and the relative electronic energies of the decomposition products and the ΔG^o_{rxn} values for the conversion of hydroperoxide “I” to the products are shown. ΔG^o_{rxn} values have been calculated as the difference between the G^o values of the products and the reactants. The total electronic energy considerations of the final products and the ΔG^{o}_{rxn} values for the conversion of hydroperoxide to the corresponding products have shown parallel trends.

Table 2-4. The total and the relative electronic energy values (UB3LYP/6-31G(d,p)) of "Hydroperoxide I and A" and their decomposition products and ΔG^{o}_{rxn} values (from the lowest to the highest).

Name	E_{total} (kJ/mol)	E_{rel} (kJ/mol)	ΔG^{o}_{rxn} (kJ/mol)
Product-4	-1420214	0	-290
Product -1	-1420172	43	-250
Product-2	-1420159	55	-231
Product-3	-1420152	63	-221
Hydroperoxide-I	-1419932	282	-
Product-5	-1419850	364	81
Product-10	-1420216	0	-293
Product-9	-1420196	20	-273
Product-7	-1420179	37	-260
Product-8	-1420177	39	-256
Product-6	-1420136	80	-218
Hydroperoxide-A	-1419926	290	-

Since Gibbs free energy change (ΔG^{o}_{rxn}) for the Reaction-4 (see Figure 2-7) is more negative than those of other reactions, Hydroperoxide-I molecule thermodynamically prefers the carboxylic acid (ester)-alkane decomposition mechanism. Also, the total electronic energy of Product-4 is lower than those of the products 1-3 and 5 and the corresponding hydroperoxide. Therefore, Product-4, *3-cyclopentyl-tetrahydropyran-2-one*, has been found to be the most feasible decomposition product of this hydroperoxide, in terms of the thermodynamic considerations.

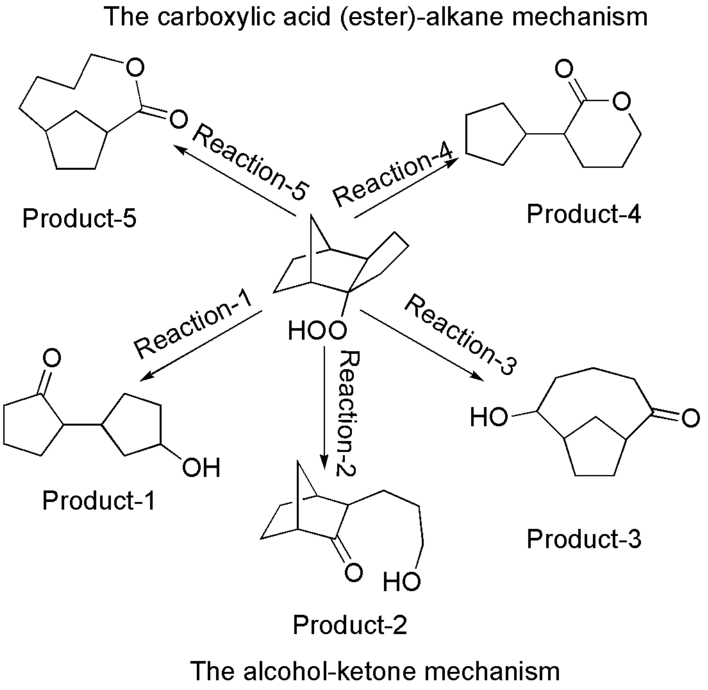

Figure 2-7. Decomposition of JP-10 Hydroperoxide labeled as “I”. Products 1-3 belong to the alcohol-ketone mechanism whereas products 4 and 5 to the carboxylic acid (ester)-alkane mechanism.

Conversion of Hydroperoxide-I to Product-5 seems to be non-spontaneous as a result of the positive ΔG^o_{rxn}. Besides, the final product is more energetic than the hydroperoxide, which is an indication of this non-spontaneity.

The hydroperoxide labeled as “A” is the second most stable hydroperoxide (see Table 2-1 and Figure 2-2). Note that, it is also a bridgehead hydroperoxide. In Table 2-4, the total electronic energies of the decomposition products and the ΔG^o_{rxn} values for the conversion of hydroperoxide “A” to the products are shown.

Hydroperoxide-A molecule prefers the carboxylic acid (ester)-alkane decomposition mechanism (Reaction-10) due to the least Gibbs free energy change (ΔG^o_{rxn}) for Reaction-10 when compared to the others (Figure 2-8). Furthermore, the total electronic energy of Product-10 is lower than those of the other products and the corresponding hydroperoxide. Consequently, Product-10, *4-ethyl-hexahydrocyclopenta[b]pyran-2(3H)-one*, has been found to be the most feasible decomposition product of this hydroperoxide regarding the thermodynamic considerations.

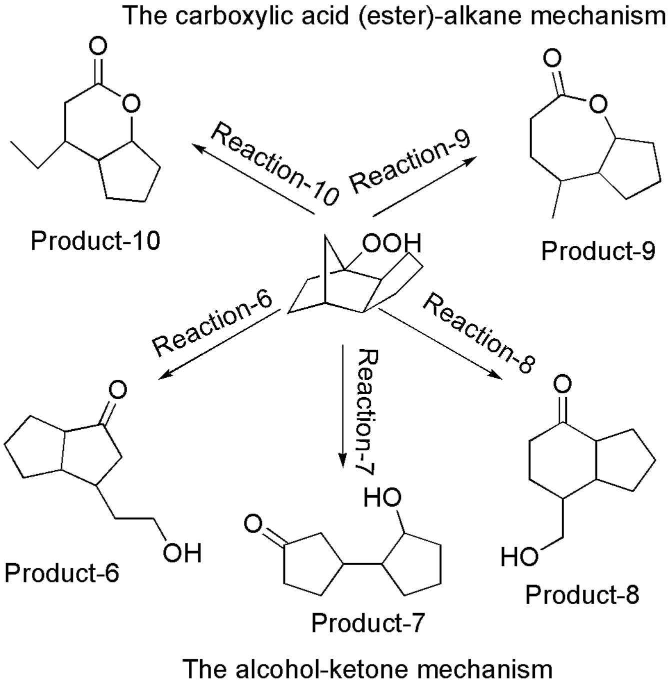

Figure 2-8. Decomposition of JP-10 Hydroperoxide labeled as "A". Products 6-8 belong to the alcohol-ketone mechanism whereas products 9 and 10 to the carboxylic acid (ester)-alkane mechanism.

2.3. Conclusion

In this work, the stability of JP-10 ($C_{10}H_{16}$), which is a cyclic, high-energy-density fuel being used in, or considered for, defense applications, has been investigated. Since hydroperoxide concentration has been found to be a factor in fuel instability, oxidation of JP-10 through hydroperoxidation mechanism has been discussed based on Density Functional Theory (DFT) calculations.

Carbon center numbered as "6" (yields radical "i") is found to be the most vulnerable point to oxidation through hydroperoxidation to produce I. Since "c" (the radical is on position-3) is the most stable radical, thermodynamically; the concentration of this radical is expected to be quite high in the medium. Therefore, one expects to see more hydroperoxide product "C"; however, this is not the case. Hydroperoxide "C" is not stable enough and probably either forms very little or decomposes easily as a result of the thermodynamic instability of the molecule. On the other hand, "i" is not as stable as radical "c" and should have low concentration in the medium; however, it is more energetic and the hydroperoxide formed from it (Hydroperoxide-I) is the most stable one. Therefore, radical "i" is more prone to the production of Hydroperoxide-I.

The decompositions of thermodynamically the most stable hydroperoxides A and I have also been investigated. The calculations have shown that both the bridgehead hydroperoxide (A) and the tertiary hydroperoxide (I) prefer the carboxylic acid (ester)-alkane decomposition mechanism.

CHAPTER 3

JP-900 HYDROPEROXIDATION and DECOMPOSITION

3.1. Introduction

The demand for a fuel with superior thermal properties motivated a group of synthetic chemists. Consequently, they have produced a thermally stable coal based jet fuel that absorbs significant quantities of heat, while remaining stable at 900 ^{o}F (482 ^{o}C) as an alternative to JP-8. This fuel has been nominated as jet propulsion 900, JP-900, due to its high temperature stability [109, 117-118]. JP-900 was produced from blending refined chemical oil (RCO) and light cycle oil (LCO) at a 50:50 blend ratio and hydrogenating the mixture. This process yields a fuel rich in cycloalkanes, most notably decahydronaphthalene (decalin). Cycloalkanes have been investigated as potential fuels in gasoline, diesel, and jet engines [6,9,10] Cycloalkanes have unique characteristics, some of which are very advantageous for jet fuels in terms of thermal stability (as hydrogen donor species), combustion properties, and energy density. The thermal stability of a jet fuel refers to the resistance of the fuel to decompose and form solid carbon deposits that spoil foul valves, nozzles and other engine parts of jet planes [119].

The JP-900 consists of *cis*- and *trans*-isomer of decalin (Figure 3-1). The studies in the literature have shown that the isomers have different thermal stability [117-119]. In each of these studies, the results have shown in varying degrees that *trans*- is the more stable isomer.

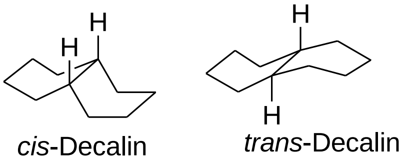

Figure 3-1. The structures of *cis*- *trans*-Decalin

The formation of hydroperoxide compounds in partial oxidations of hydrocarbons is a preliminary point for the understanding of subsequent cracking mechanisms in organic materials [111-112]. We thought that JP-900 is a potential substance to be vulnerable to oxidation through hydroperoxide formation as in the previous chapter. This has inspired us to investigate hydroperoxide formation of JP-900, theoretically.

3.2. Results and Discussion

All the calculations have been done as expressed in section 1.3.5. We have investigated the total electronic energies of both isomers of JP-900. The *trans*-decalin (E_{total}= -1028394.57 kj/mol) has been found more stable than *cis*-one (E_{total}=-1028356.40 kj/mol). Consequently, we have done our calculations on that isomer. *Trans*-decalin is considered as JP-900 in the present work. These results are consistent with other studies that examined the two 9-decalyl radicals [120-122].

3.2.1. The Formation Tendencies of JP-900 Radicals and Hydroperoxides

Numberings of the hydrogen and carbon atoms of JP-900 are shown in Figure 3-2. Numberings of the radicals and hydroperoxides have been done in the same way.

Table 3-1 shows the labeling of both the radicals and hydroperoxides obtained from the corresponding atoms. Radicals are labeled with small letters; whereas hydroperoxides are labeled with capital letters.

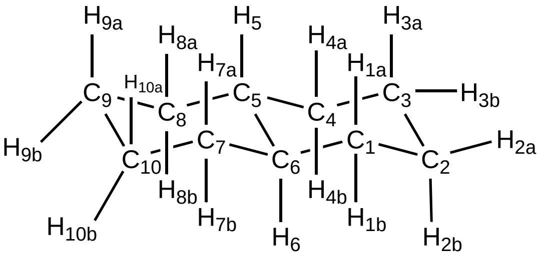

Figure 3-2. Numberings of hydrogen and carbon atoms of JP-900

Table 3-1. Labelings of the radicals and hydroperoxides originated from JP-900.

The Atoms	Radical Label	The Atoms	Hydroperoxide Label
C_1-H_{1a}	**a**	C_1-OOH_{1a}	**A**
C_1-H_{1b}	**b**	C_1-OOH_{1b}	**B**
C_2-H_{2a}	**c**	C_2-OOH_{2a}	**C**
C_2-H_{2b}	**d**	C_2-OOH_{2b}	**D**
C_3-H_{3a}	**e**	C_3-OOH_{3a}	**E**
C_3-H_{3b}	**f**	C_3-OOH_{3b}	**F**
C_4-H_{4a}	**g**	C_4-OOH_{4a}	**G**
C_4-H_{4b}	**h**	C_4-OOH_{4b}	**H**
C_5-H_5	**i**	C_5-OOH_5	**I**
C_6-H_6	**j**	C_6-OOH_6	**J**
C_7-H_{7a}	**k**	C_7-OOH_{7a}	**K**
C_7-H_{7b}	**l**	C_7-OOH_{7b}	**L**
C_8-H_{8a}	**m**	C_8-OOH_{8a}	**M**
C_8-H_{8b}	**n**	C_8-OOH_{8b}	**N**
C_9-H_{9a}	**o**	C_9-OOH_{9a}	**O**
C_9-H_{9b}	**p**	C_9-OOH_{9b}	**P**
C_{10}-H_{10a}	**r**	C_{10}-OOH_{10a}	**R**
C_{10}-H_{10b}	**s**	C_{10}-OOH_{10b}	**S**

JP-900 molecule belongs to C_i point group, which means that it has no symmetry plane and all the hydrogen atoms belonging to the molecule are unlike (18 different atoms). Therefore, in the present study, JP-900 itself, 18 different radicals and 18 different hydroperoxides originated from JP-900 have been examined computationally. A semi-empirical method, PM3, has been applied over DFT optimized geometry of JP-900 to calculate the heat of formation value at the standard state. The gas phase heat of formation value of JP-900 has been calculated as -176.522 $kJ.mol^{-1}$. JP-900 is said to be a nonpolar fuel. We have calculated the dipole moment as zero Debye, which support this nonpolarity.

JP-900, like all hydrocarbons, is susceptible to oxidation through hydroperoxide formation under storage conditions [114]. This has directed us to study hydroperoxide formation of JP-900, computationally. The following mechanism has been proposed: Firstly, homolytic H-abstraction from a specific position of JP-900 occurs. Then, the radical reacts with $^{\cdot}OOH$ radical in order to produce the corresponding JP-900 hydroperoxide. Figure 3-3 shows one example of the hydroperoxide formation routes. Also, the decomposition of hydroperoxide has been discussed in the subsequent paragraphs**.**

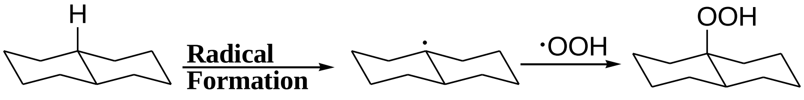

Figure 3-3. A suggested hydroperoxide formation route

As indicated in Table 3-2, stabilities of the radicals are in the following sequence: i=j > c=d=e=o=p=s > a=b=f=g=k=l=m=n=r > h. The tertiary radicals (i and j) are found to be more stable than other radicals as expected.

Table 3-2. Total and relative electronic energy values of radicals and hydroperoxides originated from JP-900 (from the lowest to the highest).

Radical Energies			Hydroperoxide Energies		
Label	**E_{total} (kJ/mol)**	**E_{rel} (kJ/mol)**	**Label**	**E_{total} (kJ/mol)**	**E_{rel} (kJ/mol)**
i	-1026692	0	**P**	-1423106	0
j	-1026692	0	**C**	-1423106	0
d	-1026681	10	**S**	-1423105	1
o	-1026681	10	**D**	-1423105	1
e	-1026681	10	**E**	-1423105	1
c	-1026681	10	**O**	-1423104	2
p	-1026681	10	**K**	-1423104	2
s	-1026681	10	**R**	-1423104	3
f	-1026681	11	**G**	-1423104	3
r	-1026681	11	**M**	-1423103	3
l	-1026681	11	**B**	-1423103	3
b	-1026680	11	**F**	-1423103	3
m	-1026680	11	**I**	-1423091	15
g	-1026680	11	**A**	-1423091	15
k	-1026680	11	**J**	-1423091	16
a	-1026680	11	**N**	-1423091	16
n	-1026680	11	**H**	-1423090	16
h	-1026680	12	**L**	-1423071	35

Table 3-3 displays the ΔG^o_{rxn} values of the formation of radicals originated from JP-900. ΔG^o_{rxn} has been calculated as the difference between the G^o values of the products and the reactants at UB3LYP/6-31G(d,p) level. According to the $\Delta G^{\mathbf{o}}_{rxn}$ values indicated in Table 3-3, the formations of tertiary radicals "i and j" seem more probable when compared to other radicals. It is obvious that the secondary positions on both cyclohexane rings have similar tendencies for radical formation.

Table 3-3. ΔG^{o}_{rxn} values of the formation of radicals from JP-900 from the lowest to the highest (UB3LYP/6-31G(d,p)).

Label	ΔG_{rxn} (kj/mol)
i	1703
j	1703
d	1713
o	1713
c	1713
p	1713
e	1713
s	1713
f	1713
r	1713
l	1713
b	1713
m	1713
g	1714
k	1714
a	1714
n	1714
h	1714

Labeling of hydroperoxides has been accomplished in same method with radical labeling. Stability order is in the following manner: C=P > D=E=S > K=O > B=F=G=M=R > A=I > H=J=N > L (Table 3-2).

We have also designated "the most feasible carbon centers" by comparing the total electronic energies of the hydroperoxide molecules. These are carbons which are potent sites to be oxidized through hydroperoxidation. Carbon centers C_2 and C_9 are very susceptible to oxidation through hydroperoxidation because the corresponding hydroperoxides C and P are very low in total electronic energies (Table 3-2). The carbon center C_7 seems to be least feasible position for oxidation as a result of the highest total electronic energy of "Hydroperoxide L" when compared to others.

3.2.2. Decomposition of JP-900 Hydroperoxides

The hydroperoxides designed may decompose to different products having more negative total electronic energies. In this part of the study, we have investigated the decomposition of the three most stable hydroperoxides, namely "C" (decahydro-2-hydroperoxynaphthalene), "K" (decahydro-1-hydroperoxynaphthalene) and "I" (decahydro-4-hydroperoxynaphthalene). "C", "K" and "I" hydroperoxides are the isomeric structures, hydroperoxide-C has –OOH group at 2 position; hydroperoxide-K has –OOH group at 1 position and hydroperoxide-I has –OOH group at 4 position (see the nomenclature of hydroperoxides in Figure 3-4).

The previous decomposition mechanisms for JP-10 hydroperoxides have also been used in the present work, namely carboxylic acid (ester)-alkane, alcohol-aldehyde and alcohol-ketone mechanisms. The selection of these mechanisms is based on analytic information as well as the distribution of products formed from the oxidative cracking of hydroperoxides [111, 112, 116].

Currently, the decompositions of the most stable JP-900 hydroperoxides, labeled as "C", "K" and "I" have been inspected in the light of the suggested mechanisms revealed above. As seen from Table 3-4 and Figure 3-4, we have made total electronic energy as well as G^o calculations on these 10 different but isomeric products over DFT optimized structures (using B3LYP method and 6-31G(d,p) basis set). The total electronic energies were corrected for zero point vibrational energies (ZPE).

The hydroperoxide labeled as "C" is the most stable hydroperoxide of all. Note that it bears the hydroperoxy group on position-2 as its name implies. In Table 3-4, the total and the relative electronic energies of the decomposition products and the $\Delta G^{\mathbf{o}}_{rxn}$ values for the conversion of hydroperoxide "C" to the corresponding products are shown. $\Delta G^{\mathbf{o}}_{rxn}$ values have been calculated as the difference between the G^o values of the products and the reactants. The total electronic energy considerations of the final products and the $\Delta G^{\mathbf{o}}_{rxn}$ values for the conversion of hydroperoxide to the corresponding products have shown parallel trends.

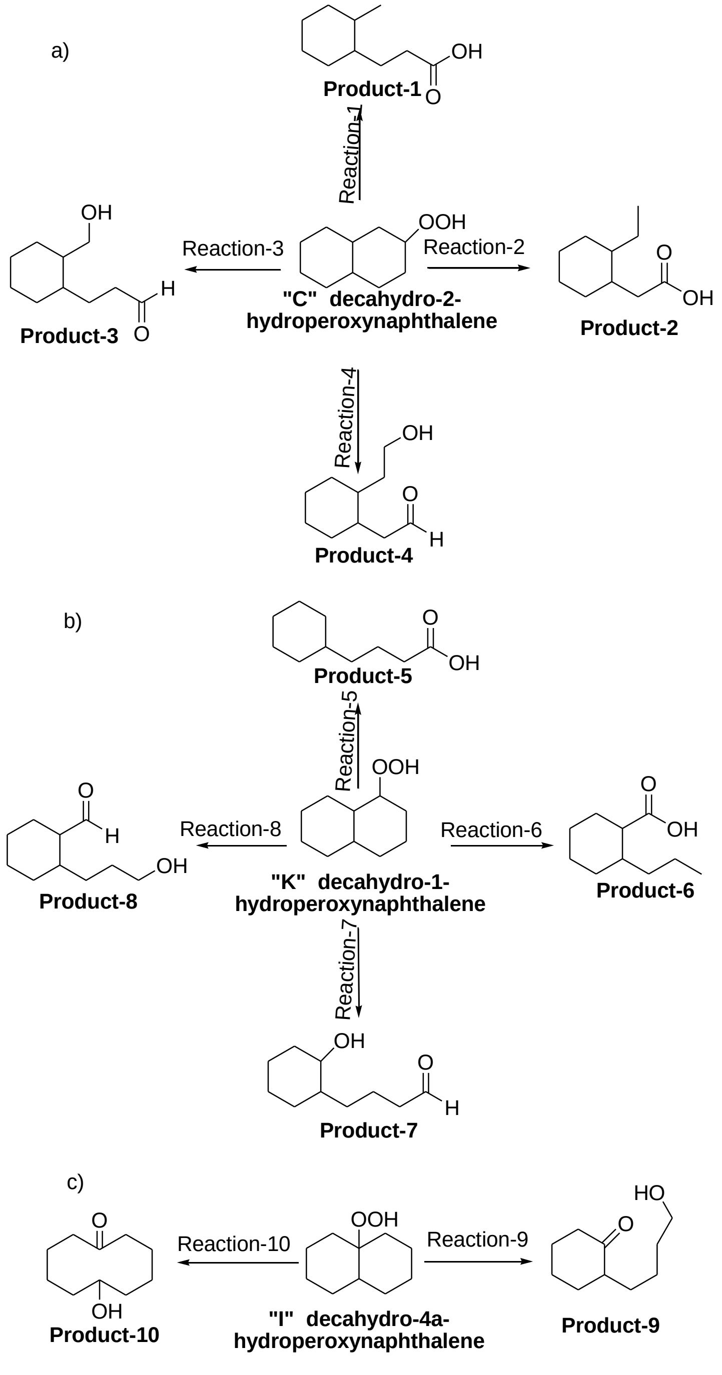

Figure 3-4. a)Decomposition of JP-900 “hydroperoxide-C’’. Products 1 and 2 belong to the carboxylic acid (ester)-alkane mechanism whereas products 3 and 4 belong to the alcohol–aldehyde mechanism. b) Decomposition of JP-900 “hydroperoxide-K’’. Products 5 and 6 belong to the carboxylic acid (ester)-alkane mechanism whereas products 7 and 8 belong to the alcohol–aldehyde mechanism. c) Decomposition of JP-900 "hydroperoxide-I’’. Products 9 and 10 belong to the ketone – alcohol mechanism.

Table 3-4. The total and the relative electronic energy values of ‘‘Hydroperoxide-C, K and I’’ and their decomposition products and ΔG_{rxn} values (from the lowest to the highest).

Label	**E_{total} (kJ/mol)**	**E_{rel} (kJ/mol)**	**ΔG_{rxn} (kJ/mol)**
Product-1	-1423397	0	-294
Product-2	-1423364	34	-259
Product-3	-1423272	126	-168
Product-4	-1423271	126	-168
Hydroperoxide-C	-1423106	291	-
Product-5	-1423381	0	-278
Product-6	-1423375	6	-271
Product-7	-1423299	82	-196
Product-8	-1423274	107	-171
Hydroperoxide-K	-1423104	277	-
Product-9	-1423291	0	-203
Product-10	-1423272	19	-183
Hydroperoxide-I	-1423091	200	-

Since Gibbs free energy change (ΔG^{o}_{rxn}) for the Reaction-1 (see Figure 3-4) is more negative than those of other reactions, Hydroperoxide-C favors the carboxylic acid (ester)-alkane decomposition mechanism thermodynamically. Besides, the total electronic energy of Product-1 is lower than those of the products 2-4 and the corresponding hydroperoxide. Therefore, Product-1, *3-(2-methylcyclohexyl)propanoic acid*, has been assigned to be the most reasonable decomposition product of this hydroperoxide, in terms of the thermodynamic considerations.

The hydroperoxide labeled as “K” is the most stable hydroperoxide bearing hydroperoxide group on position-1. In Table 3-4, the total electronic energies of the decomposition products and the ΔG^{o}_{rxn} values for the conversion of hydroperoxide “K” to the corresponding products are shown. Hydroperoxide-K molecule chooses the carboxylic acid (ester)-alkane decomposition mechanism (Reaction-5) due to the greatest Gibbs free energy change (ΔG^{o}_{rxn}) for Reaction-5 when compared to the others (Figure 3-4). Additionally, the total electronic energy of Product-5 is lower than those of both the other products and the corresponding hydroperoxide. Therefore, Product-5, *4-cyclohexylbutanoic acid*, has been found to be the most viable decomposition product of this hydroperoxide regarding the thermodynamic contemplations.

The hydroperoxide labeled as “I” is the most stable hydroperoxide bearing hydroperoxide group on position-4. Table 3-4 shows the total electronic energies of the decomposition products and the ΔG^{o}_{rxn} values for the conversion of hydroperoxide “I” to the corresponding products. Since Gibbs free energy change (ΔG^{o}_{rxn}) for the Reaction-9 (see Figure 3-4) is more negative than those of other reactions, Hydroperoxide-I molecule prefers the ketone-alcohol decomposition mechanism, contrary to Hydroperoxides C and K. Product-9, *2-(4-hydroxybutyl)cyclohexanone*, has been assigned to be the most feasible product of Hydroperoxide-I.

3.3. Conclusion

Presently, the stability of JP-900 ($C_{10}H_{18}$), *trans*-decalin, has been investigated. Oxidation of JP-900 through hydroperoxidation mechanism has been discussed based on Density Functional Theory (DFT) calculations as the hydroperoxide concentration has been found to be a factor in fuel instability.

Carbon center numbered as “2” (yields radical “c”) is found to be the most susceptible point to oxidation through hydroperoxidation to produce Hydroperoxide-C. Radical “c” is a thermodynamically energetic radical, and it may easily react with O_2 molecule and then abstract H. radical from any medium to form Hydreperoxide-C of good stability. On the other hand, radical “i” (the radical on carbon 5) is thermodynamically the most stable radical; the concentration of this radical is expected to be quite high in the medium. Therefore, one may assume to get more hydroperoxide product “I”; however, a different circumstance occurs. Hydroperoxide “I” is not stable enough to survive and undoubtedly either is produced in small amount or decomposes easily as a result of the thermodynamic instability of the molecule.

The decompositions of thermodynamically stable hydroperoxides C, K and I have also been studied. The calculations have shown that both the hydroperoxide-C and K prefer the carboxylic acid (ester)-alkane; whereas hydroperoxide-I favors the ketone-alcohol decomposition mechanism.

CHAPTER 4

DESENSITIZATION of TNAZ via STRUCTURAL MOLECULAR MODIFICATION and EXPLOSIVE PROPERTIES- A DFT STUDY

4.1. Introduction

Highly nitrated small ring heterocycles and carbocycles are interesting energetic materials due to their increased performance originating from the additional energy release (manifested as a higher heat of formation) upon opening of the strained ring system during decomposition. Nowadays, the most widely studied energetic small-ring compound is 1, 3, 3-trinitroazetidine, TNAZ [1]. It is a highly nitrated four membered nitrogen heterocyclic ring with improved performance in comparison to conventional melt castable explosive trinitrotoluene (TNT). The additional contribution of energy is expected from the strained ring system [124-129] There are more than 16 methods reported for the synthesis of 1,3,3-trinitroazetidine [130].

TNAZ, a high performance, melt castable explosive, has been proposed as potential replacement for TNT. The low melting point of TNAZ (101 ^{o}C) [131] enables processing of formulations on modified production lines. Its performance is approximately 30% greater than TNT. It shows excellent thermal stability (>180 ^{o}C) [132].

TNAZ has many added advantages over known explosives. It is a highly energetic material, more powerful than RDX, and is less vulnerable than most other nitramines [133]. Unlike HMX, TNAZ is soluble in molten TNT, and is compatible with aluminum, steel, brass and glass [134-136].

Desensitization of explosives is of great value in reducing their sensitivity in military use. One approach that is being tried toward these objectives is to use additives and coatings for explosives in which surfaces may play an important role. Many of the examples exist in the literature, especially on RDX [137].

Another approach would be to attempt some molecular level chemical changes in the explosive that bring the expected decrease in sensitivity without significant loss in power. TNAZ has three NO_2 groups. We thought that on converting the -NO_2 groups to -NO or -NH_2 groups (Figure 4-1), one might decrease the sensitivity as well as brisance values. Furthermore, an understanding of the trend in energetic properties in going from TNAZ to azetidine derivatives might reveal factors which can be used in altering the sensitivity of explosives, in general, via structural modification. Ballistic desensitization makes explosives much safer compared to their parents by preventing some accidental explosions triggered by various factors such as thermal or mechanical shock, static electric discharging, etc.

In the present study, some theoretical studies have been performed for TNAZ itself and fifteen different azetidine derivatives.

4.2. Results and Discussion

All the calculations have been done as expressed in section 1.3.5.

4.2.1. The Geometries

All the structures presently considered have been thought to be the potential candidates of explosives (Figure 4-1). The geometry optimizations of the structures in Figure 4-1 were done at the B3LYP/6-31G(d,p) level. The bond lengths for the geometry optimized structures are presented in Table 4-1. The numbering in Table 4-1 is consistent with the numbering manner in Figure 4-2. The corresponding experimental X-ray diffraction values of TNAZ [138] are also shown in Table 4-1. The compatibility of the experimental and theoretical values of the bond lengths for TNAZ and the absence of imaginary frequencies in the potential energy diagrams are indications of the successful geometry optimization of the molecules. This compatibility also guarantees that bond lengths of other azetidine derivatives are close to the real values. Note that there are no experimental data for the azetidine derivatives to the best of our knowledge.

On the whole, a comparison between the experimental and theoretical bond lengths shows that the calculated results are slightly longer than the experimental values. For example, the observed crystal structure of TNAZ has shorter N-NO_2 bonds by ca. 0.04 Å than the calculated values, and the experimental C-NO_2 bonds are shorter than the calculated results by about 0.02 Å. These minor inconsistencies are mainly due to the solid-state effect, i.e., intermolecular interactions. Such interactions are not represented in the DFT calculations [139].

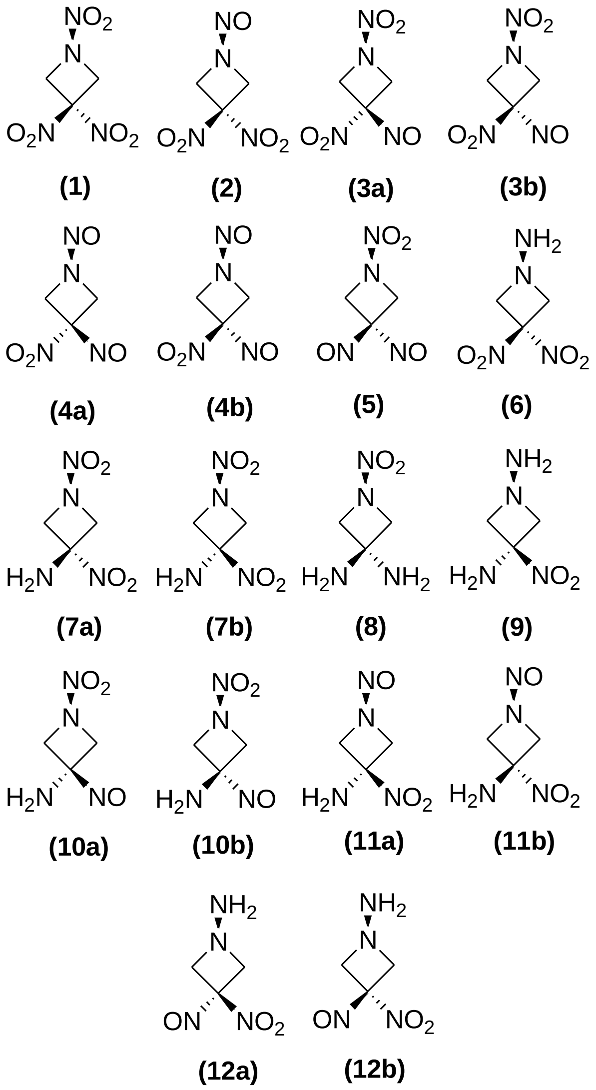

Figure 4-1. The Structures of TNAZ (1) and some azetidine derivatives

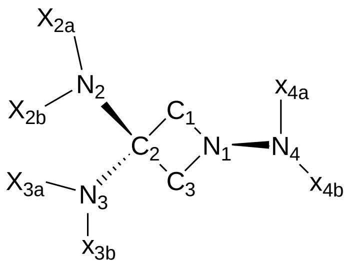

Figure 4-2. The numbering manner of TNAZ and azetidine derivatives

Table 4-1. The bond lengths (Å) of the geometry optimized TNAZ and azetidine derivatives calculated at the theoretical level of (DFT) B3LYP/6–31G(d.p)

	Bond Lengths in (Å)												
	TNAZ[a]	**1**	**2**	**3a**	**4a**	**5**	**6**	**7b**	**8**	**9**	**10a**	**11a**	**12b**
C_2 - N_2	1.501	1.523	1.524	1.538	1.523	1.507	1.519	1.547	1.447	1.573	1.529	1.568	1.508
N_2-X_{2a}	1.210	1.224	1.224	1.198	1.197	1.205	1.224	1.227	1.019	1.226	1.207	1.226	1.201
N_2-X_{2b}	1.212	1.219	1.219	-	-	-	1.221	1.227	1.019	1.228	-	1.225	-
C_2 - N_3	1.512	1.513	1.513	1.497	1.492	1.509	1.517	1.421	1.458	1.412	1.424	1.410	1.500
N_3-X_{3a}	1.212	1.223	1.223	1.226	1.227	1.204	1.223	1.016	1.019	1.016	1.018	1.016	1.227
N_3-X_{3b}	1.212	1.222	1.222	1.225	1.226	-	1.224	1.016	1.019	1.016	1.018	1.016	1.227
N_1 - N_4	1.356	1.397	1.347	1.396	1.343	1.394	1.464	1.389	1.381	1.468	1.385	1.337	1.464
N_4-X_{4a}	1.221	1.225	1.221	1.225	1.223	1.228	1.023	1.227	1.229	1.024	1.228	1.226	1.023
N_4-X_{4b}	1.224	1.225	-	1.226	-	1.225	1.023	1.227	1.230	1.023	1.228	-	1.023
C_1 – C_2	1.538	1.543	1.545	1.532	1.548	1.566	1.533	1.547	1.561	1.544	1.559	1.559	1.538
C_3 – C_2	1.534	1.542	1.545	1.551	1.547	1.534	1.533	1.545	1.572	1.544	1.561	1.556	1.539
C_1 - N_1	1.472	1.481	1.475	1.483	1.474	1.475	1.487	1.479	1.477	1.486	1.474	1.469	1.484
C_3 - N_1	1.473	1.481	1.477	1.478	1.477	1.482	1.487	1.480	1.475	1.487	1.474	1.472	1.486

[a] Experimental values at 298 K reported in ref. [138]. All molecules possess C_1 point group. Only the most stable isomers are included.

4.2.2. Relative Total Energies

In Table 4-2, the corrected absolute and relative total energies of the geometry optimized compounds calculated at the theoretical level of B3LYP/6-31G(d,p) are shown. When Table 4-2 is considered, it is obvious that compounds 3a, 4a, 7b, 11a and 12b are more stable than their stereoisomers 3b, 4b, 7a, 11b and 12a. The structures 10a and 10b are equal in energy. (See Figure 4-1 for structures).

It is essential to compare the energies of the isomeric structures in the evaluation of the stabilities. There are 5 different isomer groups on the basis of substituent groups. Note that 2, 3a, 3b (having 2 nitro and 1 nitroso groups); 4a, 4b, 5 (having 1 nitro and 2 nitroso groups); 6, 7a, 7b (2 nitro and 1 amino bearing isomeric group); 8, 9 (having 1 nitro and 2 amino groups); and 10a, 10b, 11a, 11b, 12a, 12b (possessing 1 nitro, 1 amino and 1 nitroso group) are isomers. It can be inferred from Table 4-2 that 2, 5, 7b, 8 and 11a seem to be the most stable in their corresponding isomer groups. Since the total electronic energies of 3a, 4a, 10a, 11a, 7b and 12b are less than 3b, 4b, 10b, 11b, 7a and 12a (see Table 4-2), we continued the calculations with these less energetic molecules.

Table 4-2. The calculated (corrected) absolute and relative total energies of TNAZ and azetidine derivatives at (DFT) B3LYP/6–31G(d,p) theoretical level.

Compound	E_{total} (kj/mol)	E_{rel}
1	-2065237	0
2	-1867847	197390
3a	-1867801	197436
3b	-1867799	197438
7b	-1673680	391557
7a	-1673669	391568
6	-1673570	391667
5	-1670411	394826
4a	-1670409	394828
4b	-1670351	394886
11a	-1476294	588943
11b	-1476257	588980
10a	-1476226	589011
10b	-1476226	589011
12b	-1476131	589106
12a	-1476128	589109
8	-1282065	783172
9	-1282003	783234

4.2.3. Bond Dissociation Energies (BDE)

In the present study, in order to compare the C-NO_2 and N–NO_2 bond strengths of the compounds, homolytic bond dissociation energy (BDE) calculations for the removal of nitrogen dioxide moiety from the structures were performed at UB3LYP/6-31G(d,p) level of theory as stated in Section 1.3.5. BSSE has also been performed.

The sensitivity behavior of an energetic material under different heat, impact, friction conditions may vary. In the present study, the “sensitivity” term denotes the “impact sensitivity” of a considered energetic material. Impact sensitivities of energetic compounds can be determined experimentally by physical tests, especially by drop height test. Moreover, there are theoretical approaches for the computational determination of impact sensitivity. Murray et al. [143] have indicated that there is a relationship between the BDEs of the N–NO_2 and C–NO_2 trigger linkages and the electrostatic potentials on the molecular surfaces of some energetic molecules. There are various valuable studies in the literature [140, 144-147] on the homolytic BDE of the nitro compounds such as nitroaromatic and nitramine molecules, which have revealed that there is a parallel correlation between the BDE for the weakest R–NO_2 bond scission in the molecule and its sensitivity. The usual trend is that the larger the homolytic BDE value for scission of R–NO_2 or C-NO_2 bond, the lower the sensitivity is.

Desensitization of explosives is a hot topic in military use. Our approach in the current study is to attempt small structural changes in the explosive that bring the expected decrease in sensitivity without significant loss in power. TNAZ has three -NO_2 groups. We thought that on converting the -NO_2 groups to -NO or -NH_2 groups, one might decrease the sensitivity. To visualize the effect, we attributed the lowest sensitivity to the highest N-NO_2 and C-NO_2 BDEs. Furthermore, an understanding of the trend of energetic properties in going from TNAZ to azetidine derivatives might reveal the factors which can be used in altering the sensitivity of explosives, in general, via structural modification. Table 4-3 indicates BDE values. The consistency of our BDE values and the literature data (available for some of the compounds) [148-149] increases the reliability of the method employed in the present article.

Table 4-3. The homolytic bond dissociation energies (BDE) of $C-NO_2$ and $N-NO_2$ bonds of TNAZ and azetidine derivatives calculated at (DFT) UB3LYP/6–31G(d.p) theoretical level.

	BDE (kJ/mol)		
	$C_{(2)}$ - $N_{(2)}O_2$	**$C_{(2)}$-$N_{(3)}O_2$**	**$N_{(1)}$-$N_{(4)}O_2$**
1	165.23 (167)*	165.23	160.22 (162.8)*
2	163.85	163.81	-
3a	-	62.29	163.1
4a	62.85	-	-
5	-	-	167.02
6	166.48	166.48	-
7b	186.1	-	155.82
8	-	-	181.36
9	211.82	-	-
10a	-	-	173.14
11a	198.31	-	-
12b		231.65	

*Data in parenthesis are the literature values taken from ref. [148] for BDE of $C-NO_2$ bond of TNAZ and ref. [149] for BDE of $N-NO_2$ bond of TNAZ. Numbers in parenthesis below the element symbols indicate the positions. Only the most stable isomers are considered.

We have designated the smallest BDE of the molecules and compared them with those of other molecules. When the nitro (NO_2) group on N_1 atom of TNAZ is replaced with nitroso (NO) group (compound-2), the difference between the smallest BDEs becomes 3.59 kJ/mol. This extra energy resulted in desensitization of TNAZ. However, the conversion of nitro (NO_2) group on C_2 atom of TNAZ in the same manner (compound 3a), drops the BDE dramatically to 62.29 kJ/mol. The molecule becomes more sensitive. We thought that this drop is due to the instability of isomer (compound-3a) when compared with the isomers in its group (2 nitro and 1 nitroso groups having isomer group).

When both nitro groups on C_2 of TNAZ are replaced with nitroso groups (compound-5), the difference between the smallest BDEs becomes 6.80 kJ/mol, which supports the idea of desensitization. However, conversion of TNAZ into compound 4a results in sensitization of TNAZ. This is again due to the instability of compound 4a in its isomer group (1 nitro and 2 nitroso groups bearing isomer group).

Conversion of the nitro group on N_1 of TNAZ into amino group (NH_2) (compound-6) results in a difference of 6.26 kJ/mol between the smallest BDEs. Conversion of nitro group on C_4 atom into amino group (compound-7b) does not decrease the BDE dramatically. This conversion is not useful for desensitization.

Alteration of both nitro groups on C_2 with amino groups (compound-8) and conversion of one of the nitro group on C_2 and other nitro group on N_1 with amino groups increases BDE tremendously. Thus, this type molecular structural modification seems to be beneficial for desensitization purpose.

Stereochemically variable introduction of one nitroso and one amino groups into TNAZ accomplishes compounds 10a, 11a and 12b (each one having one nitro, one nitroso and one amino groups). All the conversions lead to a remarkable rise in BDEs, accordingly an effective decrease in sensitivity is expected theoretically. Such type of variation of functional groups of TNAZ is very advantageous for depressing sensitivity.

In conclusion, introduction of an amino group into TNAZ desensitizes more as compared to the introduction of nitroso group. Additionally, replacement of two of the nitro groups with nitroso groups produces the same effect with the replacement of one nitro group with an amino group.

4.2.4. The Frontier Molecular Orbitals

Mulliken electro negativities (χ_M) and chemical hardness (η) are significant assets in mirroring chemical reactivity of compounds. The χ_M and η values are calculated according to formulas given:

$$\chi_M = (I+A)/2 \qquad \textbf{(9)}$$

$$\eta = (I-A)/2 \qquad \textbf{(10)}$$

where I and A are the ionization potential and electron affinity, respectively [150]. Note that $I = -\varepsilon_{HOMO}$ and $A = -\varepsilon_{LUMO}$ within the rationality of the Koopmans' theorem [151] The HOMO, LUMO, $\Delta\varepsilon$ energies ($\Delta\varepsilon = \varepsilon_{LUMO} - \varepsilon_{HOMO}$), Mulliken electro negativities (χ_M) and chemical hardnesses (η) of TNAZ and other azetidine derivatives calculated at HF/6–31G(d,p)//B3LYP/6–31G(d,p) theoretical level are shown in Table 4-4. Hartree-Fock is preferred over DFT in the frontier molecular orbital calculations due to the absence of Hartree-Fock type orbital concept in DFT [152].

χ_M values indicates Mulliken electro negativities. The more electronegative the compound is (the higher the χ_M value), the less susceptible to oxidations than the others. It is essential to evaluate the χ_M values of the isomeric structures. TNAZ (1) is the most electronegative of all; therefore it is less susceptible to oxidation when compared to others. The χ_M trend of the compounds shows partial parallelism with the total electronic energies. Generally, the most stable isomers in the corresponding isomer groups are more electronegative than the other group members, except for 3 and 10a.

The chemical hardness (η) value of a compound expresses the kinetic stability of the corresponding compound [153-163] and it is acknowledged that the harder compounds show higher kinetic stability.[41] The chemical hardness values of the questioned compounds are between 6 and 7b. TNAZ, the thermodynamically most stable of all, shows also good kinetic stability [153]. The highest value belongs to compound 8. It is the kinetically most stable one; whereas it shows very poor thermodynamic stability (Table 4-4).

Table 4-4. The HOMO, LUMO, Δε energies ($\Delta\varepsilon = \varepsilon_{LUMO} - \varepsilon_{HOMO}$), Mulliken electronegativities (χ_M) and chemical hardnesses (η) values of TNAZ and azetidine derivatives calculated at HF/6–31G(d.p)//B3LYP/6–31G(d.p) theoretical level.

	E_{HOMO} (eV)	E_{LUMO} (eV)	Δε	χ_m	η
1	-13.03	0.99	14.02	6.02	7.01
2	-11.95	1.13	13.08	5.41	6.54
3a	-12.35	0.81	13.16	5.77	6.58
4a	-11.65	1.68	13.33	4.99	6.67
5	-11.98	1.06	13.04	5.46	6.52
6	-10.54	1.67	12.21	4.44	6.11
7b	-12.15	2.00	14.15	5.08	7.08
8	-11.22	3.17	14.39	4.03	7.20
9	-9.78	2.70	12.48	3.54	6.24
10a	-11.11	2.10	13.21	4.51	6.61
11a	-11.16	2.20	13.36	4.48	6.68
12b	-10.29	1.84	12.18	4.23	6.07

4.2.5. Explosive Properties

Explosive outcomes of energetic materials can be evaluated by the determination of the ballistic properties, namely detonation velocity (D) and detonation pressure (P). The empirical Kamlet-Jacobs [38-53] equations are employed for the calculations of these properties.

TNAZ ($C_3H_4O_6N_4$) and other azetidine derivatives are in accordance with $2a+b/2>c\geq b/2$ parameters. Therefore relations belonging to that set of parameters are employed in the calculations. The predicted densities and detonation properties of TNAZ and other azetidine derivatives are listed in Table 4-5. It also includes experimental and theoretical performance values of TNT [165], RDX [21, 164-167] and HMX [21, 167] taken from the literature.

The detonation velocity and pressure values for TNAZ are in accordance with the literature data [180-181].When Table 4-5 is considered, it is obvious that the performance of TNAZ lies between well-known explosives HMX and RDX and is better in usage than its alternate, TNT.

The performances of TNAZ and other azetidine derivatives are in the following manner: TNAZ (1) >2> 3a> 5> 7b> 4a> 6> 12b> 10a> 11a> 9> 8> TNT. The results show that the more nitro groups the compounds have, the better the ballistic properties are. TNAZ has the highest detonation properties as we expected.

Replacement of nitro groups with nitroso groups (on going from TNAZ to compounds 2, 3, 4a and 5) slightly decreases ballistic properties. Whereas, amino group replacements (from TNAZ to compounds 6, 7b, 8 and 9) decreases detonation velocity and pressure more. The compounds 10a, 11a and 12b have one nitro, one nitroso and one amino group. These isomers (10a, 11a and 12b) are better in performance and the most insensitive isomer groups in the present study.

4.2.6. Detonation Products

The detonation of a $C_aH_bO_cN_d$ type explosive will result in the formation of smaller molecules, i.e., CO_2, CO, H_2O, etc. In order to clarify the decomposition products, a set of rules was developed by Kistiakowsky and Wilson [29-30]. Table 4-6 shows the number of moles of detonation products of the compounds questioned in the present study.

Table 4-5. Predicted densities and detonation properties of TNAZ and azetidine derivatives at the theoretical level of B3LYP/6–31G(d,p).

Compound	**Ω (%)**	ΔH^{o}_{f} ^{a} **(kJ/mol)**	***Q*** **(kJ/g)**	V^{b} **(cm^3/mol)**	***ρ*** **(g/cm3)**	***D*** **(km/s)**	***P*** **(GPa)**
1 (TNAZ)	-16.67	127.46 (125.05)	1740.43	109.275	1.773 (1.76)	8.92 (8.68)	34.97 (35.68)
2	-27.27	189.02	1715.06	101.649	1.754	8.73	33.25
3a	-27.27	202.39	1733.22	103.962	1.711	8.60	31.80
4a	-40.00	266.20	1707.95	98.491	1.645	8.23	28.40
5	-40.00	293.05	1748.05	96.256	1.688	8.42	30.25
6	-49.38	171.56	1613.76	99.078	1.653	8.22	28.44
7b	-49.38	123.82	1543.32	97.333	1.688	8.25	29.01
8	-96.97	115.44	1084.77	92.112	1.450	7.13	19.62
9	-96.97	175.71	1193.9	91.638	1.459	7.33	20.84
10a	-65.75	209.41	1530.48	92.065	1.606	7.82	25.25
11a	-65.75	183.76	1488.49	92.607	1.592	7.72	24.47
12b	-65.75	252.54	1601.07	93.129	1.589	7.85	25.28
TNT	-73.98	53.12	1417.5	137.32	1.64	6.95	19.00
RDX	-21.61	168.90	1597.39	124.920	1.78	8.88 (8.75)	34.75 (34.70)
HMX	-21.61	270.41	1633.88	157.530	1.88	9.28 (9.10)	39.21 (39.30)

[a] Gas phase standard heat of formation values obtained from the PM3 single point calculations over B3LYP/6–31G(d,p) geometry optimized structures. [b] Average molar volumes from 100−single point calculations at the B3LYP/6–31G(d,p) level.Data in parenthesis are the experimental values taken from ref. [168] for ΔH^{o}_{f} of TNAZ, ref. [169] for density of TNAZ, ref.[170] for detonation velocity of TNAZ, ref.[171] for detonation pressure of TNAZ, ref.[165] for TNT, refs.[21, 164-167] for RDX and refs.[21, 167] for HMX.

Table 4-6. Gaseous decomposition products of TNAZ and other azetidine derivatives using the Kistiakowsky and Wilson Rules

		Number of moles of detonation products						Total
	Formula	N_2	H_2O	CO	CO_2	H_2	C	
1	$C_3H_4N_4O_6$	2	2	2	1	-	-	7
2	$C_3H_4N_4O_5$	2	2	3	-	-	-	7
3a	$C_3H_4N_4O_5$							
4a	$C_3H_4N_4O_4$	2	2	2	-	-	1	7
5	$C_3H_4N_4O_4$							
6	$C_3H_6N_4O_4$	2	3	1	-	-	2	8
7b	$C_3H_6N_4O_4$							
8	$C_3H_8N_4O_2$	2	2	-	-	2	3	9
9	$C_3H_8N_4O_2$							
10a	$C_3H_6N_4O_3$	2	3	-	-	-	3	8
11a	$C_3H_6N_4O_3$							
12b	$C_3H_6N_4O_3$							
Picric Acid	$C_6H_3N_3O_7$	3/2	3/2	11/2	-	-	1/2	9
TNT	$C_7H_5N_3O_6$	3/2	5/2	7/2	-	-	7/2	11
RDX	$C_3H_6N_6O_6$	3	3	3	-	-	-	9
HMX	$C_4H_8N_8O_8$	4	4	4	-	-	-	12

When total amount of gas produced upon detonation is considered, the compounds 8 and 9 seem to be the most gas releasing ones. These compounds produce as much gas as well-known explosives Picric Acid and RDX. The next group of compounds producing less gas upon detonation contain 5, 6, 10a, 11a and 12b. TNAZ produces the least amount of gas upon detonation.

The most hazardous detonation product is carbon monoxide (CO). It is a colorless, odorless poisonous gas that is extremely harmful to human health. Compounds 2 and 3 produce 3 moles of carbon monoxide upon detonation. TNAZ, compounds 4 and 5 produce 2 moles whence compounds 6 and 7 only produce 1 mole of carbon monoxide. TNAZ is the only compound that produces CO_2 upon detonation.

Compounds 8, 9, 10, 11 and 12 seem to be the most environments friendly when detonation products of other azetidine derivatives are considered. TNAZ and other derivatives produce less CO when compared to those of Picric Acid, TNT, RDX and HMX. It is appropriate to consider TNAZ as an environment friendly explosive in terms of detonation products.

4.2.7. Explosive Power and Power Index

Heat and gases are released in an explosive reaction. The volume of gas produced will provide information on the amount of work done by the explosive. Standard conditions must be established in order to measure the volume of generated gas, since the volume of gas varies according to the temperature. The standard conditions (273 K, 1atm) also enable one to make comparisons between different explosives. Division of the value of total volume of gas produced upon detonation by the molecular weight gives an idea of how much gas is released per gram of explosive. Explosive power and power index have been calculated as stated in section 1.2.2.5.

Table 4-7 shows the power index values of TNAZ, azetidine derivatives, Picric Acid, TNT, RDX and HMX. The power index values of TNAZ and other azetidine derivatives are between 118 – 163% and in the following manner: 12b> 10a> 11a> 9> 6> HMX> 5> 7b> 4a> 8> 3a> TNT> 2> HMX> RDX> TNAZ (1)> Picric Acid. The results show that TNAZ is as favorable as RDX and HMX in terms of power index. The compounds 10a, 11a and 12b having one nitro, one nitroso and one amino group have the highest power index value of all.

Table 4-7. The power index values of TNAZ, azetidine derivatives, Picric Acid, TNT, RDX and HMX

Compound	Q (kJ/g)	V(dm^3/g)	QxV	Power Index %
TNAZ (1)	1740.43	0.817	1421.35	118
2	1715.06	0.891	1527.96	126
3a	1733.22	0.891	1544.14	128
4a	1707.95	0.980	1673.80	139
5	1748.05	0.980	1713.09	142
6	1613.76	1.106	1785.09	148
7b	1543.32	1.106	1707.18	141
8	1084.77	1.527	1656.75	137
9	1193.90	1.527	1823.42	151
10a	1530.48	1.227	1878.50	155
11a	1488.49	1.227	1826.97	151
12b	1601.07	1.227	1965.15	163
Picric Acid	1372.86	0.880	1208.07	100
TNT	1417.54	1.085	1538.69	127
RDX	1598.39	0.908	1450.86	120
HMX	1634.89	0.908	1484.66	123

4.3. Conclusion

Presently, theoretical studies have been performed on TNAZ itself and fifteen different azetidine derivatives. The corrected absolute and relative total energies of the geometry optimized structures have been calculated at the theoretical level of B3LYP/6-31G(d,p). We have correlated the bond dissociation energies with sensitivity. TNAZ has three NO_2 groups. We have proved that by converting the nitro groups to nitroso and amino groups, it is possible to decrease the sensitivity without significant loss in power. The introduction of an amino group into TNAZ desensitizes the molecule more when compared to the introduction of nitroso group. Besides, replacement of two of the nitro groups with nitroso groups makes the same effect with the replacement of one nitro group with an amino group. It is obvious that as the number of amino group increases, BDE values also increases, consequently sensitivity decreases. As for explosive effects, replacement of nitro groups with nitroso groups (on going from TNAZ to compounds 2-5) slightly decreases ballistic properties. Whereas, amino group replacements (from TNAZ to compounds 6, 7b, 8 and 9) decrease detonation velocity and pressure more. Compounds 8-12 seem to be the most environment friendly when detonation products of all azetidine derivatives are considered. Note that the compounds 10a, 11a and 12b have one nitro, one nitroso and one amino group. These isomers not only have the highest power index values but also are optimum structures in performance and the most insensitive isomer group in the present study. TNAZ is as favorable as RDX and HMX in terms of power index. All the compounds investigated showed better ballistic properties than TNT. They are all potential candidates for insensitive high explosives. They are all alternative to TNT whenever lower sensitivity is required. We have proved that molecular modification is a functioning method in both desensitization of TNAZ and reduction of its explosive effects.

CHAPTER 5

PREDICTION of EXPLOSIVE PERFORMANCE PROPERTIES OF z-DBBD and ITS ISOMERS by QUANTUM CHEMICAL COMPUTATIONS - A DFT STUDY

5.1. Introduction

Recently, experts in organic materials focus on compounds having large content of nitrogen and low content of hydrogen. Such compounds attract theoretical as well as practical attention. They are employed not only in traditional fields where high-energy substances are required (propellants, explosives, etc.), but also for some other purposes, e.g. gas-generating substances or components of pyrophobic compositions [172]. If the target compounds are employed as components of energetic compositions, they should have favorable detonation and/or combustion properties, which depend on the enthalpy of formation (or enthalpy of combustion) and molecular crystal density [35-41].

One of the most interesting energetic skeleton rich in nitrogen, low in hydrogen is dibenzo-tetraazapentalene [173]. It is a planar system with six electrons delocalized over four nitrogen atoms [174-175]. The high temperature environment of guided missiles, especially which created by long-time aerodynamic heating due to carrying by supersonic aircraft, has stimulated a demand for high explosives which have superior ability to withstand such an environment [176]. TACOT (2, 4, 8, 10-tetranitrobenzotriazolo [2, 1-a] benzotriazol-6-ium inner salt) ($C_{12}H_4N_8O_8$) (see Figure 5-1), which was first discovered by chemists at DuPont, is a product of this necessity [177-178].

TACOT has been developed as insensitive energetic material for a variety of engineering and military applications. It has favorable insensitivity to heat, impact, and electric shock. The density and ballistic properties (detonation velocity, detonation pressure) of TACOT is inferior to those observed for the explosives RDX and HMX [13]. It finds extensive use in applications where high temperature resistance is needed. It is available commercially in the form of flexible linear shaped charges (FLSC), plastic bonded explosive (PBX), high-density charges, and in mild detonating fuse. TACOT is also reported to be used in the manufacture of high-temperature resistant detonators [21].

Due to excellent characteristic properties of TACOT, we decided to conduct our search for new high explosives with a high energy content, superior crystal density and reasonable stability among substances whose molecules are similar to TACOT from the structural point of view. Therefore, a sequence of molecules (TACOT, z-DBBD (4,11-dinitro[1,2,5]-oxadiazolo[3,4-e] [1,2,5]oxadiazolo[3’,4’:4,5] benzotriazolo- [2,1-a] benzotriazol-6-ium inner salt 1,8-dioxide) and its three hypothetical isomers, see Figure 5-1) that possess the tetraazapentalene core have been considered in the present study.

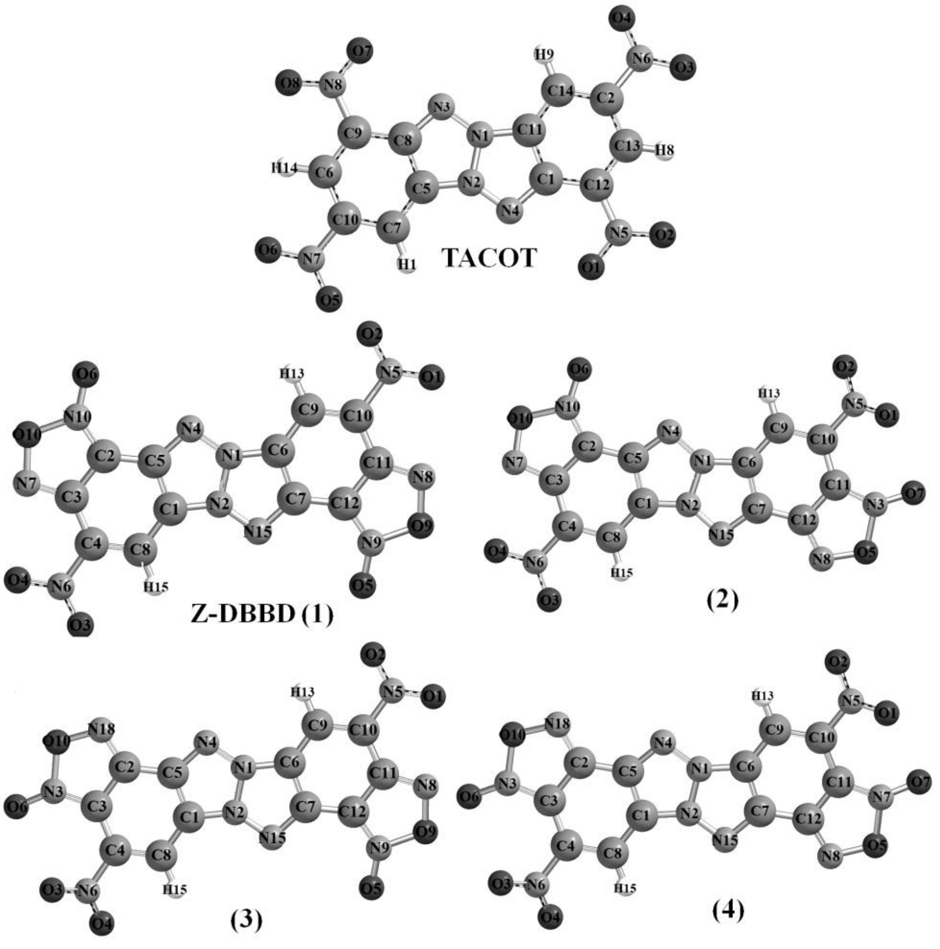

Figure 5-1. The geometry optimized structures of TACOT, z-DBBD and its three isomers.

5.2. Results and Discussion

All the calculations have been done as expressed in section 1.3.5.

5.2.1. The Geometries

All the structures currently studied have been deliberated as the potential candidates of high explosives (Figure 5-1). The geometry optimizations of the structures shown in Figure

5-1 were done at the B3LYP/6-31G(d,p) level. The bond lengths for the geometry optimized structures are presented in Table 5-1.

The experimental X-ray diffraction [179] and calculated bond length values of TACOT are also shown in Table 5-1. The similarity of the experimental and theoretical values of the bond lengths for TACOT indicates the successful geometry optimization of the molecules at the used level of calculations. This compatibility also assurances that bond lengths of *z*-DBBD and its isomers are close to the actual values. Note that there are no experimental X-ray data for *z*-DBBD to the best of our knowledge.

Table 5-1. The bond lengths (Å) of the geometry optimized TACOT, z-DBBD and its three isomers calculated at the theoretical level of B3LYP/6–31G(d,p).

Bond Lengths in (Å)										
BOND	**TACOT**[a]	**TACOT**	**BOND**	**1**	**BOND**	**2**	**BOND**	**3**	**BOND**	**4**
C5-C8	1.411	1.437	**C2-C5**	1.421	**C2-C5**	1.422	**C1-C5**	1.416	**C1-C5**	1.416
C8-C9	1.417	1.422	**C3-C2**	1.434	**C3-C2**	1.434	**C2-C5**	1.437	**C2-C5**	1.437
C9-C6	1.364	1.379	**C4-C3**	1.449	**C4-C3**	1.449	**C3-C2**	1.436	**C3-C2**	1.436
C6-C10	1.388	1.408	**C4-C8**	1.371	**C4-C8**	1.371	**C2-N18**	1.313	**C2-N18**	1.313
C10-C7	1.379	1.385	**C4-N6**	1.462	**C4-N6**	1.460	**N18-O10**	1.355	**N18-O10**	1.355
C7-C5	1.385	1.389	**N6-O4**	1.227	**N6-O4**	1.227	**O10-N3**	1.480	**O10-N3**	1.480
C8-N3	1.360	1.354	**N6-O3**	1.232	**N6-O3**	1.233	**N3-O6**	1.209	**N3-O6**	1.209
C5-N2	1.380	1.371	**C8-C1**	1.411	**C8-C1**	1.410	**N3-C3**	1.347	**N3-C3**	1.348
N3-N1	1.341	1.336	**C1-C5**	1.420	**C1-C5**	1.420	**C4-C3**	1.438	**C4-C3**	1.438
N1-N2	1.361	1.367	**C2-N10**	1.337	**C2-N10**	1.337	**C4-N6**	1.465	**C4-N6**	1.464
N2-N4	1.341	1.336	**C3-N7**	1.322	**C3-N7**	1.322	**N6-O3**	1.227	**N6-O3**	1.227
C11-N1	1.380	1.371	**N7-O10**	1.366	**N7-O10**	1.367	**N6-O4**	1.230	**N6-O4**	1.231
C1-N4	1.360	1.354	**O10-N10**	1.459	**O10-N10**	1.458	**C4-C8**	1.370	**C4-C8**	1.370
C1-C12	1.417	1.422	**N10-O6**	1.214	**N10-O6**	1.214	**C8-C1**	1.415	**C8-C1**	1.416
C12-C13	1.364	1.379	**C5-N4**	1.347	**C5-N4**	1.346	**C5-N4**	1.347	**C5-N4**	1.347
C13-C2	1.388	1.408	**N4-N1**	1.337	**N4-N1**	1.339	**C1-N2**	1.368	**C1-N2**	1.369
C2-C14	1.379	1.385	**N1-N2**	1.377	**N1-N2**	1.378	**N4-N1**	1.332	**N4-N1**	1.334
C14-C11	1.385	1.389	**N2-N15**	1.337	**N2-N15**	1.332	**N1-N2**	1.378	**N1-N2**	1.379

Table 5-1 **continued**

Bond Lengths in (Å)										
BOND	**TACOT**[a]	**TACOT**	**BOND**	**1**	**BOND**	**2**	**BOND**	**3**	**BOND**	**4**
C11-C1	1.411	1.438	**C1-N2**	1.369	**C1-N2**	1.371	**N2-N15**	1.339	**N2-N15**	1.334
C10-N7	1.461	1.471	**N1-C6**	1.369	**N1-C6**	1.367	**N15-C7**	1.346	**N15-C7**	1.347
N7-06	1.225	1.228	**N15-C7**	1.347	**N15-C7**	1.348	**N1-C6**	1.371	**N1-C6**	1.369
N7-05	1.222	1.230	**C6-C7**	1.420	**C6-C7**	1.416	**C6-C7**	1.420	**C6-C7**	1.416
C9-N8	1.459	1.468	**C6-C9**	1.411	**C6-C9**	1.414	**C7-C12**	1.422	**C7-C12**	1.437
N8-07	1.226	1.227	**C9-C10**	1.371	**C9-C10**	1.370	**C12-C11**	1.434	**C12-C11**	1.437
N8-08	1.227	1.230	**C10-N5**	1.462	**C10-N5**	1.465	**C12-N9**	1.337	**C12-N8**	1.313
C2-N6	1.461	1.472	**N5-O1**	1.227	**N5-O1**	1.227	**N9-O5**	1.214	**N8-O5**	1.355
N6-03	1.222	1.228	**N5-O2**	1.232	**N5-O2**	1.230	**N9-O9**	1.459	**N7-O5**	1.479
N6-04	1.225	1.229	**C10-C11**	1.449	**C10-C11**	1.438	**O9-N8**	1.366	**O7-N7**	1.209
C12-N5	1.459	1.468	**C11-C12**	1.434	**C11-C12**	1.436	**N8-C11**	1.322	**N7-C11**	1.348
N5-O1	1.227	1.227	**C7-C12**	1.421	**C7-C12**	1.437	**C11-C10**	1.449	**C11-C10**	1.438
N5-O2	1.226	1.230	**C12-N9**	1.337	**C12-N8**	1.313	**C10-N5**	1.460	**C10-N5**	1.464
-	-	-	**C11-N8**	1.322	**C11-N3**	1.347	**N5-O2**	1.233	**N5-O2**	1.230
-	-	-	**N8-O9**	1.366	**N8-O5**	1.355	**N5-01**	1.227	**N5-01**	1.227
-	-	-	**N9-O9**	1.459	**O5-N3**	1.48	**C10-C9**	1.371	**C10-C9**	1.371
-	-	-	**N9-O5**	1.214	**N3-O7**	1.209	**C9-C6**	1.410	**C9-C6**	1.413

[a] Experimental values at 298 K reported in ref. [179]. All molecules possess C_1 point group.

On the whole, a comparison between the experimental and theoretical bond lengths of TACOT shows that the calculated results are slightly greater than the experimental values. Note that our calculated results are for gas phase, the experimental data are for solid state. Though the bond lengths in Table 5-1 appear to be sufficiently comparable with the experimental results, one possible source of discrepancy is the inadequate modeling of dispersion forces in most forms of DFT. Other reason is due to the solid-state effect, i.e., intermolecular interactions. Such interactions are not considered in the DFT calculations [49].

5.2.2. Relative Total Energies

Zero point (ZPE) and zero point corrected total electronic energies (B3LYP/6-31G(d,p)) of the compounds presently considered are given in Table 5-2. It is well known that the lower the total electronic energy, the more stable the compound. Among the *z*-DBBD isomers, the most stable structure is computed to be 1 (*z*-DBBD) due to the lowest total electronic energy. The stability order is 1> 3~ 2> 4. When total energy values for structures 1-4 are compared, stability order of 1>2=3>4 is obtained. It is obvious from Table 5-2 that position and orientation of furoxan ring influence the energy of the molecules.

Table 5-2. Calculated ZPE and total energies (zero point corrected) of z-DBBD and its three isomers at (DFT) B3LYP/6–31G(d,p) theoretical level (Energies in kJ/mol).

	Formula	ZPE	E_{total}
1	$C_{12}H_2N_{10}O_8$	465.27	-4219201.08
2		465.34	-4219191.22
3		465.28	-4219191.26
4		465.22	-4219181.00
TACOT	$C_{12}H_4N_8O_8$	499.61	-3935138.08

5.2.3. Bond Dissociation Energies (BDE)

In the present study, in order to compare the C-NO_2 and N–NO_2 bond strengths of the compounds, homolytic bond dissociation energy (BDE) calculations for the removal of nitrogen dioxide moiety from the structures were performed at UB3LYP/6-31G(d,p) level of theory as stated in Section 1.3.5. BSSE has also been performed.

Table 5-3 represents BDE values for the nitro bonds of the compounds investigated in the present study. Note that C2-NO_2 bond of TACOT and C10-NO_2 bond of the isomers, and

C10-NO_2 bond of TACOT and the C4-NO_2 bonds are similar. Chung et al. [50] suggest that a molecule should have more than 20.00 kcal/mol (83.74 kJ/mol) dissociation energy to be considered as a feasible candidate for high energy density material (HEDM). It is obvious from Table 5-3 that according to this criterion, all of the studied compounds are viable candidates for HEDMs.

The BDE for TACOT in the literature is computed by a package program in Naval Weapons Center, China Lake [180]. The closeness of our BDE value and the calculated literature data increases the reliability of the method employed in the present article. When the values in Table 5-3 are considered, TACOT and *z*-DBBD have similar BDEs. Their sensitivities are very close to each other. The closeness of the BDEs of the isomers (which are nonexistent yet) labeled as 2, 3 and 4 shows that these isomers should have similar sensitivities.

Table 5-3. The homolytic bond dissociation energies (BDE) of C−NO_2 bond of TACOT, z-DBBD and its three isomers at (DFT) UB3LYP/6–31G(d,p) theoretical level.

	BDE (kJ/mol)				
Compound	C(2)–NO_2	C(4)–NO_2	C(9)–NO_2	C(10)–NO_2	C(12)–NO_2
TACOT	274.64 (282.4)	-	263.24	274.63	263.25
z-DBBD (1)	-	273.74	-	265.17	-
2	-	266.56	-	251.99	-
3	-	252.02	-	266.60	-
4	-	253.14	-	253.13	-

*Datum in parenthesis is the calculated literature value for BDE of TACOT [180]

5.2.4. The Frontier Molecular Orbitals

Mulliken electro negativities (χ_M) and chemical hardness (η) are significant parameters in inquiring the chemical reactivity of the compounds. The χ_M and η values are calculated as expressed as section 4.2.3. Hartree-Fock is preferred over DFT in the frontier molecular orbital calculations due to the lack of Hartree-Fock type orbital concept in DFT [152].

Table 5-4. The HOMO, LUMO, Δε energies ($\Delta\varepsilon = \varepsilon_{LUMO} - \varepsilon_{HOMO}$), Mulliken electronegativities (χ_M) and chemical hardnesses (η) values of TACOT, *z*-DBBD and its three isomers calculated at HF/6–31G(d,p)//B3LYP/6-31G(d,p) theoretical level.

	E_{HOMO} (eV)	E_{LUMO} (eV)	Δε	χ_M	η
1	-9.05	-1.41	7.64	5.23	3.82
2	-8.94	-1.29	7.65	5.12	3.83
3	-8.94	-1.29	7.65	5.12	3.83
4	-8.81	-1.18	7.63	5.00	3.82
TACOT	-9.45	-1.43	8.02	5.44	4.01

The energy difference, Δε, between the HOMO and LUMO energies follows the order of TACOT>2=3>1>4 in Table 5-4. The Δε values of the molecules 1-4 are very close to each other. The differences among the results are due to the relative positions of the substituent groups. It is well known that hard molecules have a large HOMO-LUMO gap, contrary to soft molecules which have small HOMO-LUMO gaps. TACOT is calculated to be the hardest molecule in the present treatment. Compounds 1-4 show similar hardness values.

χ_M values indicate Mulliken electro negativities. The more electronegative the compound is (the higher the χ_M value), the less susceptible to oxidations than the others are. The most electronegative one is compound 1, whereas the least electronegative one is compound 4.

The chemical hardness (η) value of a compound expresses the kinetic stability of it [153-163] and it is acknowledged that harder compounds show higher kinetic stability [153]. The chemical hardness values of the questioned compounds are very close to each other. Hence, they show similar kinetic stabilities.

5.2.5. Explosive Properties

Hazardous effects of energetic materials can be evaluated by the determination of the ballistic properties, namely detonation velocity (D) and detonation pressure (P). The empirical Kamlet-Jacobs [38-53] equations are employed for the calculations of these properties.

The molecules in the present study are in accordance with $2a+b/2>c\geq b/2$ relation. Therefore relations belonging to that set of parameters are employed in the calculations. The predicted densities and detonation properties of molecules are listed in Table 5-5. It also includes the experimental and theoretical performance values of TNT [154], RDX [21, 164-167] and HMX [21, 167] excerpted from the literature.

Table 5-5. Predicted densities and detonation properties of molecules at the theoretical level of B3LYP/6–31G(d,p).

Compound	**Ω (%)**	**ΔH^{o}_{f}[a] (kJ/mol)**	**Q (kJ/g)**	**V[b] (cm^3/mol)**	**ρ (g/cm^3)**	**D (km/s)**	**P (GPa)**
1[c]	-65.67	1338.89	1706.79	216.907	1.92 (1.96)	8.24(7.52)	31.27(24.5)
2	-65.67	1345.90	1710.83	218.872	1.91	8.19	30.81
3	-65.67	1345.78	1710.77	217.836	1.92	8.22	31.07
4	-65.67	1355.04	1716.11	220.729	1.89	8.14	30.24
TACOT[c]	-74.19	742.29	1481.56	216.203	1.81 (1.85)	7.56 (7.20)	25.41 (24.5)
TNT[d]	-73.98	52.47	1361.62	137.32	(1.64)	7.11 (6.95)	21.26 (19.00)
RDX[e]	–21.61	168.90	1597.39	124.92	1.78 (1.81)	8.88 (8.75)	34.75 (34.70)
HMX[e]	–21.61	270.41	1633.88	157.53	1.88 (1.90)	9.28 (9.10)	39.21 (39.30)

[a] Standard heat of formation values obtained from the PM3 single point calculations over B3LYP/6–31G(d,p) geometry optimized structures.

[b] Average molar volumes from 100−single point calculations at the B3LYP/6–31G(d,p) level.

[c] Data in parenthesis are the calculated values taken from literature for compound 1 and TACOT [181]

[d] Experimental data values (in parenthesis) of TNT are excerpted from ref. [165].

[e] Data in parenthesis are the experimental values taken from refs.[21, 164-167] for RDX and refs.[21, 167] for HMX.

The density, detonation velocity and pressure values for TACOT are in accordance with the literature data [181]. The molecules 1-4 show superior crystal density when compared to that of TACOT. ΔH^o_f values of the compounds are quite higher than TACOT. The performances of *z*-DBBD and other isomers are in the following manner *z*-DBBD(1)~3>2>4>TACOT>TNT. *z*-DBBD has the highest detonation properties. When Table 5-6 is considered, it is obvious that the performance of *z*-DBBD and its isomers are all better than TACOT. All compounds (1-4) are as successful as RDX and better than TNT in terms of ballistic properties. Hence, they are all potential candidates for high explosives.

5.2.6. Detonation Products

The detonation of a $C_aH_bO_cN_d$ type explosive will result in the formation of smaller molecules, i.e., CO_2, CO, H_2O, etc. In order to clarify the decomposition products, a set of rules by Kistiakowsky and Wilson have been employed [29-30]. Since the compounds 1-4 are isomers, their decomposition products are the same. Decomposition of 1 mole compound 1 gives 5 moles of N_2, 1 mole of H_2O, 7 moles of CO and 5 moles of C.

5.2.7. Explosive Power and Power Index

Heat and gases are released in an explosive reaction. The volume of gas produced will provide information on the amount of work done by the explosive. Standard conditions must be established in order to measure the volume of generated gas, since the volume of gas varies according to the temperature. The standard conditions (273 K, 1atm) also enable one to make comparisons between different explosives. Division of the value of total volume of gas produced upon detonation by the molecular weight gives an idea of how much gas is released per gram of explosive. Explosive power and power index have been calculated as stated in section 1.2.2.5.

Table 5-6 shows the power index values of TACOT, *z*-DBBD, its three isomers, Picric Acid, TNT, RDX and HMX**.** The power index values of *z*-DBBD and its isomers are very close to each other and around 290 %. The results show that *z*-DBBD and the isomers are better than TACOT as in the case of detonation properties. Since the amount of gas produced upon detonation is much more than those of TNT, RDX, HMX, power index values are higher than those of HMX and RDX. These isomers may easily be employed where more amount of gas is required upon detonation.

Table 5-6. The comparative power index values of TACOT, *z*-DBBD and its three isomers.

Compound	**Formula**	**Q (kJ/g)**	**V(dm^3/g)**	**QxV**	**Power Index (%)**
1	$C_{12}H_2N_{10}O_8$	1706.79	2.05	3494.74	289
2	$C_{12}H_2N_{10}O_8$	1710.83	2.05	3503.02	290
3	$C_{12}H_2N_{10}O_8$	1710.77	2.05	3502.89	290
4	$C_{12}H_2N_{10}O_8$	1716.11	2.05	3513.82	291
TACOT	$C_{12}H_4N_8O_8$	1481.56	1.04	1538.76	127
HMX	$C_4H_8N_8O_8$	1634.89	0.91	1484.66	123
RDX	$C_3H_6N_6O_6$	1598.39	0.91	1450.86	120
Picric Acid	$C_6H_3N_3O_7$	1372.86	0.88	1208.07	100
TNT	$C_7H_5N_3O_6$	1361.62	0.61	823.21	68

5.3. Conclusion

Presently, theoretical studies have been performed on TACOT itself, z-DBBD and its three different isomers. The corrected absolute and relative total energies of the geometry optimized structures have been calculated at the theoretical level of B3LYP/6-31G(d,p). We have correlated the bond dissociation energies with sensitivity. Mulliken electro negativities (χM) and chemical hardness (η) are questioned employing Frontier Molecular Orbitals at HF/6–31G(d,p)//B3LYP/6-31G(d,p) theoretical level. The detonation performance analysis showed that z-DBBD and its isomers (nonexistent yet) are better than TACOT and all (compounds 1-4) are as successful as RDX. These compounds shall be preferred where high density explosive is necessary. The power index results showed that z-DBBD and its isomers are better than TACOT, RDX and HMX. Consequently, these molecules shall preferably be employed where much gas generation upon detonation is required. The compounds 2-4 are all reasonable candidates for HEDMs. The influence of substitution of the position of furoxan ring on the physical properties is also showed in the present study.

CHAPTER 6

EFFECTS of EPOXIDATION AND NITRATION ON BALLISTIC PROPERTIES of FOX-7 – A DFT STUDY

6.1. Introduction

In both modern civil and military applications, there is developing attention for novel energetic materials with greater performance and lower susceptibility to stimuli for the personnel safety and to reduce the warhead vulnerability problems. In order to explore new energetic materials with those required properties, a promising method is to explore compounds with compact structure and high nitrogen content, which has been proved by many recent research and development efforts [132, 182-184].

FOX-7 or DADNE, 1,1-diamino-2,2-dinitroethylene is an insensitive high power explosive compound [185]. In 1998, the FOA, Defence Research Establishment of Sweden reported the prosperous synthesis of FOX-7 [186-187]. It is expected to be a high-performance explosive, since Politzer et al. [188] have reported that FOX-7 has the same molecular stoichiometry as hexahydro-1,3,5-trinitro-1,3,5-triazine (RDX) and octahydro-1,3,5,7-tetranitro-1,3,5,7-tetrazocine (HMX), which are among the most powerful explosives that are presently used for explosive formulation and monopropellants applications. In addition, it has relatively high crystal density.

Compared with typical C-H-N-O explosives, FOX-7 (Figure 6-1) is a small and relatively symmetric energetic molecule [171]. The reported energetic properties of FOX-7 indicate its use as energetic filler in insensitive munitions. Efforts are on to produce 1,1-diamino-2,2-dinitroethylene in multigram quantity for its use in insensitive applications [189]. These features make FOX-7 a striking system for theoretical studies.

The theoretical simulations on energetic materials aid to decrease the risk associated with laborious and repetitive tests. Such studies can be used to identify and characterize explosive properties [186].

Due to the outstanding characteristics of FOX-7, we decided to conduct a research for new high explosives with a high energy content, better crystal density, and reasonable stability among substances whose molecules are similar to FOX-7 from a structural point of view. Therefore, a series of molecules (FOX-7, its epoxide and further nitrated forms, compound 1-6, see Figure 6-1) that possess the FOX-7 core were considered in the present study.

6.2. Results and Discussion

All the calculations have been done as expressed in section 1.3.5.

6.2.1. The Geometries

The presently considered structures have been thought to be the potential nominees of high explosives (Figure 6-1). The geometry optimizations of the structures shown in Figure 6-1 were done at the (DFT) B3LYP/6-31G(d,p) level. The bond length data for the geometry optimized structures are presented in Table 6-1. The numbering in Table 6-1 is consistent with the numbering manner in Figure 6-2. The literature X-ray diffraction [190] and calculated bond lengths of FOX-7 are also shown in Table 6-1. The similarity of the literature and calculated values of the bond lengths for FOX-7 indicates that the method and basis set used for the geometry optimizations are successful. This similarity also promises that bond lengths of other compounds are close to the actual values.

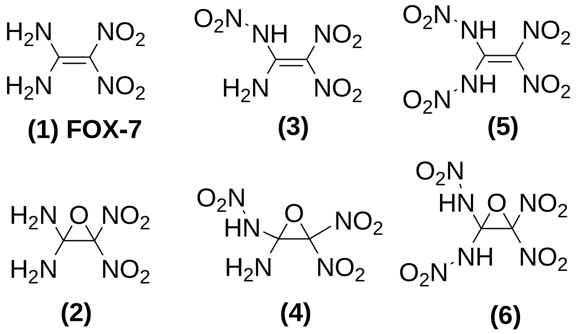

Figure 6-1. The Structures of FOX-7 (1) and other derivatives in the presently considered.

In general, an assessment between the experimental and theoretical bond lengths shows that the calculated results are slightly different from the experimental values. These minor inconsistencies are mainly due to the solid-state effect, i.e., intermolecular interactions. Such interactions are not represented in the DFT calculations [49].

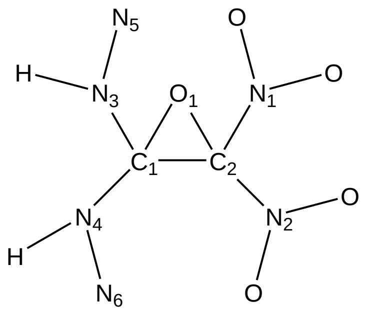

Figure 6-2. The numbering manner of the present structures

Table 6-1. The bond lengths (Å) of the geometry optimized FOX-7 and its derivatives calculated at the theoretical level of (DFT) B3LYP/6–31G(d,p)

	Bond Lengths in (Å)						
	FOX-7*	**1**	**2**	**3**	**4**	**5**	**6**
C1-C2	1.456	1.427	1.533	1.423	1.551	1.382	1.474
C1-N3	1.319	1.344	1.318	1.379	1.346	1.384	1.425
C1-N4	1.325	1.344	1.313	1.325	1.298	1.378	1.411
C2-N1	1.399	1.432	1.719	1.434	1.727	1.440	1.523
C2-N2	1.426	1.432	1.662	1.441	1.646	1.473	1.519
C1-O1	-	-	2.367	-	2.365	-	1.467
C2-O1	-	-	1.228	-	1.231	-	1.364
N3-N5	-	-	-	1.392	1.405	1.401	1.407
N4-N6	-	-	-	-	-	1.437	1.419

*Experimental values at 298 K reported in ref [190].

6.2.2. Relative Total Energies

Table 6-2 shows the ZPE corrected absolute total electronic energies of the geometry optimized compounds calculated at the theoretical level of B3LYP/6-31G(d,p). When Table 6-2 is considered, it is obvious that as the molecular weight of compounds get higher, the total electronic energy values get lower.

Table 6-2. The calculated corrected total electronic energies of FOX-7 and derivatives at (DFT) B3LYP/6–31G(d,p) theoretical level.

Compound	Energy (kj.mol^{-1})
FOX-7 (1)	-1570661
2	-1768114
3	-2107475
4	-2304916
5	-2644215
6	-2841633

6.2.3. Bond Dissociation Energies (BDE)

In the present study, in order to compare the C-NO_2 and N–NO_2 bond strengths of the compounds, homolytic bond dissociation energy (BDE) calculations for the removal of nitrogen dioxide moiety from the structures were performed at UB3LYP/6-31G(d,p) level of theory as stated in Section 1.3.5. BSSE has also been calculated.

Table 6-3 indicates BDE values. The conformity of our BDE value and the literature datum [185] for FOX-7 increases the reliability of the method employed in the present article. The drop hammer tests showed that impact sensitivity of FOX-7 is 15-40 Nm, those of RDX (BDE=175.26 kJ/mol) and HMX (BDE=180.02 kJ/mol) are 7.4 Nm [191]. When BDE values are considered, the same trend is observed. FOX-7 is more insensitive than both RDX and HMX.

Table 6-3. The homolytic bond dissociation energies (BDE) of C−NO_2 and N−NO_2 bonds of FOX-7 and derivatives calculated at (DFT) UB3LYP/6–31G(d.p) theoretical level.

	BDE (kJ/mol)			
	C2-N1	**C2-N2**	**N3-N5**	**N4-N6**
FOX-7 (1)	285.97	280.08 (267.78*)	-	-
2	47.94	48.30	-	-
3	268.32	263.37	157.48	-
4	25.46	25.61	35.66	-
5	241.15	202.54	104.73	84.76
6	184.96	189.01	160.03	129.52

*Datum in parenthesis is the literature value taken from ref. [185] for BDE of C-NO_2 bond of FOX-7.

The Table 6-3 shows that FOX-7 is the most insensitive explosive in the current study. Compounds 3 and 6 are as insensitive as well-known explosives, RDX and HMX. Compounds 2, 4 and 5 are more sensitive than other compounds. They can be regarded as primary explosives and shall be easily employed in detonators to trigger larger charges of less sensitive secondary explosives.

6.2.4. The Frontier Molecular Orbitals

Mulliken electro negativities (χ_M) and chemical hardness (η) are significant parameters in inquiring the chemical reactivity of the compounds. The χ_M and η values are calculated as expressed as section 4.2.3. Hartree-Fock is preferred over DFT in the frontier molecular orbital calculations due to the lack of Hartree-Fock type orbital concept in DFT [152].

Table 6-4. The HOMO, LUMO, $\Delta\varepsilon$ energies ($\Delta\varepsilon = \varepsilon_{LUMO} - \varepsilon_{HOMO}$), Mulliken electronegativities (χ_M) and chemical hardnesses (η) values of FOX-7 and its derivatives calculated at HF/6–31G(d.p)//B3LYP/6–31G(d.p) theoretical level.

Compound	**E_{HOMO} (eV)**	**E_{LUMO} (eV)**	$\Delta\varepsilon$	χ_m	η
FOX-7 (1)	-10.44	1.69	12.13	4.38	6.07
2	-11.04	1.70	12.74	4.67	6.37
3	-11.17	0.49	11.66	5.34	5.83
4	-11.59	-0.28	11.31	5.94	5.66
5	-11.97	-0.73	11.24	6.35	5.62
6	-13.54	0.31	13.85	6.62	6.93

The energy difference, $\Delta\varepsilon$, between the HOMO and LUMO energies follows the order of 6>2>1>3>4>5. It is acknowledged that hard molecules have a large HOMO-LUMO gap, counter to soft molecules which have small HOMO-LUMO gaps [33]. When we consider the parent structures and their epoxide derivatives (compound pairs 1-2, 3-4 and 5-6) are considered, 1-2 and 3-4 pairs show similar behavior. Compound 6 is far harder than its parent molecule (5). It is calculated to be the hardest molecule among the structures considered.

χ_M values indicate Mulliken electronegativities. The more electronegative the compound is (the higher the χ_M value), the less vulnerable to oxidations than the others are. χ_M values follow the order of 6>5>4>3>2>1. Similarly, when parent structures and their epoxide derivatives (compound pairs 1-2, 3-4 and 5-6) are investigated, the parent molecules are lower in electronegativity values. This was expected because each parent molecule (1, 3 and 5) is oxidized to obtain the compounds 2, 4 and 6.

The chemical hardness (η) value of a compound explains the kinetic stability of that compound [158-159] and it is approved that harder compounds show higher kinetic stability [148]. The chemical hardness values are also given in Table 6-4. η values follow the order of 6>2>1>3>4>5. Likewise, when the parent structures and their epoxide derivatives (compound pairs 1-2, 3-4 and 5-6) are examined, 1-2 and 3-4 pairs show similar manners. Compound 6 shows far more kinetic stability than its parent molecule (5).

6.2.5. Explosive Properties

Explosive outputs of energetic materials can be estimated by the determination of the detonation velocity (D) and detonation pressure (P). The empirical Kamlet-Jacobs [38-41] equations are used

When Table 6-5 is considered, it is obvious that compounds 1 and 2 are underoxidized like TNT, RDX and HMX. However, compounds 3-6 are overoxidized like nitroglycerine, $C_3H_5N_3O_9$ (%3.52) [11]. The calculated density and detonation properties of FOX-7 and its derivatives are listed in Table 6. It also includes experimental and theoretical performance values (in parenthesis) of TNT [165], RDX [21, 164-167] and HMX [21, 167] obtained from the literature.

Table 6-5. Predicted densities and detonation properties of FOX-7 and its derivatives at the theoretical level of B3LYP/6–31G(d,p).

Compound	Ω (%)	ΔH^{o}_{f} (kJ.mol^{-1})	Q (kJ.g^{-1})	V (cm^{3}.mol^{-1})	ρ (g.cm^{-3})	D (km.s^{-1})	P (GPa)
FOX-7 (1)	-21.61	-24.11	2005.28	83.23	1.80 (1.88)*	9.46 (9.09)*	39.69(36.6)*
2	-9.75	-62.77	2040.03	89.71	1.85	9.79	43.23
3	4.14	63.02	1501.29	119.28	1.64	8.34	29.08
4	11.48	105.95	1435.48	109.12	1.94	9.28	39.95
5	20.16	213.92	1247.64	120.91	2.00	9.09	38.88
6	25.19	187.31	1144.04	129.51	1.98	8.85	36.70
TNT	-73.98	52.47	1361.62	124.92	1.64	7.11 (6.95)	19
RDX	-21.61	168.9	1597.39	124.92	1.78 (1.81)	8.88 (8.75)	34.75 (34.70)
HMX	-21.61	270.41	1633.88	157.53	1.88 (1.90)	9.28 (9.10)	39.21 (39.30)

The detonation velocity and pressure values for FOX-7 are in accordance with the literature data [9]. When Table 6-5 is considered, it is obvious that all compounds (1-6) are strong nominees for high explosives. Their explosive character follows the order 2>1>4>HMX>5>RDX>6>3>TNT.

Epoxidation of FOX-7 gives the most powerful explosive (compound 2) of all. However, further nitration of amino group of FOX-7 does not create a better explosive (compound 3). The values of detonation velocity and pressure decreases slightly. Epoxidation of compound 3 gives compound 4. Similarly, this epoxidation yields a better explosive (compound 4). The value of detonation velocity increases by 0.94 km/s. Further nitration of compound 3 produces compound 5. This nitration seems worthy due to the increase in detonation velocity by 0.75 km/s. However, neither mono-nitrated FOX-7 (compound 3) nor doubly nitrated FOX-7 (compound 5) is as powerful as FOX-7 itself. One can conclude that further nitration of FOX-7 is not a convenient method in the enhancement of ballistic properties. Nevertheless, all compounds are better than a well-known explosive, TNT, and some are as influential as RDX and HMX. Epoxidation is a superior method than further nitration in the improvement of explosive character of FOX-7.

6.2.6. Detonation Products

In order to clarify the quantity and identity of the decomposition products, a set of rules developed by Kistiakowsky and Wilson was used [29-30]. For instance, complete decomposition of FOX-7 gives 2 moles of CO, 2 moles of N_2 and 2 moles of H_2O. Similarly, the moles of products of all compounds were calculated for the determination of volume. The decompositipon products of other products are shown in Table 6-6.

Table 6-6. The identity and quantity of the decomposition products of the compounds 1-6.

Compound	Formula	N_2	H_2O	CO	CO_2	O_2	n_{total}
1	$C_2H_4N_4O_4$	2	2	2	-	-	6
2	$C_2H_4N_4O_5$	2	2	2	-	0.5	6.5
3	$C_2H_3N_5O_6$	2.5	1.5	2	-	1.25	7.25
4	$C_2H_3N_5O_7$	2.5	1.5	2	-	1.75	7.75
5	$C_2H_2N_6O_8$	3	1	2	-	2.5	8.5
6	$C_2H_2N_6O_9$	3	1	2	-	2	8

6.2.7. Explosive Power and Power Index

Heat and gases are released in an explosive reaction. The volume of gas produced will provide information on the amount of work done by the explosive. Standard conditions must be established in order to measure the volume of generated gas, since the volume of gas varies according to the temperature. The standard conditions (273 K, 1atm) also enable one to make comparisons between different explosives. Division of the value of total volume of gas produced upon detonation by the molecular weight gives an idea of how much gas is released per gram of explosive. Explosive power and power index have been calculated as stated in section 1.2.2.5.

Table 6-7 shows the power index values of FOX-7, its derivatives, Picric Acid, RDX and HMX. The power index values of considered compounds reside between 75 – 151 % and in the following manner: 1> 2>HMX>RDX>3>PA>4>5>6. The results show that FOX-7 has the greatest power index value. Compound 2 shows better performance than both HMX and RDX. When the compound pairs (1-2, 3-4 and 5-6) are compared, epoxidized compounds (2, 3 and 6) are lower in power index value than their parent structures.

Table 6-7. The power index values of FOX-7, derivatives, Picric Acid, RDX and HMX

Compound	Q (kJ.g^{-1})	V(dm^3.g^{-1})	QxV	Power Index %
FOX-7 (1)	2005.28	0.91	1820.06	151
2	2040.03	0.89	1810.30	150
3	1501.29	0.84	1262.77	105
4	1435.48	0.83	1191.92	99
5	1247.64	0.80	997.81	83
6	1144.04	0.79	907.77	75
Picric Acid	1372.86	0.88	1208.07	100
RDX	1598.39	0.91	1450.86	120
HMX	1634.89	0.91	1484.66	123

6.3. Conclusion

Presently, theoretical studies have been performed on FOX-7 itself and 5 different derivatives. The corrected absolute and relative total energies of the geometry optimized structures have been calculated at the theoretical level of B3LYP/6-31G(d,p). Mulliken electro negativities (χ_M) and chemical hardness (η) have been reviewed using Frontier Molecular Orbitals at HF/6–31G(d,p)//B3LYP/6-31G(d,p) theoretical level. The results have showed that the parent molecules have lower electronegativity values than their epoxide derivatives. The bond dissociation energies have been correlated with sensitivity. The insensitivity order has been determined as FOX-7>HMX>RDX>3>6>5>2>4. As for explosive effects, the order is 2>1>4>HMX>5>RDX>6>3. Compound 2 has showed better explosive character than FOX-7, but its sensitivity is higher. Furthermore, compounds 4 and 5 are as successful as RDX and HMX. Power index values have also supported that phenomenon. It has been shown that epoxidation is a better method than further nitration in the enhancement of explosive properties of FOX-7. An explosive engineer should evaluate the explosive performance, power index and sensitivity of explosives prior to use. He should decide the employment of an explosive on the basis of these properties according to the requirements of the system. For instance, if insensitivity is required as in the case of detonator use, compounds 3 and 6 shall be used. If higher detonation velocity and pressure are essential, compound 2 shall be employed. All the compounds in the present article are potential candidates for high explosives.

CHAPTER 7

NITRO DERIVATIVES OF PARABANIC ACID AS POTENTIAL EXPLOSIVES—A DFT STUDY

7.1. Introduction

Lately, explosive scientists have concentrated on compounds of high density with high content of nitrogen and low content of hydrogen. These types of compounds appeal both theoretical and practical considerations. They are not only applicable in conventional fields where high-energy substances are essential (propellants, explosives, etc.), but also applicable in some other purposes, e.g. gas-generating substances or components of pyrophobic compositions [192]. Such compounds are used as components of energetic compositions on condition that they have promising detonation and/or combustion properties, which depend on the enthalpy of formation (or enthalpy of combustion) and molecular crystal density [38-41].

One of the most remarkable energetic skeleton, rich in nitrogen, low in hydrogen is parabanic acid (PA) [193]. Parabanic acid, 2,4,5-Imidazolidinetrione, is a crystalline nitrogenous acid ($C_3N_2H_2O_3$) obtained by the oxidation of uric acid. It is also called oxalylurea (see Figure 7-1) [194-195]. Ulrich and Sayigh *et. al*. have reported the synthesis of PA by the reaction of oxalychloride and urea [196].

The great magnitude of the calculated density data (1.753 $g.cm^{-3}$) of parabanic acid and high content of nitrogen (24.5 %) have inspired us to investigate the parabanic acid frame. We have designed a series of molecules (1-8) by nitration and imination. Figure 7-1 shows the structures of parabanic acid and its derivatives (compounds 1-8).

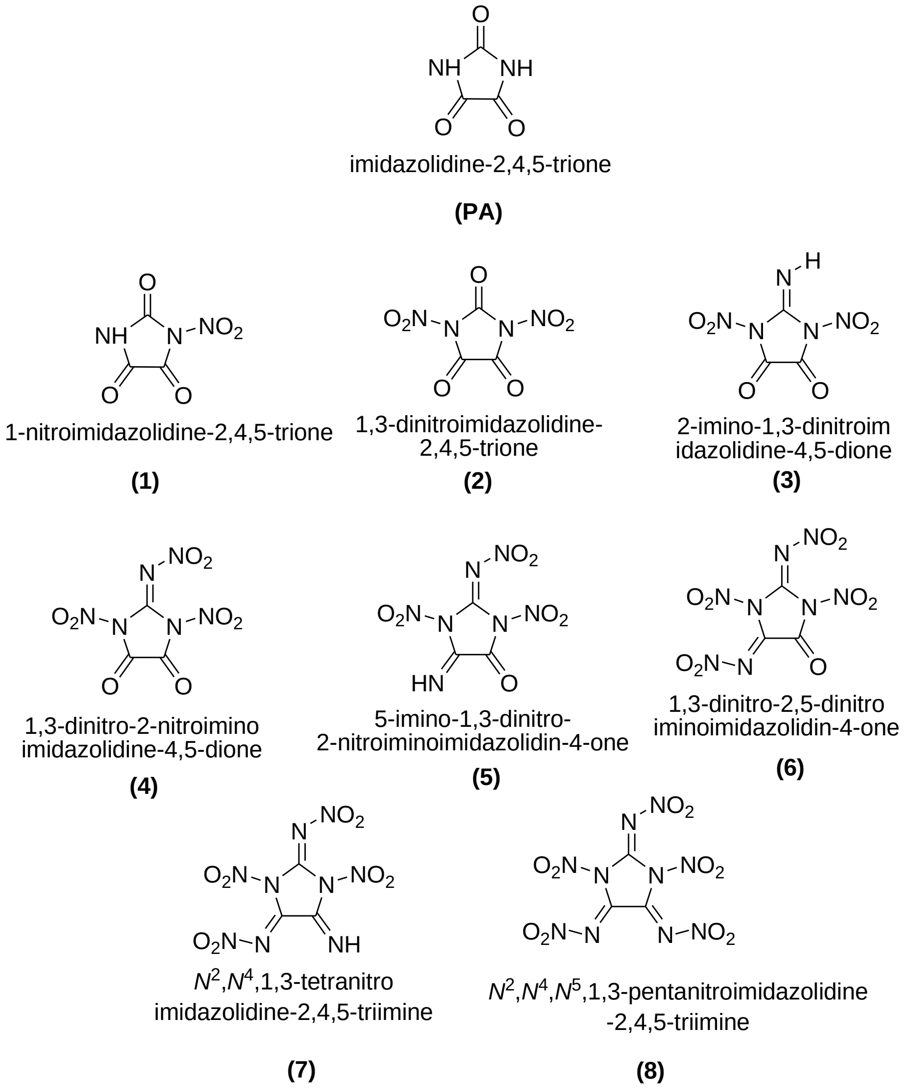

imidazolidine-2,4,5-trione

(PA)

1-nitroimidazolidine-2,4,5-trione

(1)

1,3-dinitroimidazolidine-2,4,5-trione

(2)

2-imino-1,3-dinitroimidazolidine-4,5-dione

(3)

1,3-dinitro-2-nitroimino imidazolidine-4,5-dione

(4)

5-imino-1,3-dinitro-2-nitroiminoimidazolidin-4-one

(5)

1,3-dinitro-2,5-dinitro iminoimidazolidin-4-one

(6)

N^2,*N*^{4},1,3-tetranitro imidazolidine-2,4,5-triimine

(7)

N^2,*N*^{4},*N*^{5},1,3-pentanitroimidazolidine-2,4,5-triimine

(8)

Figure 7-1. The structures of PA and other derivatives

7.2. Results and Discussion

All the calculations have been done as expressed in section 1.3.5.

7.2.1. The Geometries

All the structures investigated have been thought as the potential candidates for high explosives. The geometry optimizations of the structures shown in Figure 7-1 were done at the B3LYP/6-31G(d,p) level. The numbering in Table 7-1 is consistent with the numbering manner in Figure 7-2. The bond lengths for the geometry optimized structures are presented in Table 7-1. The experimental X-ray diffraction [197] and calculated bond length values of parabanic acid are also shown in Table 7-1. The similarity of the experimental and theoretical values of the bond lengths for PA guarantees satisfactory level of calculation for the geometry optimization. This compatibility also guarantees that bond lengths of other compounds are close to the actual values. Note that there are no experimental X-ray data for the new designed compounds (1-8) to the best of our knowledge.

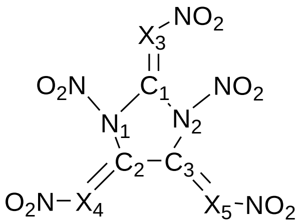

Figure 7-2. The numbering manner of the present structures

An evaluation between the experimental and theoretical bond lengths of PA indicates that the calculated results are a little greater than the experimental values. One possible source of this slight discrepancy is the inadequate modeling of dispersion forces in most forms of DFT. Other reason is due to the solid-state effect, i.e., intermolecular interactions. Such interactions are not considered in the DFT calculations [49].

Table 7-1. The bond lengths (Å) of the geometry optimized parabanic acid and its nitro derivatives (compounds 1-8) calculated at the theoretical level of B3LYP/6–31G(d,p).

	PA*	**PA**	**1**	**2**	**3**	**4**	**5**	**6**	**7**	**8**
C_1-N_1	1.396	1.400	1.430	1.423	1.417	1.406	1.401	1.410	1.414	1.398
N_1-C_2	1.360	1.388	1.416	1.411	1.395	1.409	1.419	1.384	1.380	1.409
C_2-C_3	1.551	1.556	1.553	1.553	1.546	1.544	1.517	1.524	1.507	1.504
C_3-N_2	1.362	1.388	1.387	1.410	1.424	1.422	1.405	1.423	1.422	1.386
C_1-N_2	1.399	1.400	1.396	1.423	1.442	1.408	1.410	1.401	1.394	1.408
C_1-X_3	1.203	1.206	1.198	1.192	1.252	1.274	1.276	1.274	1.276	1.276
C_2-X_4	1.213	1.204	1.196	1.195	1.199	1.196	1.258	1.275	1.279	1.269
C_3-X_5	1.210	1.204	1.202	1.195	1.194	1.194	1.200	1.194	1.257	1.276
N_1-NO_2	-	-	1.452	1.470	1.473	1.494	1.490	1.511	1.509	1.520
N_2-NO_2	-	-	-	1.470	1.436	1.492	1.486	1.499	1.499	1.515
N_3-NO_2	-	-	-	-	-	1.437	1.276	1.437	1.433	1.435
N_4-NO_2	-	-	-	-	-	-	-	1.446	1.440	1.458
N_5-NO_2	-	-	-	-	-	-	-	-	-	1.446

7.2.2. Relative Total Energies

Table 7-2 shows the Zero Point Energy (ZPE) corrected absolute total electronic energies of the geometry optimized compounds calculated at the theoretical level of B3LYP/6-31G(d,p). When Table 7-2 is considered, it is obvious that the ZPE corrected total electronic energies (E_{corr}) of compounds get lower from compound-1 to 8. It is known that as the molecular weight of compounds get higher, the total electronic energy values get lower.

Table 7-2. The calculated corrected total electronic energies of PA and derivatives at (DFT) B3LYP/6–31G(d,p) theoretical level.

	Formula	**E (kJ/mol)**	**E_{corr} (kJ/mol)**
PA	$C_3H_2N_2O_3$	-1183412	-1183249
1	$C_3HN_3O_5$	-1720174	-1720008
2	$C_3N_4O_7$	-2256927	-2256760
3	$C_3HN_5O_6$	-2204732	-2204532
4	$C_3N_6O_8$	-2741519	-2741315
5	$C_3HN_7O_7$	-2689345	-2689107
6	$C_3N_8O_9$	-3226133	-3225892
7	$C_3HN_9O_8$	-3173956	-3173682
8	$C_3N_{10}O_{10}$	-3710747	-3710470

7.2.3. Explosive Properties

Hazardous effects of explosives can be assessed by the determination of the ballistic properties, i.e. detonation velocity (D) and detonation pressure (P). The experimental Kamlet-Jacobs [38-41] equations are employed for the calculations of these properties.

When Table 7-3 is considered, it is obvious that compounds 1 and 3 are underoxidized like TNT, RDX and HMX. However, compounds 2, 4-8 are overoxidized like nitroglycerine, $C_3H_5N_3O_9$ (3.52 %) [11]. The calculated density and detonation properties of parabanic acid derivatives are listed in Table 7-3. It also includes experimental (in parenthesis) and theoretical performance values of TNT [165], RDX [21, 164-167] and HMX [21, 167] obtained from the literature.

When the detonation velocity and pressure values in Table 7-3 are considered, it is obvious that all the compounds (1-8) are strong candidates for high explosives. Their explosive character follows the order 7>HMX>8>5>6>RDX>3>4>2>1>TNT. Compounds 5-8 seem to be as effective as RDX and HMX. Others should be better than a well-known explosive, TNT.

Although Kamlet-Jacobs Equations do not explicitly relate the weight percent of nitrogen (% N) of an explosive with “D” and “P” apparently, it is an additional significant parameter that affects the ballistic properties. The order of % N value of presently considered explosives is the same as the order of detonation velocity. As the values of % N increases, detonation velocity also increases. For instance, compound 7 has the greatest %N (% 43.3) and detonation velocity (9.48 km/s); whereas, compound 1 has the lowest %N (%26.4) and detonation velocity (8.04) of all.

Table 7-3. Predicted densities and detonation properties of PA and its derivatives at the theoretical level of B3LYP/6–31G(d,p).

Compound	**Ω (%)**	**ΔH_f^o (kJ/mol)**	**Q (kJ/g)**	**% N**	**V (cm^3/mol)**	**ρ (g/cm^3)**	**D (km/s)**	**P (GPa)**
1	-15.09	-344.42	1125.89	26.4	85.39	1.88	8.04	29.46
2	7.84	-256.98	1081.73	27.4	104.1	1.98	8.38	32.94
3	-3.94	-2.76	1412.7	34.5	106.07	1.93	8.88	36.43
4	12.9	71.19	1205.98	33.9	125.39	2.01	8.8	36.61
5	3.24	295.71	1544.92	39.7	129.57	1.92	9.16	38.62
6	16.43	391.06	1285.99	38.3	145.76	2.02	9.06	38.88
7	8.25	606.66	1566.83	43.3	147.61	1.99	9.48	42.27
8	19.04	684.52	1326.27	41.7	166.22	2.04	9.24	40.62
TNT	-73.98	52.47	1361.62	18.5	138.41	1.64	7.11	19.00
RDX	-21.61	168.90	1597.39	37.8	124.92	1.78(1.81)	8.88(8.75)	34.75(34.70)
HMX	-21.61	270.41	1633.38	37.8	157.93	1.88(1.90)	9.28(9.10)	39.21(39.00)

Density of PA has been calculated as 1.753 g/cm^3. As seen from , the density increases from compound 1 to 8. Further nitration and further imination followed by nitration (from compound 1 to 8) creates compounds with greater density, accordingly superior explosives considering Kamlet-Jacobs Equations. These molecules shall easily be employed in munitions requiring limited volume.

Further nitration of lactam nitrogen of compound 1 yields a better explosive (compound-2). Similarly, the imination of compound gives an enhanced explosive character (compound-3) increasing the detonation velocity value from 8.38 to 8.88 km/s. However, nitration of the imino group of compound-3 yields compound-4 with lower detonation velocity. Additional imination of the carbonyl group of compound-4 gives compound-5 with superior detonation velocity. Conversely, nitration of that imine group produces compound-6 lessening the detonation velocity. Conversion of the last carbonyl group of compound-6 to imino derivative gives compound-7, which has the best explosive properties of all. Nitration of compound -7 decreases the ballistic properties (as in the previous cases). Computationally, it has been shown that nitration of parabanic acid is a useful method in the enhancement of ballistic properties. On the other hand, imination of carbonyl group (at least in the present case) is not a convenient method in the improvement of explosive properties; whereas nitration of the formed imine group is an effective way of increasing both the detonation velocity and pressure. All the compounds in the present article are potential candidates for high explosives.

7.2.4. Detonation Products

In order to clarify the quantity and identity of the decomposition products, a set of rules developed by Kistiakowsky and Wilson have been used [29-30]. Table 7-4 shows the decomposition products of the compounds 1-8. For instance, complete decomposition of compound-1 produces 1.5 moles of N_2, 0.5 moles of H_2O, 1.5 moles of CO and 1.5 moles of CO. Table 7-4 shows the decomposition products of the compounds 1-8. Compound-8 gives the greatest amount of hot gas upon detonation. The total moles of decomposition products data are inputs for the calculation of power index values.

Table 7-4. The identity and the quantity of the decomposition products of the compounds 1-8.

		Quantity of Decomposition Products (mol)					
Compound	Formula	N_2	H_2O	CO	CO_2	O_2	n_{total}
1	$C_3HN_3O_5$	1.5	0.5	1.5	1.5	-	5.0
2	$C_3N_4O_7$	2	-	-	3	0.5	5.5
3	$C_3HN_5O_6$	2.5	0.5	0.5	2.5	-	6.0
4	$C_3N_6O_8$	3	-	-	3	1	6.0
5	$C_3HN_7O_7$	3.5	0.5	-	3	0.25	7.25
6	$C_3N_8O_9$	4	-	-	3	1.5	8.5
7	$C_3HN_9O_8$	4.5	0.5	-	3	0.75	8.75
8	$C_3N_{10}O_{10}$	5	-	-	3	2	10

7.2.5. Explosive Power and index

Table 7-5 shows the power index values of the compounds 1-8 and Picric Acid. The power index values of the considered compounds vary between 57 – 92 % and in the following manner: 7> 5>3>8>6>1>4>2. Compound-7 seems to be the best of all. The power index values of some renowned explosives are given for comparison. Hexanitrostilbene (HNS) (109 %), Trinitrotoluene (TNT) (110 %), triamino trinitro benzene (TATB) (99 %), 5-nitro-2,4-dihydro-3H-1,24-triazol-3-one (NTO) (87%), RDX (120%), HMX (120%), [1]. The results show that compounds 7, 5 and 3 are as effective as TATB and NTO, but not as good as RDX and HMX in terms of power index concept.

Table 7-5. The power index values of the compounds 1-8 and Picric Acid.

Compound	Q (kJ/g)	V(dm^3/g)	Q.V	% Power Index
1	1125.89	0.704	792.73	69
2	1081.73	0.604	653.11	57
3	1412.70	0.662	934.99	82
4	1205.98	0.632	762.29	67
5	1544.92	0.657	1015.43	89
6	1285.99	0.652	838.31	73
7	1566.83	0.673	1055.10	92
8	1326.27	0.666	883.94	77
Picric Acid	1379.07	0.831	1146.09	100
RDX	1598.39	0.91	1450.86	120
HMX	1634.89	0.91	1484.66	123

7.2.6. Conclusion

Parabanic acid has been chosen as a starting frame due to its high nitrogen content and high density value. DFT studies have been performed on eight parabanic acid derivatives. The corrected absolute and relative total energies of the geometry optimized structures have been calculated at the theoretical level of B3LYP/6-31G(d,p). The density data of compounds 1-8 have been calculated and found to be much more than RDX and HMX. These molecules shall easily be employed in munitions requiring small volume. Detonation velocity and pressure values have been calculated employing Kamlet-Jacobs equations. The results showed that the explosive character follows the order 7>HMX>8>5>6>RDX>3>4>2>1>TNT. Compounds 5-8 are found as effective as RDX and HMX, others have been found superior than a well-recognized explosive, TNT. The identity and quantity of the decomposition products have been enlightened. Power index values have indicated that some of our explosives are as effective as TATB and NTO in terms of amount of work done by the explosive. It has been shown that nitration of parabanic acid is a useful method in the enhancement of ballistic properties. Whereas, imination of carbonyl group is not a convenient method in the improvement of explosive properties; but nitration of the formed imine group is an effective way of increasing both the detonation velocity and pressure. All the compounds in the present article are potential candidates for high explosives.

CHAPTER 8

CONCLUSION

Molecular modeling is a valuable tool that gives information about chemical and physical properties of materials without doing a physical experiment. It has been widely utilized in energetic materials field. In the present work, we have also performed molecular modeling studies of fuels and explosives. The thesis consists of six chapters (excluding introduction, Chapter-1), which have their own literature surveys, methodologies and conclusions.

Chapter-II is about JP-10, an aviation fuel widely used in aircrafts. It is a bicyclic hydrocarbon based fuel. Fuel degradation may occur under long time, low-temperature storage conditions (storage stability) or under short time high-temperature stress (thermal oxidative stability). Oxidation through hydroperoxide formation has been considered. The Carbon center numbered as “6” is found to be the most vulnerable point to oxidation through hydroperoxidation. Also decomposition of the formed fuel hydroperoxide has been reviewed. The most probable decomposition products have been identified. The calculations have shown that both the bridgehead hydroperoxide and the tertiary hydroperoxide prefer the carboxylic acid (ester)-alkane decomposition mechanism. 3-cyclopentyl-tetrahydropyran-2-one and 4-ethyl-hexahydrocyclopenta[b]pyran-2(*3H*)-one have been found to be the most feasible decomposition products of hydroperoxides.

Chapter-III is about another significant aviation fuel, JP-900. It has also been studied in this perspective. Carbon center numbered as “2” is found to be the most vulnerable point to oxidation through hydroperoxidation to produce its corresponding hydroperoxide. The decompositions of thermodynamically stable hydroperoxides have been studied. The calculations have shown that some hydroperoxides prefer the carboxylic acid (ester)-alkane; whereas some hydroperoxides favors the ketone-alcohol decomposition mechanism.

Chapter-IV focuses on explosive, 1,3,3-trinitroazetidine, TNAZ. The explosive properties of TNAZ and its derivatives have been studied. A decrease in the sensitivity of TNAZ has been tried by making molecular level changes on the molecule. The nitro groups have been converted to nitroso and amino groups. It has been proved that molecular modification is a functioning method in both desensitization of TNAZ. The isomeric compounds having one nitro, one nitroso and one amino group not only have the highest power index values but also are optimum structures in performance and the most insensitive isomer group in the present study.

Chapter-V is on explosive TACOT, and its 4 novel benzofuroxan derivatives. The explosive properties of both TACOT and 4 benzofuroxan isomers have been determined and compared with TACOT (an existing molecule). The detonation performance analysis showed that z-DBBD and its isomers are better than TACOT and all (compounds 1-4) are as successful as RDX. These compounds have greater density values than TACOT. Therefore, they shall be preferred where high density explosive is necessary.

Chapter-VI concerns an explosive, FOX-7, 1, 1-diamino-2,2-dinitroethylene. The effects of further nitration of the amino groups on the molecule and effects of epoxidation of the double bond in the middle of the molecule on the explosive performance have been investigated. All the six compounds in the present article are potential candidates for high explosives. It has been shown that epoxidation is a better method than further nitration in the enhancement of explosive properties of FOX-7. Each epoxide derivatives have higher detonation velocity and pressure than its parent molecule.

Chapter VII deals with the design of novel explosives based on parabanic acid structures. The great magnitude of the calculated density of parabanic acid and its high nitrogen content has inspired us to investigate the parabanic acid frame. A series of molecules have been designed by nitration and imination. It has been shown that nitration of parabanic acid is a beneficial method in the enhancement of ballistic properties. Whereas, imination of carbonyl group is not a convenient method in the improvement of explosive properties; but nitration of the formed imine group is an effective way of increasing both the detonation velocity and pressure.

An explosive engineer should evaluate the explosive performance, power index and sensitivity of explosives prior to use. He should decide the employment of an explosive on the basis of these properties according to the requirements of the system. For instance, if sensitivity is required as in the case of detonator use, sensitive explosives (See Figure 8-1) shall be used.

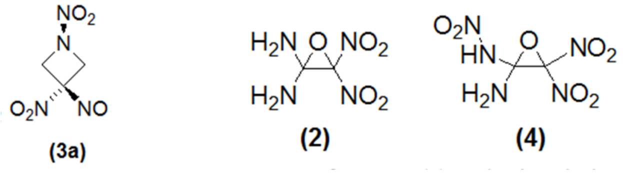

(3a) (2) (4)

Chapter-4 **Chapter-6**

Figure 8-1. Examples of Sensitive Explosives

If higher detonation velocity and pressure are essential as in the case of munition use, the compounds with great detonation values shall be employed. The examples from thesis work are listed in Figure 8-2.

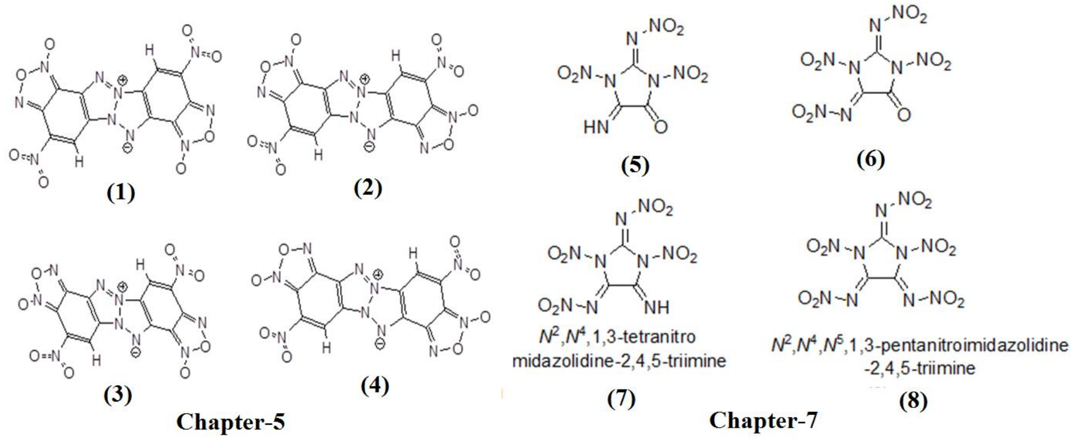

Figure 8-2. Examples of explosives with high detonation velocity and pressure

If high amount of hot gases is required as in the case of gas generators of rocket motors, the explosives with high power index (see Figure 8-3) shall be employed.

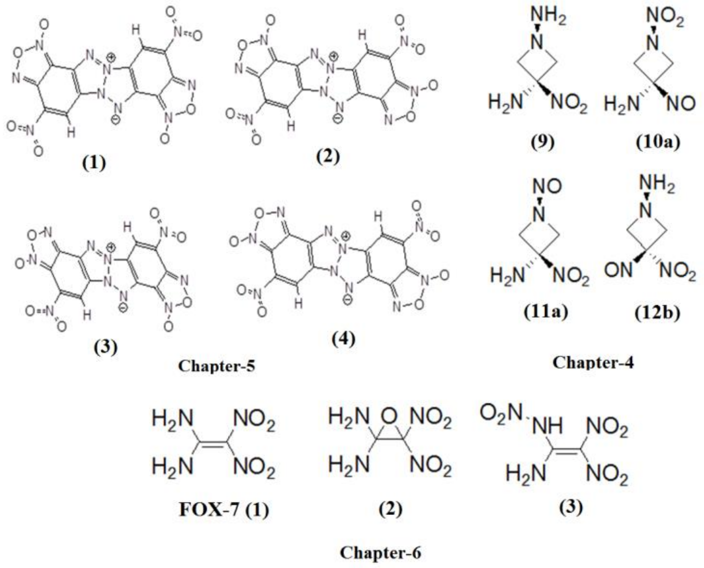

Figure 8-3. Examples of explosives with high power index values.

If insensitive explosives are required for safety reasons, the explosive with high BDEs shall be employed. Some examples are shown in Figure 8-4.

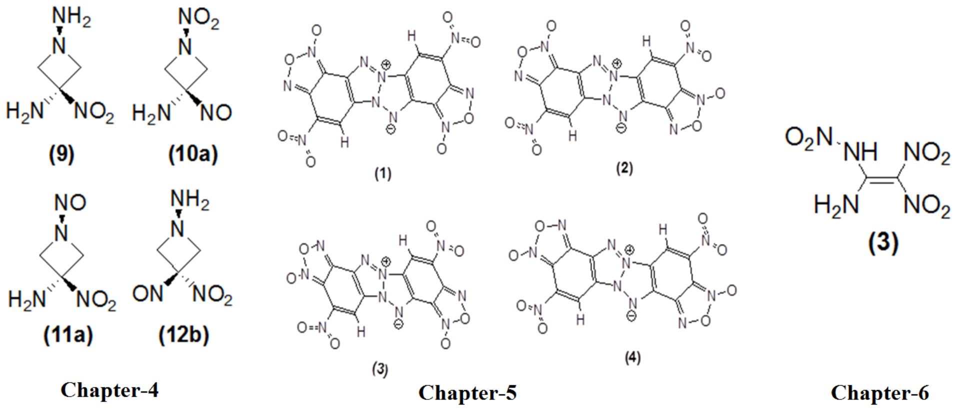

Figure 8-4. Examples of explosives with high BDE values.

REFERENCES

[1] Akhavan, J., *The Chemistry of Explosives*, The Royal Society of Chemistry, Cambridge 1998.

[2] Sprengel, H., XXXII.—On a new class of explosives which are non-explosive during their manufacture, storage, and transport, *J. Chem. Soc.*, 1873,26: 796-808.

[3] Abel, F. A., XLVI.—Researches on gun-cotton.—Second memoir. On the stability of gun-cotton, *J. Chem. Soc.*, 1867, 20: 505-576.

[4] Silberrad, O., Farmer, R. C., CLXXI.—The hydrolysis of “nitrocellulose” and “nitroglycerine”, *J. Chem. Soc., Trans.*, 1906, 89: 1759-1773.

[5] Noy, M. J., Sujansky, V. J., *Anfo Composition*, Patent no: WO 1999061395 A1.

[6] Mills, E. J., XVIII.—On nitro-compounds. (Part. I), *J. Chem. Soc.*, 1864, 17: 153-164.

[7] Mitra, B. N., Srinivasan, M., Estimation of tetryl, alone or in mixtures with TNT by ferrous ammonium sulphate, *Analyst*, 1945,70: 418-419.

[8] Smith, G. C., *TNT. Trinitrotoluenes and Mono- and Dinitrotoluenes, Their Manufacture and Properties*, New York, 1918, pp. 17-18.

[9] Herz E. V., *Explosives*, Patents no: 1402693, 1922.

[10] Wright, G. E. S., *Purification of Cyclotetramethylene Teranitramine*, Patent no: 3853847, 1974.

[11] Cooper, P. W., *Explosives Engineering*, New York: Wiley-VCH, 1996.

[12] Alam, N., *Dictionary of Explosions & Explosives*, Tisha Printers, Bangladesh, 2005.

[13] Türker, L., Variş, S., A Review of Polycyclic Aromatic Energetic Materials, *Polycyclic Aromatic Compounds*, 2009, 29: 228–266.

[14] Türker, L., Gümüş, S., Atalar, T., Çamur, Y., Theoretical Treatment of Some Novel Nitropyrimidines, in Barey, P. B., *New Research on Hazardous Materials*, 2007, pp. 371-404.

[15] Lothrop, W. C., Handrick, G. R., The Relationship between Performance and Constitution of Pure Organic Explosive Compounds, *Chem. Reviews*, 1949, 44: 419-445.

[16] Schmidt, A., Chimie et Industrie, 1952, 67: 253.

[17] Stettbacher, A., Die Sensibilität der Azide, *Angew. Chem*. 1917, 30: 33-39.

[18] T. Urbanski, *Chemistry and technology of explosive*, Warszawa, Vol. 10, 1961,pp.1-3,

[19] Shackelford, S. A., J. de Physique IV, 1995, C4, 485-499.

[20] Atalar, T., *Molecular Design of Some Potential Explosives*, Ph.D. Thesis, Department of Chemistry , METU, January 2009.

[21] Meyer, R., Köhler, J., Homburg, A., *Explosives, 6th edition*, Wiley-VCH & Co. KGaA, Weinheim, 2007.

[22] Altgilbers, L. L., Baird, J., Freeman, B. L., Cooper, Lynch, C. S., Explosive Pulsed Power, Imperial College Press, Singapore, 2011.

[23] Politzer, P. A., Murray, J. S., *Detonation, Combustion Theoretical and Computational Chemistry*, Vol. 13, Chapter 7, Elsevier, 2003.

[24] Fickett, W., Davis, W. C., *Detonation Theory and Experiment*, University of California Press, Berkeley, 1979. 130

[25] Andersen, W. H., Comments on “The chemistry of detonations, *Combustion and Flame,* 1982, 45: 309-316.

[26] Chapman, D. L., On the rate of explosion in gases, *Philos Mag*, 1899, 47: 90-95.

[27] Deal, W. E, Measurement of Chapman-Jouguet Pressure for Explosives, *J. Chem. Phys.* 1957, 27: 796-800.

[28] Dremin, A. N., Towards detonation theory, *Journal de Physique*, 1995, 5, C4: 259-276.

[29] Cowan, R. D., Fickett W., Calculation of the Detonation Products of Solid Explosives with the Kistiakowsky-Wilson Equation of State, *J. Chem. Phys.* 1956, 24: 932.

[30] Muthurajan, H., Sivabalan R., Talawar, M.B., Asthana, S. N., Computer simulation for prediction of performance and thermodynamic parameters of high energy materials, *Journal of Hazardous Materials*, 2004, A112: 17–33.

[31] Martin, A. R., Yallop, H. J., The correlation of explosive power with molecular structure, *Journal of Applied Chemistry*, 1959, 9, Issue 6: 310–315.

[32] Zel'dovich, Y., Kompaneets, A.S., *Theory of Detonation,* Academic Press. 1960, pp. 208–210.

[33] Hougen, O. A., Watson, K., Ragatz R., *Chemical Process Principles*. John Wiley & Sons. 1954, pp. 66–67.

[34] Anderson, H.V., *Chemical Calculations*. McGraw-Hill. 1955, pp. 206.

[35] Keshavarz, M. H., Simple procedure for determining heats of detonation, *Thermochimica Acta,* 2005, 428: 95-99.

[36] Labanowski, J., Andzelm, J., *Density Functional Methods in Chemistry*, Springer-Verlag, Berlin, 1991.

[37] Politzer, P., Seminario, J. M., *Theoretical and Computational Chemistry*, Vol. 1, Elsevier Scientific,Amsterdam, 1995.

[38] Kamlet, M. J., Jacobs, S. F., Chemistry of Detonations. I. A Simple Method for Calculating Detonation Properties of C H N O Explosives, *J. Chem. Phys.*, 1968, 48: 23.

[39] Kamlet, M. J., Ablard, J. E., Chemistry of Detonations. II. Buffered Equilibria, *J. Chem. Phys.*, 1968, 48: 36-42.

[40] Kamlet, M. J., Dickenson, C., Chemistry of Detonations. III. Evaluation of the Simplified Calculational Method for Chapman-Jouguet Detonation Pressures on the Basis of Available Experimental Information, *J. Chem. Phys.* 1968, 48: 43.

[41]. Kamlet, M. J., Hurwitz, H. J., Chemistry of Detonations. IV. Evaluation of a Simple Predictional Method for Detonation Velocities of C–H–N–O Explosives, *J. Chem. Phys*. 1968, 48: 3685-3692.

[42] Hurwitz, H. J., Kamlet, M. J., The chemistry of detonations. V. Pressures of CHNO explosives at various stages of the isentropic expansion, Israel J. Tech. 1968, 7: 431.

[43] Kamlet, M. J., Short, J. M., The chemistry of detonations. VI. A “Rule for Gamma” as a criterion for choice among conflicting detonation pressure measurements, *Combust. Flame,* 1980, 38: 221.

[44] Politzer, P., Lane, P., Grice, E. M., Concha, M. C., Redfren, P. C., Comparative Computational analysis of some nitramine and difluoroamine structures, Dissociation energies and heats of formation, *J. Mol. Struct. (THEOCHEM)*, 1995, 338: 249-256.

[45] Tarver, C.M., Density estimations for explosives and related compounds using the group additivity approach, *J. Chem. Eng. Data*, 1979, 24 (2): 136-145.

[46] Keshavarz, M. H., New method for calculating densities of nitroaromatic explosive compounds, *Journal of Hazardous Materials*, 2007, 145: 263-269.

[47] Qiu, L., Xiao, H. M., Ju, X. H., Gong, X. D., Theoretical study of the structures and properties of cyclic nitramines: tetranitrotetraazadecalin (TNAD) and its isomers, *Int. J. Quantum Chem.*, 2005, 105: 48–56.

[48] Xu, X. J., Xiao, H. M., Gong, X. D., Ju, X. H., Chen, Z. X., Theoretical studies on the vibrational spectra, thermodynamic properties, detonation properties, and pyrolysis mechanisms for polynitroadamantanes, *J. Phys. Chem.* 2005, A109: 11268–11274.

[49] Qiu, L., Xiao, H., Gong, X., Ju, X., Zhu, W., Theoretical studies on the structures, thermodynamic properties, detonation properties and pyrolysis mechanisms of spiro nitramines, *J. Phys. Chem.* 2006, A110: 3797–3807.

[50] Chung, G. S., Schimidt, M. W., Gordon, M. S., An *ab initio* study of potential energy surfaces for N8 isomers, *J. Phys. Chem.*, 2000, A104: 5647–5650.

[51] Xiao, J. J., Zhang, J., Yang, D., Xiao, H. M., DFT comparative studies on the structures and properties of heterocyclic nitramines, *Acta Chim. Slovenica*, 2002, 60: 2110-2114.

[52] Eaton, P. E., Gilardi, R. L., Zhang, M. X., Polynitrocubanes: Advanced high density, high-enegy matrials, *Advanced Materials,* 2000, 12: 1143-1148.

[53] Cho, S. G., Park, B. S., Cho, J. R., Theoretical studies on the structure of 1,2,4,5-tetranitroimidazole, *Propellants, Explosives, Pyrotechnics*, 1999, 24: 343-348.

[54] Wang, G., Xiao, H., Ju, X., Gong, X., Calculation of detonation velocity, pressure, and electric sensitivity of nitro arenes on quantum chemistry, *Propellants*, *Explosives*, *Pyrotechnics*, 2006, 31: 361-368.

[55] Ling, Q., Theoretical study on the high energy density compound hexanitroazatricyclotetradecanedifuroxan, *Chinese Journal of Chemistry*, 2006, 24:1538-1546.

[56] Zhang, J. Z., Xiao, J., Xiao, H. Theoretical studies on heats of formation for cubylnitrates using density functional theory B3LYP method and semiemprical MO methods, *Internationa Journal of Quantum Chemistry*, 2001, 86 (3): 305-312.

[57] Macek, A., Sensitivity of Explosives, *Chem. Rev.*, 1962, 62 (1): 41–63.

[58] Kamlet, M. J., Adolph, H. G., The Relationship of Impact Sensitivity with Structure of Organic High Explosives. 11. Polynitroaromatic Explosives, *Propellants, Explosives and Pyrotechnics*, 1979, 4:30-34.

[59] Licht H. H., Performance and Sensitivity of Explosives, *Propellants*, *Explosives*, *Pyrotechnics*, 2000, 25: 126-132.

[60] *Ammunition and Explosives Safety Ashore,* Technical Report No: 278680, NAVSEA OP 5, Volume 1, U.S.A Navy NOSSA, 2009.

[61] Yallop , H. J., *Explosion Investigation* , The Forensic Science Society, UK and Scottish Academic Press , Scotland.1980.

[62] Agrawal, J. P., *High Energy Materials*, Wiley-Vch Verlag GmbH & Co. KGaA, Weinheim, 2010, pp:19-23.

[63] OZM Research, http://www.ozm.cz/en/sensitivity-tests/bfh-10-bam-fall-hammer-impact-sensitivity-test/, last visited on July 2013.

[64] Rice, B. M., Sahu, S., Owens F. J., Density functional calculation of bond dissociation energies for NO_2 scission in some nitroaromatic molecules, *J. Mol. Struct. (THEOCHEM)*, 2002, 583: 69–72.

[65] Owens, F. J., Calculation of energy barriers for bond rupture in some energetic molecules, *J. Mol. Struct. (THEOCHEM)*, 1996, 370: 11-16.

[66] Politzer P., Murray J. S., Relationships between dissociation energies and electrostatic potentials of C---NO_2 bonds: applications to impact sensitivities, *J. Mol. Struct. (THEOCHEM)*. 1996, 376: 419-424.

[67] Politzer, P., Lane, P. Comparison of density functional calculations of C-NO_2, N-NO_2 and C-NF_2 dissociation energies, *J. Mol. Struct. (THEOCHEM)*, 1996, 388: 51-55.

[68] Harris, N. J., Lammertsma, K., *Ab Initio* Density Functional Computations of Conformations and Bond Dissociation Energies for Hexahydro-1,3,5-trinitro-1,3,5-triazine, *J. Am. Chem. Soc.* 1997, 119: 6583-6589.

[69] Nadentla, R. R., Molecular Modeling: A powerful tool for drug design and molecular docking, Resonance, (2004) 51-60.

[70] Andrew Leach, Molecular Modelling: Principles and Applications (2nd Edition), Pearson-Prentice Hall, 2001.

[71] Jack Simons, An Introduction to Theoretical Chemistry, Cambridge University Press, 2003.

[72] Stewart, J. J. P., Encyl. Comput. Chem. 3 (1998) 2080.

[73] Holder, A. J., Encyl. Comput. Chem. 1 (1998) 8.

[74] Daan Frenkel, Berend Smit, Understanding Molecular Simulation, Second Edition: From Algorithms to Applications (Computational Science), 2001.

[75] Jensen, F., Introduction to Computational Chemistry, John Wiley & Sons, New York 1999.

[76] W. J. Hehre, L. Radom, P. v. R. Schleyer, and J. A. Pople, *Ab Initio* Molecular Orbital Theory", Wiley, New York, 1986.

[77] Levine, N., Quantum Chemistry, Prentice Hall, Englewood Cliffs, 1991.

[78]. Stubber, J. L., Paldus, J., Fundamental World of Quantum Chemistry, 1 (2003) 67.

[79] Li, X., Paldus, J., Recent Advances in Computational Chemistry, 3 (1997) 183.

[80] Muthurojan, H., Sivabalan, R., Talawar, M. B., Asthana, S. N., Computer simulation for prediction of performance and thermodynamic parameters of high energy materials, *Journal of Hazardous Materials*, 2004, A112:17-33.

[81] Stine, J. R., *Prediction of crystal densities of organic explosives by group additivity*, Los Alamos National Laboratory's Report, New Mexico, 1981.

[82] Lipkowitz, K. B., Boyd, D. B., Kohn-Sham Density Functional Theory: Predicting and Understanding Chemistry, In Reviews in Computational Chemistry, Volume 15, Volume 15 (eds K. B. Lipkowitz and D. B. Boyd), John Wiley & Sons, Inc., Hoboken, NJ, USA.

[83] Zhang, J., Xiao, H., Computational studies on the infrared vibrational spectra, thermodynamic properties, detonation properties, and pyrolysis mechanism of octanitrocubane, *Journal of Chemical Physics*, 2002, 116 (24): 10674.

[84] Liu, M. H., Chen, C., Hong, Y. S., Theoretical study on the detonation properties of energetic TNAD molecular derivatives, *Journal of Molecular Structure (THEOCHEM)*, 2004, 710: 207.

[85] Persson, P. A., *TIGER, WIN-a window PC code for computing explosive performance and thermodynamic properties*, in Proceedings of 2000 High-Tech Seminar, State of the Art Blasting Technology and Explosives Applications, 2000.

[86] Fried, L. E., *CHEETAH 1.39*, Lawrence Livermore National Laboratory 1996.

[87] Muthurajan, H., Sivalan, R., Talawar, M., B., Asthana, S. N., *Development of Computer Code for Qualitative Prediction of Heat of Formation of High Energetic Materials*, New Trends in New Research of Energetic Materials, 2007, 202.

[88] Sućeska, M., Evaluation of Detonation Energy from EXPLO5 Computer Code Results, *Propellants, Explos. Pyrotech.* 1999, 24: 280-285.

[89] *Gaussian 03, Revision C.02*, Frisch, M. J.; Trucks, G. W.; Schlegel, H. B.; Scuseria, G. E.; Robb, M. A.; Cheeseman, J. R.; Montgomery, Jr., J. A.; Vreven, T.; Kudin, K. N.; Burant, J. C.; Millam, J. M.; Iyengar, S. S.; Tomasi, J.; Barone, V.; Mennucci, B.; Cossi, M.; Scalmani, G.; Rega, N.; Petersson, G. A.; Nakatsuji, H.; Hada, M.; Ehara, M.; Toyota, K.; Fukuda, R.; Hasegawa, J.; Ishida, M.; Nakajima, T.; Honda, Y.; Kitao, O.; Nakai, H.; Klene, M.; Li, X.; Knox, J. E.; Hratchian, H. P.; Cross, J. B.; Bakken, V.; Adamo, C.; Jaramillo, J.; Gomperts, R.; Stratmann, R. E.; Yazyev, O.; Austin, A. J.; Cammi, R.; Pomelli, C.; Ochterski, J. W.; Ayala, P. Y.; Morokuma, K.; Voth, G. A.; Salvador, P.; Dannenberg, J. J.; Zakrzewski, V. G.; Dapprich, S.; Daniels, A. D.; Strain, M. C.; Farkas, O.; Malick, D. K.; Rabuck, A. D.; Raghavachari, K.; Foresman, J. B.; Ortiz, J. V.; Cui, Q.; Baboul, A. G.; Clifford, S.; Cioslowski, J.; Stefanov, B. B.; Liu, G.; Liashenko, A.; Piskorz, P.; Komaromi, I.; Martin, R. L.; Fox, D. J.; Keith, T.; Al-Laham, M. A.; Peng, C. Y.; Nanayakkara, A.; Challacombe, M.; Gill, P. M. W.; Johnson, B.; Chen, W.; Wong, M. W.; Gonzalez, C.; and Pople, J. A.; Gaussian, Inc., Wallingford CT, 2004.

[90] *SPARTAN 06*, Wavefunction Inc., Irvine CA, USA.

[91] *Hyperchem Program*, Hypercube, Canada, 1996.

[92] Stewart, J. J. P., Optimization of parameters for semiempirical methods I. Method, *J. Comput. Chem.* 1989, 10: 209-220.

[93] Leach, A. R., *Molecular Modeling*; Pearson: Essex, 2001.

[94] Fletcher, P. *Practical Methods of Optimization*; second edition, Wiley: Sussex, 1987.

[95] Kohn, W., Sham, L. J., Self-Consistent Equations Including Exchange and Correlation Effects, *Phys. Rev.* 1965, 140: A1133-A1138.

[96] Parr, G. R., Yang, W., *Density Functional Theory of Atoms and Molecules*, Oxford University Press: New York, 1989.

[97] Becke, A. D., Density-functional exchange-energy approximation with correct asymptotic behavior, *Phys. Rev.* 1988, A38: 3098-3100.

[98] Vosko, S. H., Vilk, L., Nusair, M. Accurate spin-dependent electron liquid correlation energies for local spin density calculations: a critical analysis, *Can. J. Phys.*, 1980, 58: 1200-1211.

[99] Lee, C., Yang, W., Parr, R. G. Development of the Colle-Salvetti correlation-energy formula into a functional of the electron density, *Phys. Rev. B.,* 1988, 37: 785-789.

[100] Boys, S. F., Bernardi, F. Calculation of Small Molecular Interactions by Differences of Separate Total Energies - Some Procedures with Reduced Errors, *Mol. Phys.,* 1970, 19: 553-562.

[101] The Coordinating Research Council, Inc, *Handbook of aviation fuel properties.* Coordinating Research Council (CRC) ATLANTA GA; 1983. CRC Report No: 530.

[102] Botteri, B.P., Cretcher, R., Fultz, J.R., Lander, H. R. *A review and analysis of the safety of jet fuel. Wright-Patterson, Air Force Aero Propulsion Laboratory,* Research and Technology Division, Air Force Systems Command, Ohio; 1966 March. Report No: AFAPL-TR-66-9.

[103] Maurice, L, Q, Lander, H., Edwards, T., Harrison, W. E., Advanced aviation fuels: A look ahead via a historical perspective. *Fuel,* 2001, 80:747-56.

[104] Milton, B. E., Pianthong, K., Pulsed, supersonic fuel jets: A review of their characteristics and potential for fuel injection. *Int. J. Heat Fluid*, 2005, Fl, 26:656-71.

[105] Lander, H., Nixon, A. C., Endothermic fuels for hypersonic vehicles. *J Aircraft,* 1971, 8: 200-07.

[106] Maurice, L. Q., Edwards, J. T., Griffiths, J.F., *Liquid hydrocarbon fuels for hypersonic propulsion*. In: Curran ET and Murthy SNB, editors. *Scramjet Propulsion*, Reston, VA, American Institute of Aeronautics and Astronautics; 2000, p.757-822.

[107] Goodger, E. M., *Hydrocarbon fuels: Production, properties, and performance of liquids and gases.* New York: Wiley; 1975.

[108] Li, S.C., Varatharajan, B., Williams, F.A., *Chemistry of JP-10 ignition.* 39th AIAA Aerospace Sciences Meeting & Exhibit, Reno NV, 8-11 January 2001, 39: 2351-2356.

[109] Watkins, J.M., Mushrush, G. W., Hazlett, R. N., Beal, E.J., Hydroperoxide formation and reactivity in jet fuels. *Energy & Fuels,* 1989, 3: 231-236.

[110] Nadler, C., *Effect of oxidizing fuels on aircraft fuel system elastomers and sealants.* Naval Air Development center, Warminster, PA; 1980 May 20. Report No: NADC-80076-60.

[111] Jensen, R. K., Korceck, S., Mahoney, L. R. , Zinbo, M. J., Liquid-phase autoxidation of organic compounds at elevated temperatures. 1. The stirred flow reactor technique and analysis of primary products from n-hexadecane autoxidation at 120-180 ^{o}C. *J. Am. Chem. Soc.* 1979: 101(25): 7574-7584.

[112] Blaine, S., Savage, P. E., Reaction pathways in lubricant degradation. 2. n-Hexadecane autoxidation. *Ind. Eng. Chem. Res.*, 1991, 30:2185-2191.

[113] Yang, F., Guo, Y., Xing, Y., Li, D., Fang, W., Lin, R., Densities and viscosities of binary mixtures of JP-10 with n-octane or n-decane at several temperatures. *J. Chem. Eng. Data*, 2008, 53: 2237-2240.

[114] Hayashi, J., Nakahara, T., Kusakabe, K., Pyrolysis of polypropylene in the presence of oxygen, *Fuel Process. Technol*., 1988, 55:265-275.

[115] Nonhebel, D. C., Walton J. C., *Free-radical chemistry*. London: Cambridge University Press; 1974.

[116] Camara, L.D.T., Furtado, N. C., Monteiro, R. S., Aranda, D. A. G., Taft, C.A., Molecular orbital approach for investigating the kinetics of cracking hydroperoxides. *J. Mol. Struc. (Theochem)*, 2006, 776: 41-45.

[117] Song, C., Eser, S., Schobert, H. H., Hatcher, P., Pyrolytic degradation studies of a coal-derived and a petroleum-derived aviation jet fuel. *Energy Fuels*, 1993, 7: 234–243.

[118] Yu, J., Eser, S., Thermal decomposition of jet fuel model compounds under near-critical and supercritical conditions. 2. Decalin and tetralin. *Ind. Eng. Chem. Res.*, 1998, 4601–4608.

[119] Ullah, K. Aging of polymer in diesel and biodiesel blended fuel, M.Sc. Thesis, CHALMERS UNIVERSITY OF TECHNOLOGY, Sweden, 2013.

[120] Greene, F. D., Lowry, N. N., 9-Decalyl free radicals. Decomposition of *cis*- and *trans*-9-decalylcarbinyl hypochlorite. *J. Org. Chem.* 1967, 32: 875–881.

[121] Bartlett, P. D., Pincock, R. E., Rolston, J. H., Schindel, W. D., Singer, L. A., The stereochemistry of 9-decalyl free radicals. *J. Am. Chem. Soc.* 1965, 87 (12): 2590–2596.

[122] Lloyd, R. V., Williams, R. V., Bridgehead decalin radicals: Evidence for nonplanarity at the radical site, *J. Phys. Chem.* 1985, 89: 5379–5381.

[123] Pagoria, P. F., Lee, G. S., Mitchell, R. A., Schmidt, R. D., A review of energetic materials synthesis, *Thermochim. Acta.* 2002, 384: 187-204.

[124] Archibald, T. G., Gilardi, R., Baum, K., George, C. J., Synthesis and x-ray crystal structure of 1,3,3-trinitroazetidine,J. Org. Chem. 1990, 55: 2920-2924.

[125] Mckenny, L. R., Floyed, G. T., Synthesis and thermal properties of 1, 3-dinitro-3-(1′, 3′-dinitroazetidin-3′-yl) azetidine (tndaz) and its admixtures with 1, 3, 3-trinitroazetidine (TNAZ), *J. Energ. Mater.* 1999, 16: 199-235.

[126] Hiskey, A. M., Johnson, M. C., Chavez, E. D., Preparation of 1-substituted-3,3-dinitroazetidines, *J. Energ. Mater.* 1999, 17, 233-252.

[127] Zhang, J., Rongzu, H., Chunhua, Z., Guofu, F., Quihe, L., Thermal behavior of 1,3,3-trinitroazetidine *Thermochim. Acta.* 1997, 298: 31-35.

[128] Zeman, S., The thermoanalytical study of some aminoderivatives of 1,3,5-trinitrobenzene *Thermochim. Acta.* 1993, **216:**157-168.

[129] Keshavarz, M. H., Approximate prediction of melting point of nitramines, nitrate esters, nitrate salts and nitroaliphatics energetic compounds *J. Hazard. Mater.* 2006, 138: 448–451.

[130] Jalovy, Z., Zeman, S., Suceska, M., Vavra, P., Dudek, K., Rajic, J. M., 1,3,3-trinitroazetidine (TNAZ). Part I. Syntheses and properties, *J. Energ. Mater.* 2001, 19: 219–239.

[131] Talawar, M. B., Singh, A., Naik, N. H., Polke, B. G., Gore, G. M., Asthana, S. N., Gandhea, B. R., Effect of organic additives on the mitigation of volatility of 1-nitro-3,3′-dinitroazetidine (TNAZ): Next generation powerful melt cast able high energy material, *J. Hazard. Mater.* 2006, A134: 8–18.

[132] Sikder, A. K., Sikder, N., A review of advanced high performance, insensitive and thermally stable energetic materials emerging for military and space applications

J. Hazard. Mater. 2004, A112: 1–15.

[133] Iyer, S., Sarah, E. Y., Yoyee, M., Perz, R., Alster, J., Stoc, D., *TNAZ based composition C-4 development*, 11th Annual Working Group, Institute on Synthesis of High Density Materials (Proc.), Kiamesha Lakes, 1992.

[134] Doali, J. O., Fifer, R. A., Kruzezynski, D. I., Nelson, B. J., *The mobile combustion diagnostic fixture and its application to the study of propellant combustion Part-I. Investigation of the low pressure combustion of LOVA XM-39 Propellant*, Technical report No: BRLMR- 3787/5, US Ballistic Research Laboratory, Maryland, 1989.

[135] Agrawal, J. P., Recent trends in high-energy materials, *Prog. Energ. Combust. Sci.* 1998, 24/1: 1–30.

[136] Coburn, M. D., Hiskey, M. A., Archibald, T. G., Scale-up and waste-minimization of the Los Alamos process for 1,3,3-trinitroazetidine (TNAZ), *Waste Management.* 1997, 17: 143-146.

[137] Iyer, S., Explosive desensitization studies via chemical group modification. Nitroso-Derivatives of RDX and 3-Amino-TNT, *Propellants, Explosives, Pyrotechnics*, 1982, 7: 37-39.

[138] Sikder, N., Sikder, A. K., Bulakh, N. R., Gandhe, B. R., 1,3,3-Trinitroazetidine (TNAZ), a melt-cast explosive: synthesis, characterization and thermal behaviour *J. of Hazard. Mat.* 2001, 113: 35-43.

[139] Qui, L., Gong X., Wang, G., Zheng, J., Xiao, H. Looking for High Energy Density Compounds among 1,3-Bishomopentaprismane Derivatives with CN, NC, and ONO_2 Groups, *J. Phys. Chem. A*, 2009, 113 (11), 2607–2614.

[140] Rice, B. M., Hare, J. J., A, Quantum Mechanical Investigation of the Relation between Impact Sensitivity and the Charge Distribution in Energetic Molecules, *J. Phys. Chem. A, 2002, 106 (9): 1770–1783.*

[141] Shao J., Cheng X., Yang X. Density functional calculations of bond dissociation energies for removal of the nitrogen dioxide moiety in some nitroaromatic molecules, *J. Mol. Struct. (THEOCHEM).* 2005, 755: 127–130.

[142] Young, D. C., *Computational Chemistry: A Practical Guide for Applying Techniques to Real World Problems,* John Wiley & Sons, Inc. 2001.

[143] Murray, J. S., Concha, M. C., Politzer P., Links between surface electrostatic potentials of energetic molecules, impact sensitivities and $C-NO_2/N-NO_2$ bond dissociation energies, *Mol. Phys.* 2009, 107: 89-97.

[144] F. J. Owens, Calculation of energy barriers for bond rupture in some energetic molecules, *J. Mol Struct. (THEOCHEM),* 1996, 370: 11-16.

[145] Politzer, P., Murray, J. S., Relationships between dissociation energies and electrostatic potentials of C-NO2 bonds: applications to impact sensitivities, J. *Mol. Struct. (THEOCHEM),* 1996, 376, 419-424.

[146] Politzer, P., Lane, P., Comparison of density functional calculations of C-NO2, N-NO2 and C-NF2 dissociation energies, J. Mol. Struct. (THEOCHEM),1996, 388, 51-55.

[147] Harris, N. J., Lammertsma, K., *Ab initio* density functional computations of conformations and bond dissociation energies for hexahydro-1, 3, 5-trinitro-1, 3, 5-triazine, *J. Am. Chem. Soc.* 1997, 119, 6583-6589.

[148] Hilal, R., Elroby, S. A. K., DFT investigation of sites of protonation of antitumor of 2-(4-aminophenyl)benzazoles in the gas phase and in solution, *Int. J. Quantum Chem.* 2005, 103, 449-459.

[149] Fried, L. E., Manaa, M. R., Pagoria, P. F., Simpson, R. L., Design and synthesis of Energetic Materials, *Annu. Rev. Mater. Res.* 2001, 31: 291–321.

[150] Pearson, R. G., *Chemical Hardness. Applications from Molecules to Solids*, Wiley–VCH: Weinheim, 1997.

[151] Cramer, C. J., *Essentials of Computational Chemistry: Theories and Models*, 2nd ed.; Wiley: Chichester, West Sussex, England, 2004.

[152] Koch, W., Holthausen, M. C., *A Chemist's Guide to Density Functional Theory*, Second Edition, Wiley-VCH :Verlag GmbH, 2001.

[153] Manolopoulos, D. E., May, J. C., Down, S. E., Theoretical studies of the fullerenes: C34 to C70, *Chem. Phys. Lett.* 1991, 181: 105-111.

[154] Hess, B. A. Jr., Schaad, L. J., Hueckel molecular orbital .pi. resonance energies. Benzenoidhydrocarbons , *J. Am. Chem. Soc.* 1971, 93: 2413-2416.

[155] Pearson, R. G., *Hard and Soft Acids and Bases*, Dowden, Hutchinson and Ross, Stroudsburg, 1973.

[156] Haddon, R. C., Fukunaga, T., Unified theory of the thermodynamic and kinetic criteria of aromatic character in the [4n+2] annulenes, *Tetrahedron Lett.* 1980, 21: 1191-1192.

[157] Schmalz, T. G., Seitz, W. A., Klein, D. J., Hite, G. E., *Elemental carbon cages*, *J. Am. Chem. Soc.* 1988, 110: 1113-1127.

[158] Zhou, Z., Parr, R. G., Garst, J. F., Absolute hardness as a measure of aromaticity, *Tetrahedron Lett.* 1988, 29:4843.

[159] Zhou, Z., Parr, R. G., New measures of aromaticity: absolute hardness and relative hardness, *J. Am. Chem. Soc.* 1989, 111: 7371-7379.

[160] Zhou, Z., Parr, R. G., Activation hardness: new index for describing the orientation of electrophilic aromatic substitution, *J. Am. Chem. Soc.* 1990, 112:5720-5724.

[161] Liu, X., Schmalz, T. G., Klein, D. J., Favorable structures for higher fullerenes, *Chem. Phys. Lett.* 1992, 188: 550-554.

[162] Parr, R. G., Zhou, Z. Absolute hardness: unifying concept for identifying shells and subshells in nuclei, atoms, molecules, and metallic clusters, *Acc. Chem. Res.* 1993, 26: 256-258.

[163] Aihara, J., Oe, S., Yoshida, M., Ōsawa, E., Further test of the isolated pentagon rule: Thermodynamic and kinetic stabilities of C84 fullerene isomers, J. Comput. Chem. 1996, 17: 1387-1394.

[164] Sikder A. K., Maddala, G., Agrawal, J. P., Singh, H., Important aspects of behaviour of organic energetic compounds: a review, *J. Hazard. Mater.* 2001, A84: 1–26.

[165] Dong, H. S., Zhou, F. F., *Performance of High Energetic Explosive and Related Compounds*. Beijing: Science Press, 1989.

[166] Lowe–Ma, C. K., Structure of 2,4,8,10-tetranitro-2,4,8,10-tetraazaspiro[5.5]undecane (TNSU), an energetic spiro bicyclic nitramine, *Acta Crystallogr.* 1990, C46: 1029–1033.

[167] Mader, C. L., *Numerical Modeling of Explosives and Propellants*. New York: CRC Press, 1998.

[168] Wilcox, C. F., Zhang, Y. X., Bauer, S. H., The thermochemistry of TNAZ (1,3,3-trinitroazetidine) and related species: models for calculating heats of formation, J. *Mol. Struct. (THEOCHEM)*, 2000, 528, 95-109.

[169] Jadhav, H. S., Talawar, M. B., Dhavale, D. D., Asthana, S. N., Krishnamurthy, V. N., Alternate method for synthesis of 1,3,3-trinitroazetidine (TNAZ): Next generation melt castable high energy material, *Ind. Journal of Chem. Tech.* 2006, 13: 41-46.

[170] Hanson-Parr, D. M., Parr, T. P., Thermal properties measurements of solid rocket propellant oxidizers and binder materials as a function of temperature, *J. Energ. Mater.* 1999, 17, 1-48.

[171] Badgujar, D. M., Talawar, M. B., Asthana, S. N., Mahulikar, P. P., Advances in science and technology of modern energetic materials: An overview, *J. of Hazard. Mat.* 2008, 151: 289-305.

[172] Molchanova, M. S., Pivina, T. S., Arnautova, E. A., Zefirov, N. S., Computer-aided search for high-density energetic compounds among hydrogen-free heterocycles, *J. Mol. Struct. (THEOCHEM)*, 1999, 465: 11–24.

[173] Carboni, R. A., Castle, J. E., Dibenzo-1, 3a, 4, 6a-Tetraazapentalene - A new heteroaromatic system. J. Am. Chem. Soc. 1962, 84: 2453–2454.

[174] Carboni, R. A., Castle J. E., Kauer J. C., Simmons, H. E., Aromatic azapentalenes I.Dibenzo-1,3a,4,6a-tetraazapentalene and dibenzo-1,3a,6,6a-tetraazapentalene. New heteroaromatic systems. *J. Am. Chem. Soc.* 1967, 89: 2618–2625.

[175] Carboni, R. A., Kauer, J. C., Aromatic azapentalenes. III. 1,3a,6,6atetraazapentalenes, *J. Am. Chem. Soc.* 1967, 89: 2633–2637.

[176] Murphy, M. F., Coleburn, N. L. *A preliminary evaluation of TACOT, a new heat resistant explosive*, Defense Technical Information Center. Report No: AD0329452. 1961.

[177] Nair, U. R., Gore, G. M., Sivabalan, R., Pawar, S. J., Asthana, S.N., Venugopalan, S. Preparation and thermal studies on tetranitrodibenzotetraazapentalene (TACOT): A thermally stable high explosive. *J. Hazard. Mat.* 2007, 143:500–505.

[178] Agrawal, J. P., Hodgson, R. D., *Organic Chemistry of Explosives*, Wiley-VCH, 2007.

[179] Karen, L. A., Lawrence, H. M., William, P. N., William, S. W., Gilardi, R. High Nitrogen Explosives Part 2. , Technical Report No: NAWCWPNS TP 8277, Naval Air Warfare Center Weapons Division China Lake, Ca. 1996.

[180] Tan, B., Long, X., Peng, R., Li, H., Jin, B., Chu, S., Dong, H. Two important factors influencing shock sensitivity of nitro compounds: Bond dissociation energy of X–NO_2 (X = C, N, O) and Mulliken charges of nitro group, J. Hazard. Mat., 2010, 183: 908–912.

[181] Subramanian, G., Eck, G., Boyer, J. H., Stevens, E. D., Trudell, M. L. Synthesis of Benzotriazolo[1,2-*a*]benzotriazole Derivatives as New High Density, Insensitive Energetic Materials, *J. Org. Chem.* 1996, 61: 5801-5803.

[182] Millar, R. W., Philbin, S. P., Claridge, R. P., Hamid, J., Studies of Novel Heterocyclic Insensitive High Explosive Compounds: Pyridines, Pyrimidines, Pyrazines and Their Bicyclic Analogues, *Propellants, Explosives, Pyrotechnics*, 2004, 29: 81.

[183] Chapman, R. D., Wilson, W. S., Fronabarger, J.W., Merwin, L. H., Ostrom, G. S., Prospects of fused polycyclic nitroazines as thermally insensitive energetic materials, *Thermochim. Acta,* 2002, 384: 229.

[184] Singh, R. P., Verma, R. D., Meshri, D. T., Shreeve, J. M., Energetic Nitrogen-Rich Salts and Ionic Liquids, *Angew. Chem. Int. Edit*. 2006, 45: 3584-3601.

[185] Dorsett, H., Computational Studies of FOX-7, a New Insensitive Explosive, Weapons Systems Division Aeronautical and Maritime Research Laboratory, DSTO-TR-1054, 2000.

[186] Ostmark, H., Langlet, A., Bergman, H., Wingborg, N., Wellmar, U., Bemm, U., FOX-7-A new explosive with low sensitivity and high performance. In 11th international Symposium on Detonation (1998), pp. 31-08.

[187] Latypov, N.V., Bergman, J., Langlet, A., Wellmar, U., Bemm, U., Synthesis and reactions of 1,1-diamino-2,2-dinitroethylene, *Tetrahedron*, 1998, 54, 11525-11536

[188] Politzer, P., Concha, M. C., Grice, M. E., Murray, J. S., Lane, P. Computational investigation of the structures and relative stabilities of amino/nitro derivatives of ethylene, *J. Mol. Struct. (THEOCHEM),* 1998, 452: 75-83.

[189] Herve, G., Jacob, G., Latypov, N., The reactivity of 1,1-diamino-2,2-dinitroethene (FOX-7), *Tetrahedron*, 2005, 61, 6743-6748.

[190] Bemm, U., Östmark, H., 1,1-Diamino-2,2-dinitroethylene: a Novel Energetic Material with Infinite Layers in Two Dimensions, *Acta Crystallographica*, 1998, C54, 1997-1999.

[191] Teipel, U., *Energetic Materials Particle Processing and Characterization*, WILEY-VCH Verlag GmbH & Co. 2005

[192] Molchanova, M. S., Pivina, T. S., Arnautova, E. A., Zefirov, N. S., J. Mol. Struct. (THEOCHEM), 1999, 465: 11–24.

[193] a) Organic Syntheses, 1963, Coll. Vol. 4: 744; b) Organic Syntheses, 1957, Coll. Vol. 37:71.

[194] Ribeiro da Silva, M. D. M. C., Ribeiro da Silva, M. A.V., Freitas, V. L.S., Roux, M. V., Jimenez, P., Davalos J. Z., Cabildo, P., Claramunt, R. M., Elguero, J., Structural studies of cyclic ureas: 2. Enthalpy of formation of parabanic acid, *J. Chem. Thermodyn.,* 2008, 40, 1378–1385.

[195] Lewis, T. C., Tocher, D. A., Day, G. M., Price, S. L., A computational and experimental search for polymorphs of parabanic acid – a salutary tale leading to the crystal structure of oxo-ureido-acetic acid methyl ester, *Cryst. Eng. Comm.*, 2003, 5(2): 3–9.

[196] Ulrich, H., Sayigh, A. A. R., The Reaction of Oxalyl Chloride with Substituted ureas and Thioureas, *J. of Org. Chem.*, 1965, 2781-2873.

[197] Craven, B. M., McMullan, R. K., Charge density in parabanic acid from X-ray and neutron diffraction, *Acta Cryst.*, 1979, B35, 934-945.

APPENDIX A

THE CARTESIAN COORDINATES OF THE STRUCTURES CONSIDERED IN CHAPTER-2

The Cartesian Coordinates of JP-10 (ZPE=634.76 kj/mol)

	Coordinates		
Atom	**x**	**y**	**z**
C	-1.704300	-0.521100	1.494300
C	-0.251300	0.010900	1.449300
C	-0.342300	-1.393100	-0.333700
C	-0.186300	-0.003100	-0.996700
C	-1.768300	-1.485100	0.262300
C	-0.129300	0.972900	0.243300
C	1.121700	0.243900	-1.783700
C	1.205700	1.743900	0.107300
C	1.547700	1.669900	-1.392700
C	0.506700	-1.239100	0.950300
H	-1.816259	-1.107965	2.381968
H	-2.364966	0.299896	1.308867
H	0.063844	0.464503	2.365722
H	-0.110693	-2.193566	-1.004902
H	-0.975677	0.118332	-1.708766
H	-1.912515	-2.480766	0.626650
H	-2.452755	-1.071065	-0.448331
H	-0.886008	1.723416	0.338268
H	1.861331	-0.432581	-1.409242
H	0.880142	0.249021	-2.826064
H	1.954864	1.197052	0.640789
H	1.017360	2.768972	0.349490
H	2.610645	1.738361	-1.494485
H	0.915047	2.359302	-1.911714
H	0.322091	-2.062321	1.608424
H	1.511020	-0.975492	0.691935

JP-10-Hydroperoxide-A (ZPE=653.43 kj/mol)

	Coordinates		
Atom	**x**	**y**	**z**
C	-1.685605	-0.741368	0.895053
C	-0.233605	-0.213368	0.829053
C	-0.326605	-1.610368	-0.938947
C	-0.164605	-0.221368	-1.603947
C	-1.753605	-1.701368	-0.335947
C	-0.116605	0.760632	-0.370947
C	1.153395	0.019632	-2.376947
C	1.214395	1.536632	-0.495947
C	1.578395	1.445632	-1.989947
C	0.529395	-1.464368	0.339053
O	0.312395	0.235632	2.056053
O	-0.458605	1.406632	2.481053
H	-1.788189	-1.328619	1.783598
H	-2.348646	0.079264	0.716615
H	-0.102824	-2.410436	-1.613272
H	-0.949156	-0.101846	-2.321648
H	-1.897516	-2.697431	0.027438
H	-2.440124	-1.285630	-1.043587
H	-0.873632	1.511588	-0.282209
H	1.887219	-0.656263	-1.990207
H	0.923901	0.019425	-3.422047
H	1.958554	1.000664	0.055293
H	1.016881	2.563537	-0.269332
H	2.643074	1.508707	-2.075856
H	0.956843	2.133083	-2.524722
H	0.345319	-2.286663	0.998483
H	1.533465	-1.201741	0.078724
H	0.141549	2.155908	2.481053

JP-10-Hydroperoxide-B (ZPE=654.02 kj/mol)			
	Coordinates		
Atom	**x**	**y**	**z**
C	-1.44437	-0.99187	1.58763
C	-0.00837	-0.41487	1.51563
C	-0.06837	-1.87087	-0.22737
C	0.08963	-0.50387	-0.93537
C	-1.49837	-1.95987	0.36063
C	0.12063	0.50813	0.27163
C	1.41563	-0.29287	-1.70137
C	1.45863	1.27713	0.14763
C	1.88763	1.12513	-1.32437
C	0.77763	-1.66187	1.05163
O	-1.00737	1.39313	0.32963
O	-1.04037	2.19613	-0.88937
H	-1.52275	-1.57920	2.47859
H	-2.13346	-0.19248	1.41146
H	0.27827	0.08575	2.41681
H	0.16695	-2.69429	-0.86885
H	-0.68664	-0.39928	-1.66432
H	-1.64470	-2.95397	0.72838
H	-2.17818	-1.54920	-0.35639
H	2.12983	-0.98675	-1.30976
H	1.18889	-0.29141	-2.74707
H	2.18171	0.76768	0.74972
H	1.25363	2.31312	0.31966
H	2.95699	1.13715	-1.35934
H	1.32542	1.82556	-1.90593
H	0.61143	-2.47003	1.73292
H	1.77582	-1.38344	0.78517
H	-0.44021	2.94541	-0.88937

JP-10-Hydroperoxide-C (ZPE=655.28 kj/mol)			
	Coordinates		
Atom	**x**	**y**	**z**
C	-1.89071	-1.08742	1.25913
C	-0.43971	-0.59042	1.04813
C	-0.87971	-1.71642	-0.86987
C	-0.76271	-0.24842	-1.35587
C	-2.20371	-1.84542	-0.07487
C	-0.49671	0.53658	-0.01587
C	0.43529	0.06858	-2.29287
C	0.81129	1.33758	-0.25087
C	1.55529	0.65858	-1.41387
C	0.15729	-1.78542	0.27313
O	1.71529	1.37058	0.85213
O	1.07029	2.13358	1.91813
H	-1.88494	-1.80281	2.05480
H	-2.53084	-0.23176	1.31365
H	0.05931	-0.27766	1.94148
H	-0.78763	-2.41679	-1.67355
H	-1.63618	-0.00152	-1.92243
H	-2.35335	-2.87923	0.15698
H	-2.96069	-1.29948	-0.59816
H	-1.21956	1.25715	0.30533
H	0.79201	-0.86341	-2.67893
H	0.11855	0.83952	-2.96386
H	0.51430	2.34917	-0.43357
H	2.11955	-0.15636	-1.01091
H	2.04747	1.42246	-1.97879
H	0.02095	-2.68665	0.83358
H	1.12681	-1.52883	-0.09982
H	1.67044	2.88286	1.91813

JP-10-Hydroperoxide-D (ZPE=654.93kj/mol)

	Coordinates		
Atom	x	y	z
C	-1.85497	-1.11624	1.53434
C	-0.38897	-0.63324	1.42334
C	-0.57197	-2.11824	-0.28266
C	-0.39797	-0.76624	-1.01766
C	-1.98197	-2.14024	0.35834
C	-0.27397	0.25976	0.16734
C	0.89603	-0.60224	-1.85566
C	1.08003	0.97276	-0.04566
C	1.39103	0.81976	-1.54266
C	0.32003	-1.92724	0.96534
O	1.15403	2.30576	0.46734
O	0.18303	3.13276	-0.24566
H	-1.95981	-1.65201	2.45459
H	-2.49564	-0.28576	1.32280
H	-0.03596	-0.14565	2.30796
H	-0.38343	-2.95682	-0.91994
H	-1.20512	-0.65069	-1.71052
H	-2.14088	-3.11126	0.77878
H	-2.67672	-1.74501	-0.35301
H	-1.00497	1.03706	0.24697
H	1.62079	-1.29114	-1.47483
H	0.62119	-0.63183	-2.88934
H	1.84730	0.51533	0.54336
H	2.45382	0.83695	-1.66542
H	0.77887	1.51178	-2.08236
H	0.13371	-2.71190	1.66854
H	1.32262	-1.70518	0.66470
H	0.78318	3.88204	-0.24566

JP-10-Hydroperoxide-E (ZPE=654.70 kj/mol)

	Coordinates		
Atom	x	y	z
C	-2.25803	-0.89018	2.08761
C	-0.79003	-0.41118	1.96561
C	-1.03803	-1.77618	0.16761
C	-0.88003	-0.37918	-0.47939
C	-2.42603	-1.83618	0.85261
C	-0.70703	0.57082	0.77361
C	0.38097	-0.16618	-1.34439
C	0.64497	1.28982	0.57261
C	0.88297	1.22982	-0.94339
C	-0.10703	-1.67618	1.39661
O	2.26897	1.46582	-1.17139
O	2.45397	1.56782	-2.61539
H	-2.34200	-1.48283	2.97452
H	-2.89701	-0.04345	1.94747
H	-0.40386	0.00929	2.87058
H	-0.87461	-2.56901	-0.53212
H	-1.71008	-0.21381	-1.13404
H	-2.57481	-2.83195	1.21484
H	-3.14210	-1.39489	0.19124
H	-1.42625	1.34813	0.92658
H	1.11545	-0.88054	-1.03593
H	0.07351	-0.12312	-2.36836
H	1.40304	0.70279	1.04763
H	0.51462	2.31651	0.84429
H	0.37152	1.96208	-1.53255
H	-0.27810	-2.50606	2.05001
H	0.88760	-1.44049	1.08026
H	3.05413	2.31709	-2.61539

JP-10-Hydroperoxide-F (ZPE=654.58kj/mol)			
	Coordinates		
Atom	x	y	z
C	-1.88643	-0.89804	2.02874
H	-2.07643	-1.42104	2.97174
C	-0.41543	-0.41904	1.95374
H	-0.04143	0.00596	2.88974
C	-0.58643	-1.83404	0.18774
H	-0.36743	-2.68304	-0.46626
C	-0.39443	-0.45604	-0.49126
C	-2.00343	-1.87304	0.80974
H	-2.77543	-1.56704	0.09574
H	-2.25343	-2.88604	1.14074
H	-2.59243	-0.06304	1.97274
C	-0.28043	0.52796	0.73774
H	-1.25743	-0.21304	-1.12026
C	0.91257	-0.27704	-1.29626
H	1.65557	-1.03204	-1.00726
H	0.77757	-0.36404	-2.37826
H	-1.08343	1.27196	0.73474
C	1.08457	1.23996	0.57774
H	1.86357	0.73796	1.16374
H	1.06457	2.28696	0.89274
C	1.44057	1.10796	-0.90826
H	2.50757	1.24596	-1.12326
C	0.29157	-1.69904	1.45274
H	1.35557	-1.56004	1.23874
H	0.18757	-2.54604	2.13974
O	0.70657	2.16496	-1.54726
O	1.03157	2.12696	-2.96826
H	0.12569	1.97905	-3.24952

JP-10-Hydroperoxide-G (ZPE=656.40 kj/mol)			
	Coordinates		
Atom	x	y	z
C	-2.53545	-1.08011	0.87000
C	-1.25345	-1.61211	0.18100
C	-1.15545	0.61789	-0.21300
C	0.00455	0.38589	0.79600
C	-2.47345	0.45889	0.58900
C	-0.03745	-1.17011	1.03300
C	1.46155	0.68489	0.35300
C	1.34555	-1.72411	0.58300
C	2.03555	-0.61411	-0.23300
C	-1.17345	-0.68011	-1.04700
O	1.67855	1.86989	-0.41600
O	1.15755	1.67989	-1.76800
H	-2.43371	-1.23050	1.92448
H	-3.38220	-1.47942	0.35187
H	-1.26155	-2.66838	0.01034
H	-1.05782	1.54269	-0.74226
H	-0.16808	1.05770	1.61072
H	-2.35596	0.96343	1.52524
H	-3.28823	0.71215	-0.05667
H	-0.16946	-1.52141	2.03503
H	2.02484	0.96978	1.21697
H	1.92891	-1.87815	1.46667
H	1.15932	-2.53974	-0.08405
H	3.08166	-0.64257	-0.00996
H	1.70227	-0.69422	-1.24661
H	-0.23225	-0.80837	-1.53953
H	-2.08300	-0.73904	-1.60749
H	1.66393	0.86431	-1.76800

JP-10-Hydroperoxide-H (ZPE=654.21kj/mol)			
	Coordinates		
Atom	x	y	z
C	-1.85375	-0.38736	2.09580
H	-2.04575	-0.89836	3.04580
C	-0.40675	0.15964	2.05080
C	-0.46075	-1.30336	0.31380
H	-0.17875	-2.14736	-0.32120
C	-0.31975	0.06764	-0.38820
C	-1.89175	-1.39336	0.89780
H	-2.65775	-1.13936	0.15680
H	-2.10475	-2.41036	1.24480
H	-2.59775	0.41164	2.00180
C	-0.27775	1.08264	0.81580
H	-1.16375	0.26264	-1.06120
C	0.98225	0.30664	-1.18620
H	1.75425	-0.42336	-0.90520
H	-1.11175	1.79164	0.77280
C	1.06225	1.84664	0.66780
H	1.84225	1.37264	1.27680
H	0.99125	2.88664	1.00180
C	1.42425	1.73164	-0.82320
H	2.47925	1.91664	-1.04020
H	0.83225	2.43864	-1.41820
C	0.37325	-1.09536	1.59980
H	1.43525	-0.91336	1.41180
H	0.28925	-1.93036	2.30380
H	-0.07675	0.62364	2.98480
O	0.81825	0.26364	-2.60220
O	0.54625	-1.12336	-2.96220
H	0.71818	-1.37537	-2.05196

JP-10-Hydroperoxide-I (ZPE=653.60 kj/mol)			
	Coordinates		
Atom	x	y	z
C	-1.43037	-0.48580	1.95809
H	-1.58437	-0.97880	2.92309
C	-0.00437	0.11120	1.87209
C	-0.04337	-1.39280	0.16809
H	0.25163	-2.24080	-0.45291
C	0.06063	-0.02780	-0.56091
C	-1.45637	-1.51780	0.78309
H	-2.23737	-1.30380	0.05209
H	-1.61337	-2.53480	1.15509
H	-2.20137	0.28420	1.85609
C	0.07063	1.01520	0.61909
C	1.35263	0.22920	-1.36191
H	2.15563	-0.42280	-0.99891
H	1.20763	0.00020	-2.42091
H	-0.81037	1.66020	0.54409
C	1.35763	1.85020	0.42409
H	2.17363	1.43520	1.03109
H	1.22863	2.89120	0.73409
C	1.69763	1.69920	-1.07091
H	2.73463	1.95720	-1.30591
H	1.05163	2.35520	-1.66691
C	0.81163	-1.12380	1.42809
H	1.86363	-0.90680	1.21909
H	0.77263	-1.94880	2.14809
H	0.32863	0.60620	2.79009
O	-1.09637	0.31320	-1.33791
O	-1.23237	-0.67680	-2.40991
H	-0.33056	-0.87754	-2.14906

JP-10-Hydroperoxide-J (ZPE=654.51kj/mol)			
	Coordinates		
Atom	**x**	**y**	**z**
C	-1.76813	0.130816	1.624737
C	-0.33813	0.728816	1.591737
C	-0.30613	-0.76518	-0.09626
C	-0.16713	0.577816	-0.85426
C	-1.75613	-0.87818	0.435737
C	-0.21613	1.620816	0.329737
C	1.173868	0.829816	-1.58426
C	1.083868	2.451816	0.204737
C	1.509868	2.295816	-1.26626
C	0.493868	-0.50918	1.201737
O	0.117868	-1.80018	-0.96526
O	0.099868	-3.06218	-0.22526
H	-1.87525	-0.42567	2.532346
H	-2.46099	0.912047	1.391235
H	-0.07786	1.253861	2.486995
H	-0.91201	0.621572	-1.62117
H	-1.89028	-1.86287	0.832332
H	-2.41848	-0.51105	-0.32017
H	-1.01821	2.328834	0.346633
H	1.918816	0.215006	-1.12387
H	0.993964	0.755067	-2.63638
H	1.830168	1.983861	0.812154
H	0.831206	3.479245	0.364269
H	2.572478	2.410554	-1.31722
H	0.875394	2.917794	-1.86249
H	0.320511	-1.30101	1.900208
H	1.494843	-0.2164	0.962515
H	0.606242	-3.87777	-0.22526

JP-10-Hydroperoxide-K (ZPE=653.97 kj/mol)			
	Coordinates		
Atom	**x**	**y**	**z**
C	-1.22037	0.11603	1.36724
C	0.21363	0.68403	1.23124
C	0.05863	-0.75597	-0.51476
C	0.16463	0.62603	-1.21276
C	-1.35437	-0.80497	0.11924
C	0.24963	1.62903	0.00524
C	1.43763	0.87803	-2.05376
C	1.55563	2.43203	-0.20676
C	1.84163	2.32403	-1.71576
C	0.97163	-0.55897	0.71624
O	-1.89137	-2.10797	0.37024
O	-1.04737	-2.81897	1.32824
H	-1.25248	-0.50079	2.24097
H	-1.91086	0.92617	1.25860
H	0.56648	1.16478	2.11965
H	0.27188	-1.58818	-1.15262
H	-0.65279	0.71983	-1.89682
H	-2.10289	-0.46004	-0.56313
H	-0.52258	2.36042	0.12206
H	2.20579	0.22917	-1.68795
H	1.15925	0.84847	-3.08649
H	2.34045	1.92200	0.31173
H	1.34752	3.45820	0.01360
H	2.89788	2.41545	-1.86029
H	1.17250	2.98344	-2.22795
H	0.84136	-1.37250	1.39895
H	1.95435	-0.27929	0.39853
H	-0.54100	-3.63456	1.32824

JP-10-Hydroperoxide-L (ZPE=653.19kj/mol)			
	Coordinates		
Atom	x	y	z
C	0.21053	-1.07968	1.73279
C	-0.34047	0.36632	1.67879
C	1.04953	0.27832	-0.12021
C	-0.34947	0.39532	-0.76721
C	1.19753	-1.12268	0.52479
C	-1.31447	0.46532	0.47979
C	-0.61247	1.68632	-1.57821
C	-2.09547	1.79332	0.33179
C	-2.03647	2.11232	-1.17521
C	0.90053	1.13232	1.16279
O	0.80553	-2.23068	-0.28721
O	1.73753	-2.28968	-1.41521
H	0.77999	-1.18598	2.63241
H	-0.59649	-1.75173	1.52790
H	-0.79179	0.68614	2.59472
H	1.82056	0.51411	-0.82363
H	-0.47399	-0.41354	-1.45652
H	2.23271	-1.28392	0.74229
H	-2.05991	-0.29400	0.59232
H	0.06521	2.43670	-1.22811
H	-0.63047	1.42356	-2.61529
H	-1.54869	2.55390	0.84893
H	-3.11710	1.60222	0.58608
H	-2.11024	3.17334	-1.29219
H	-2.72895	1.46931	-1.67712
H	1.73150	0.95713	1.81371
H	0.62659	2.13336	0.90246
H	2.24390	-3.10527	-1.41521

JP-10-Hydroperoxide-M (ZPE=654.42 kj/mol)			
	Coordinates		
Atom	x	y	z
C	-1.28955	-0.27297	0.83111
C	0.17245	0.21503	0.76311
C	0.02645	-1.22497	-0.98489
C	0.21345	0.14203	-1.68589
C	-1.39655	-1.25297	-0.37389
C	0.28645	1.14603	-0.46889
C	1.52945	0.34103	-2.47189
C	1.63045	1.89903	-0.62789
C	1.97545	1.77203	-2.12289
C	0.88945	-1.06697	0.28711
O	-1.56155	-1.07197	1.98711
O	-1.46655	-0.20097	3.15411
H	-1.95310	0.56637	0.84114
H	0.52023	0.67798	1.66289
H	0.23036	-2.04903	-1.63624
H	-0.56886	0.26174	-2.40601
H	-1.57268	-2.23531	0.01198
H	-2.07229	-0.82926	-1.08716
H	-0.46673	1.90202	-0.39079
H	2.25554	-0.33508	-2.07118
H	1.29435	0.31673	-3.51547
H	2.37285	1.36279	-0.07455
H	1.45194	2.93344	-0.42050
H	3.03962	1.82130	-2.22291
H	1.35494	2.45430	-2.66546
H	0.68669	-1.86938	0.96529
H	1.89874	-0.83863	0.01493
H	-0.86640	0.54830	3.15411

JP-10-Hydroperoxide-N (ZPE=655.13kj/mol)

	Coordinates		
Atom	**x**	**y**	**z**
C	-1.11824	-0.68655	1.252632
C	0.314763	-0.09855	1.210632
C	0.271763	-1.53955	-0.54637
C	0.468763	-0.16455	-1.22937
C	-1.17524	-1.61155	-0.00037
C	0.496763	0.835447	-0.00937
C	1.808763	0.041447	-1.97237
C	1.860763	1.565447	-0.09637
C	2.258763	1.459447	-1.58037
C	1.077763	-1.36755	0.765632
O	-2.21124	0.217447	1.441632
O	-2.48724	0.957447	0.212632
H	-1.27982	-1.22912	2.160601
H	0.583914	0.413309	2.110884
H	0.517325	-2.35447	-1.19483
H	-0.29455	-0.04234	-1.96918
H	-1.35726	-2.61233	0.331615
H	-1.82613	-1.15969	-0.71943
H	-0.24847	1.602162	0.031554
H	2.517171	-0.65012	-1.56642
H	1.603363	0.042395	-3.02247
H	2.57031	1.003466	0.474262
H	1.694199	2.59889	0.125336
H	3.32643	1.496603	-1.64043
H	1.667162	2.159274	-2.13277
H	0.860861	-2.17477	1.433649
H	2.093466	-1.11961	0.538094
H	-1.98086	0.141858	0.212632

JP-10-Hydroperoxide-O (ZPE=654.80 kj/mol)

	Coordinates		
Atom	**x**	**y**	**z**
C	-1.86445	-0.12139	1.06768
H	-2.05245	-0.64239	2.01068
C	-0.41945	0.43261	1.01568
C	-0.48045	-1.03439	-0.72632
H	-0.19245	-1.89339	-1.33832
C	-0.32745	0.33461	-1.43032
C	-1.91045	-1.11839	-0.13632
H	-2.66645	-0.84739	-0.87932
H	-2.13245	-2.13339	0.20568
H	-2.60445	0.68061	0.98468
C	-0.29445	1.35461	-0.22032
H	-1.19045	0.51761	-2.08132
C	0.98055	0.57961	-2.21932
H	1.76355	-0.11139	-1.88432
H	0.85355	0.41961	-3.29532
H	-1.14045	2.04861	-0.26132
C	1.02955	2.14261	-0.37332
H	1.82255	1.68261	0.22968
H	0.93755	3.17961	-0.03632
C	1.37955	2.02361	-1.86832
H	2.42955	2.24661	-2.08432
H	0.77255	2.73061	-2.45032
C	0.36955	-0.80839	0.54268
H	1.42555	-0.60639	0.33968
H	-0.07145	0.88561	1.94768
O	0.27355	-1.95839	1.37368
O	1.08655	-1.69539	2.55768
H	0.42531	-1.63563	3.25107

JP-10-Hydroperoxide-P
(ZPE=658.82 kj/mol)

	Coordinates		
Atom	**x**	**y**	**z**
C	-2.06309	-0.18332	1.39297
H	-2.25409	-0.75932	2.30597
C	-0.59609	0.29568	1.34097
C	-0.75109	-1.03232	-0.44903
H	-0.51809	-1.84432	-1.14003
C	-0.58009	0.37168	-1.07503
C	-2.17009	-1.10132	0.15597
H	-2.94509	-0.76432	-0.54003
H	-2.41209	-2.12332	0.46597
H	-2.78109	0.64168	1.35497
C	-0.47409	1.29068	0.16397
H	-1.45409	0.64268	-1.68003
C	0.68591	0.61368	-1.89503
H	1.46191	-0.13132	-1.69503
H	0.48091	0.57668	-2.97003
H	-1.29609	2.01768	0.17397
C	0.84991	2.04068	0.02697
H	1.65791	1.57068	0.59597
H	0.76591	3.07068	0.38897
C	1.14791	1.99868	-1.46503
H	2.20591	2.16968	-1.68203
H	0.56491	2.76768	-1.98603
C	0.08491	-0.98732	0.83997
H	-0.10809	-1.83632	1.50797
H	-0.21909	0.69468	2.28597
O	1.47991	-0.85432	0.65297
O	1.95791	-2.17432	0.26697
H	2.56130	-2.30002	1.00298

APPENDIX B

THE CARTESIAN COORDINATES OF THE STRUCTURES CONSIDERED IN CHAPTER-3

JP-900 (ZPE=694.56 kj/mol)			
	Coordinates		
Atom	**x**	**y**	**z**
H	1.69500	0.25700	-2.21700
C	1.54400	0.36700	-1.13500
C	1.55000	2.01600	0.79200
C	-0.13000	0.09800	0.75600
C	0.13800	1.55300	1.17800
C	0.13000	-0.09800	-0.75600
C	1.81000	1.81800	-0.70900
H	2.28800	1.43800	1.36500
H	0.58800	-0.54400	1.29500
H	-0.60400	2.20700	0.69600
H	-0.58800	0.54400	-1.29500
H	1.15200	2.48900	-1.28000
H	2.27900	-0.29300	-0.65100
H	1.69300	3.06700	1.07100
H	-0.01400	1.65900	2.26000
H	2.83800	2.10800	-0.95800
C	-0.13800	-1.55300	-1.17800
H	0.60400	-2.20700	-0.69600
H	0.01400	-1.65900	-2.26000
C	-1.54400	-0.36700	1.13500
H	-1.69500	-0.25700	2.21700
H	-2.27900	0.29300	0.65100
C	-1.81000	-1.81800	0.70900
H	-1.15200	-2.48900	1.28000
H	-2.83800	-2.10800	0.95800
H	-2.28800	-1.43800	-1.36500
C	-1.55000	-2.01600	-0.79200
H	-1.69300	-3.06700	-1.07100

JP-900-Hydroperoxide-A (ZPE=713.59 kj/mol)			
	Coordinates		
Atom	**x**	**y**	**z**
C	1.06014	0.49997	-1.14850
C	0.97614	2.19397	0.80650
C	-0.63386	0.21997	0.78650
C	-0.43786	1.70197	1.14250
C	-0.31686	-0.03703	-0.70750
C	1.32114	1.93797	-0.67050
H	1.69614	1.67897	1.45050
H	0.07414	-0.37103	1.38250
H	-1.17586	2.30397	0.59150
H	-1.04486	0.55797	-1.28550
H	0.70214	2.59997	-1.29250
H	1.06414	3.26597	1.02150
H	-0.64886	1.85797	2.20750
H	2.36414	2.19997	-0.88650
C	-0.51586	-1.51403	-1.08450
H	0.22814	-2.11803	-0.55250
H	-0.31786	-1.65403	-2.15450
C	-2.05486	-0.26703	1.11250
H	-2.26386	-0.11203	2.17950
H	-2.78186	0.34997	0.56250
C	-2.25986	-1.74303	0.74250
H	-1.60886	-2.36703	1.37150
H	-3.29086	-2.05103	0.95950
H	-2.66086	-1.47203	-1.36450
C	-1.92986	-1.99903	-0.73450
H	-2.02986	-3.06603	-0.97050
H	1.08614	0.49097	-2.24850
O	2.15714	-0.39903	-0.91050
O	2.35814	-0.58503	0.52750
H	3.25717	-0.25745	0.60511

JP-900-Hydroperoxide-B (ZPE=715.23 kj/mol)			
	Coordinates		
Atom	**x**	**y**	**z**
C	1.04404	0.33623	-0.77904
C	1.33104	1.87923	1.20196
C	-0.38096	0.00223	1.28996
C	-0.02996	1.42823	1.74396
C	-0.32196	-0.13577	-0.25304
C	1.38304	1.75823	-0.32604
H	2.12204	1.25923	1.64696
H	0.38104	-0.67677	1.70596
H	-0.80996	2.12023	1.39396
H	-1.07896	0.54223	-0.67804
H	0.65504	2.44123	-0.78204
H	1.54204	2.91223	1.50396
H	-0.04096	1.47823	2.84096
H	2.36904	2.03423	-0.71104
C	-0.66296	-1.57277	-0.68904
H	0.12004	-2.25177	-0.32004
H	-0.64596	-1.64077	-1.78104
C	-1.74896	-0.45677	1.82096
H	-1.75996	-0.38277	2.91596
H	-2.52296	0.23323	1.45596
C	-2.09596	-1.88577	1.38096
H	-1.38796	-2.58877	1.84196
H	-3.09196	-2.16377	1.74496
H	-2.81596	-1.41577	-0.60204
C	-2.02396	-2.02677	-0.14604
H	-2.22196	-3.06377	-0.44404
H	1.82404	-0.36277	-0.43404
O	0.95504	0.24723	-2.20804
O	2.28204	0.49823	-2.75504
H	3.11390	0.95160	-2.59986

JP-900-Hydroperoxide-C (ZPE=714.87 kj/mol)			
	Coordinates		
Atom	**x**	**y**	**z**
H	1.10255	-0.13963	-1.93269
C	0.96655	-0.03163	-0.85069
C	1.02355	1.63037	1.05431
C	-0.67345	-0.27663	1.07231
C	-0.38245	1.17837	1.47431
C	-0.44345	-0.48663	-0.44269
C	1.22955	1.42237	-0.44769
H	1.77955	1.04737	1.59631
H	0.04755	-0.92163	1.60231
H	-1.13145	1.83637	1.00931
H	-1.16845	0.15437	-0.97269
H	0.55655	2.08937	-1.00569
H	1.71655	-0.66763	-0.35969
H	1.18755	2.68337	1.30731
H	-0.49845	1.29737	2.55831
C	-0.72845	-1.94263	-0.84869
H	0.01655	-2.59763	-0.37269
H	-0.59745	-2.05863	-1.93169
C	-2.08545	-0.72463	1.48031
H	-2.21645	-0.60463	2.56331
H	-2.82245	-0.06163	1.00331
C	-2.37045	-2.17663	1.07031
H	-1.71045	-2.84863	1.63631
H	-3.39745	-2.45263	1.33931
H	-2.87945	-1.80963	-0.99869
C	-2.13645	-2.38863	-0.43269
H	-2.29345	-3.44063	-0.70069
O	2.57655	1.83237	-0.70269
O	2.73755	1.92337	-2.15069
H	3.32905	1.18165	-2.29755

JP-900-Hydroperoxide-D (ZPE=714.59 kj/mol)			
	Coordinates		
Atom	x	y	z
H	1.53119	-0.25669	-1.80584
C	1.35419	-0.14169	-0.73084
C	1.32819	1.57431	1.14116
C	-0.35981	-0.33469	1.13516
C	-0.09281	1.13131	1.51416
C	-0.07181	-0.57869	-0.36484
C	1.65619	1.30731	-0.33284
H	2.05919	1.02031	1.74516
H	0.34219	-0.96569	1.70816
H	-0.82181	1.77331	1.00416
H	-0.76981	0.05531	-0.93484
H	2.08119	-0.79169	-0.22284
H	1.47419	2.63831	1.35716
H	-0.25181	1.27231	2.59116
H	2.70919	1.54431	-0.53184
C	-0.34181	-2.04369	-0.74884
H	0.38419	-2.68769	-0.23184
H	-0.16781	-2.18469	-1.82384
C	-1.78481	-0.77869	1.49816
H	-1.95881	-0.63469	2.57216
H	-2.50281	-0.12769	0.97816
C	-2.05381	-2.23969	1.11016
H	-1.41381	-2.89769	1.71516
H	-3.08881	-2.51269	1.34716
H	-2.48681	-1.91769	-0.98384
C	-1.76481	-2.48369	-0.37784
H	-1.90981	-3.54169	-0.62884
O	0.84819	2.25031	-1.05784
O	1.29019	2.22531	-2.44684
H	0.43016	1.98870	-2.80175

JP-900-Hydroperoxide-E (ZPE=713.77 kj/mol)			
	Coordinates		
Atom	x	y	z
H	1.32518	0.00188	-2.57610
C	1.14618	0.10488	-1.49910
C	1.05418	1.81088	0.39890
C	-0.56282	-0.16812	0.35190
C	-0.34082	1.29588	0.76490
C	-0.27182	-0.37212	-1.15210
C	1.38518	1.56288	-1.07910
H	0.15818	-0.78312	0.91190
H	-1.08082	1.93688	0.26390
H	-0.98582	0.25788	-1.71210
H	0.74518	2.23088	-1.67010
H	1.87618	-0.54012	-0.99510
H	1.12918	2.88488	0.62990
H	-0.49382	1.41588	1.84190
H	2.42118	1.86288	-1.27210
C	-0.51082	-1.83312	-1.56810
H	0.23418	-2.47012	-1.06810
H	-0.33782	-1.94512	-2.64710
C	-1.97482	-0.65212	0.71190
H	-2.14482	-0.53512	1.78990
H	-2.71382	-0.00912	0.20990
C	-2.20782	-2.11112	0.29390
H	-1.54682	-2.76412	0.88190
H	-3.23482	-2.41612	0.52890
H	-2.65882	-1.75412	-1.79110
C	-1.91982	-2.31612	-1.20010
H	-2.04182	-3.37112	-1.47410
O	2.09118	1.12388	1.12190
O	1.90018	1.38488	2.54190
H	2.66472	1.94720	2.68640

JP-900-Hydroperoxide-F (ZPE=714.14 kj/mol)			
	Coordinates		
Atom	**x**	**y**	**z**
H	1.67211	-0.54546	-2.20461
C	1.43011	-0.32346	-1.15861
C	1.15011	1.53354	0.52939
C	-0.34089	-0.52146	0.64439
C	-0.23389	0.99154	0.89639
C	0.03711	-0.87146	-0.81161
C	1.53711	1.18854	-0.90961
H	0.39011	-1.02546	1.29939
H	-0.98389	1.51654	0.29139
H	-0.69389	-0.36946	-1.46761
H	0.86811	1.72854	-1.58761
H	2.18211	-0.85146	-0.55161
H	-0.44789	1.21854	1.94839
H	2.55311	1.54954	-1.10461
C	-0.07289	-2.38546	-1.06061
H	0.68911	-2.90246	-0.45961
H	0.16111	-2.60646	-2.11061
C	-1.73389	-1.06746	1.00039
H	-1.96789	-0.84046	2.04839
H	-2.48689	-0.54046	0.39439
C	-1.84289	-2.57746	0.74639
H	-1.17489	-3.10946	1.43739
H	-2.85889	-2.92646	0.96639
H	-2.20789	-2.50346	-1.38261
C	-1.46189	-2.93146	-0.69761
H	-1.49189	-4.01746	-0.84561
H	1.89811	1.10854	1.21639
O	1.29511	2.93154	0.82339
O	0.37311	3.68254	-0.02461
H	-0.22286	3.99658	0.65936

JP-900-Hydroperoxide-G (ZPE=715.62 kj/mol)			
	Coordinates		
Atom	**x**	**y**	**z**
H	1.94632	-0.47565	-2.50157
C	1.70632	-0.22765	-1.45957
C	1.53532	1.64735	0.22943
C	-0.13468	-0.27665	0.30543
C	0.09832	1.22635	0.54243
C	0.26632	-0.65565	-1.14157
C	1.92432	1.27035	-1.20557
H	2.19932	1.14135	0.94343
H	0.53332	-0.82165	0.99043
H	-0.40368	-0.09965	-1.81957
H	1.31732	1.85135	-1.91457
H	2.39932	-0.80765	-0.83357
H	1.64032	2.72335	0.39843
H	2.96832	1.54635	-1.39457
C	0.03832	-2.15765	-1.39157
H	0.73532	-2.73265	-0.76457
H	0.29032	-2.39865	-2.43257
C	-1.58268	-0.70365	0.60743
H	-1.83568	-0.45165	1.64143
H	-2.26368	-0.12365	-0.03357
C	-1.79868	-2.20165	0.35143
H	-1.19368	-2.78065	1.06343
H	-2.84468	-2.47165	0.54143
H	-2.08468	-2.10365	-1.78857
C	-1.40068	-2.58865	-1.07857
H	-1.51068	-3.66965	-1.22857
H	-0.60368	1.80235	-0.08057
O	-0.22968	1.45735	1.92043
O	-0.26768	2.89935	2.13143
H	-1.19610	3.08059	2.29512

JP-900-Hydroperoxide-H (ZPE=713.91 kj/mol)			
	Coordinates		
Atom	x	y	z
H	1.85869	-0.09563	-2.30659
C	1.71069	-0.03463	-1.22159
C	1.76269	1.51237	0.78741
C	0.04069	-0.38763	0.65841
C	0.39869	0.98937	1.26241
C	0.28869	-0.49363	-0.86659
C	1.99569	1.39137	-0.72759
H	2.53169	0.92637	1.31041
H	0.74769	-1.09063	1.13141
H	-0.41631	0.18037	-1.37059
H	1.34669	2.09737	-1.25459
H	2.43369	-0.73063	-0.77059
H	1.87069	2.54937	1.12341
H	3.03069	1.67137	-0.95759
C	0.00269	-1.92663	-1.35059
H	0.73669	-2.61263	-0.90059
H	0.15169	-1.98563	-2.43659
C	-1.37631	-0.84763	1.03341
H	-1.51331	-0.79363	2.12141
H	-2.11031	-0.15363	0.60141
C	-1.66531	-2.26863	0.52841
H	-1.01631	-2.97963	1.06041
H	-2.69731	-2.55363	0.76741
H	-2.14631	-1.77063	-1.51959
C	-1.41331	-2.38863	-0.98159
H	-1.57531	-3.42163	-1.31459
H	0.43369	0.87637	2.35541
O	-0.64931	1.97037	1.19141
O	-0.89131	2.34937	-0.20159
H	-1.82807	2.14858	-0.26284

JP-900-Hydroperoxide-I (ZPE=713.65 kj/mol)			
	Coordinates		
Atom	x	y	z
H	1.53516	0.43243	-2.45021
C	1.38916	0.57643	-1.37321
C	1.30116	2.33043	0.47479
C	-0.24184	0.27543	0.55279
C	-0.06384	1.77243	0.90779
C	-0.01184	0.09343	-0.97421
C	1.58916	2.05743	-1.00921
H	2.08516	1.87443	1.09079
H	-0.86984	2.32343	0.40779
H	-0.72984	0.78643	-1.44221
H	0.91316	2.66643	-1.62621
H	2.14816	-0.03457	-0.86721
H	1.33316	3.40843	0.67379
H	-0.20784	1.90043	1.98679
H	2.60716	2.37843	-1.25921
C	-0.37884	-1.30657	-1.50121
H	0.32716	-2.05157	-1.12121
H	-0.28584	-1.30657	-2.59521
C	-1.62984	-0.23457	0.97679
H	-1.67984	-0.22457	2.07179
H	-2.36884	0.49643	0.61979
C	-2.00884	-1.62057	0.42479
H	-1.40384	-2.38957	0.91279
H	-3.05684	-1.83157	0.67379
H	-2.51784	-1.02357	-1.59321
C	-1.80684	-1.69957	-1.09521
H	-2.03684	-2.70857	-1.45621
O	0.89116	-1.74657	1.23479
O	0.81116	-0.29557	1.37179
H	1.09412	-1.57406	2.15709

JP-900-Hydroperoxide-J
(ZPE=714.28 kj/mol)

	Coordinates		
Atom	**x**	**y**	**z**
H	1.77455	0.14164	-1.99683
C	1.67255	0.18964	-0.90683
C	1.76355	1.72664	1.11817
C	-0.03245	-0.06236	0.97717
C	0.31655	1.35364	1.47117
C	0.26155	-0.29636	-0.52983
C	2.03855	1.59164	-0.38683
H	2.44755	1.06764	1.67417
H	0.66255	-0.74136	1.50017
H	-0.36845	2.08564	1.03417
H	1.46655	2.34764	-0.93183
H	2.38755	-0.53336	-0.48983
H	1.98155	2.74864	1.45317
H	0.17455	1.39164	2.55917
H	3.09955	1.78464	-0.58983
C	0.08755	-1.80036	-0.84883
H	0.86655	-2.34336	-0.29883
H	0.27655	-1.96136	-1.91583
C	-1.45145	-0.52836	1.33317
H	-1.64145	-0.35036	2.39917
H	-2.18545	0.07064	0.77917
C	-1.64545	-2.01836	1.00517
H	-0.99745	-2.61236	1.66617
H	-2.67445	-2.32736	1.22217
H	-2.05245	-1.88936	-1.11683
C	-1.29945	-2.33536	-0.45783
H	-1.33345	-3.41836	-0.62783
O	-0.74745	0.25864	-1.41283
O	-0.80745	1.71564	-1.33283
H	-1.67701	1.84110	-0.94589

JP-900-Hydroperoxide-K
(ZPE=714.18 kj/mol)

	Coordinates		
Atom	**x**	**y**	**z**
H	1.48553	0.85097	-1.83086
C	1.45553	0.85697	-0.73786
C	1.67153	2.29797	1.33814
C	0.00453	0.36497	1.29314
C	0.31653	1.77397	1.83114
C	0.08953	0.34197	-0.25286
C	1.75853	2.25997	-0.19286
H	2.47353	1.67797	1.76114
H	0.78553	-0.31603	1.67014
H	-0.48047	2.46197	1.51014
H	-0.68947	1.01897	-0.63986
H	1.03653	2.97497	-0.61386
H	2.23653	0.15897	-0.40086
H	1.83753	3.31797	1.70714
H	0.28853	1.76197	2.92814
H	2.74953	2.58897	-0.52686
C	-0.22947	-1.06803	-0.78086
C	-1.34947	-0.15903	1.79414
H	-1.36047	-0.16303	2.89114
H	-2.14247	0.53497	1.47814
C	-1.65347	-1.56203	1.25114
H	-0.92647	-2.27703	1.66214
H	-2.64047	-1.90003	1.58614
H	-2.36747	-0.94403	-0.69986
C	-1.58047	-1.58503	-0.28086
H	-1.74247	-2.59703	-0.66486
O	-0.19947	-0.96003	-2.21086
O	-0.17347	-2.31403	-2.75286
H	-1.06406	-2.32665	-3.11102
H	0.57153	-1.75803	-0.47486

JP-900-Hydroperoxide-L (ZPE=715.00 kj/mol)			
	Coordinates		
Atom	**x**	**y**	**z**
H	0.31079	1.97772	-1.69063
C	0.86379	1.33172	-0.99763
C	2.65379	1.26072	0.78537
C	0.59479	-0.25028	1.00037
C	1.67379	0.56572	1.73637
C	-0.12621	0.60872	-0.06363
C	1.89979	2.14672	-0.21563
H	3.23579	0.50572	0.23837
H	1.10479	-1.06228	0.46137
H	1.17279	1.32872	2.35237
H	-0.69221	1.38372	0.47637
H	1.39779	2.95872	0.33037
H	1.37779	0.58972	-1.61863
H	3.37679	1.85572	1.35737
H	2.21079	-0.08828	2.43637
H	2.60179	2.62372	-0.90963
C	-1.18621	-0.19828	-0.84963
C	-0.41421	-0.87628	2.00837
H	-0.12221	-1.91428	2.21137
H	-0.34721	-0.35028	2.96937
C	-1.87321	-0.84828	1.51637
H	-2.48221	-1.54028	2.10937
H	-2.30921	0.14672	1.67637
H	-2.99121	-1.29428	-0.30363
C	-1.95321	-1.20928	0.03137
H	-1.49021	-2.19528	-0.11363
O	-0.48721	-0.86928	-1.91063
O	-1.49821	-1.41328	-2.80663
H	-1.41164	-2.35473	-2.63996
H	-1.88321	0.50972	-1.31663

JP-900-Hydroperoxide-M (ZPE=715.24 kj/mol)			
	Coordinates		
Atom	**x**	**y**	**z**
H	2.02764	0.30210	-2.74618
C	1.91264	0.40910	-1.66018
C	1.99964	2.04310	0.27182
C	0.29564	0.15010	0.27882
C	0.59264	1.60310	0.69782
C	0.50164	-0.03890	-1.24718
C	2.21564	1.85210	-1.23518
H	2.74264	1.45010	0.82282
H	1.00964	-0.50890	0.79682
H	-0.15236	2.26710	0.23182
H	-0.21836	0.62310	-1.75718
H	1.55464	2.53710	-1.78518
H	2.64864	-0.26690	-1.20118
H	2.16564	3.08910	0.55482
H	0.47064	1.70710	1.77982
H	3.24164	2.12210	-1.51318
C	0.19664	-1.47990	-1.68618
H	0.94164	-2.15690	-1.24118
H	0.31164	-1.56490	-2.77418
C	-1.11236	-0.31190	0.68582
C	-1.40236	-1.74990	0.25082
H	-0.71736	-2.41290	0.79482
H	-2.41836	-2.02190	0.55182
H	-1.95536	-1.31890	-1.79918
C	-1.20836	-1.92090	-1.26118
H	-1.38636	-2.96290	-1.54918
O	-1.16336	-0.17690	2.11382
O	-2.53036	-0.45190	2.53882
H	-2.80658	0.43119	2.79466
H	-1.85936	0.36910	0.24382

JP-900-Hydroperoxide-N
(ZPE=712.92 kj/mol)

	Coordinates		
Atom	**x**	**y**	**z**
H	2.18889	0.26902	-2.24549
C	2.01789	0.35002	-1.16449
C	1.95189	1.95002	0.80251
C	0.34389	-0.01398	0.69351
C	0.55089	1.43502	1.16451
C	0.60789	-0.16098	-0.82449
C	2.23489	1.79702	-0.69949
H	2.70489	1.38602	1.37051
H	1.09889	-0.64198	1.19951
H	-0.21211	2.06902	0.69851
H	-0.11911	0.47002	-1.35249
H	1.56489	2.46102	-1.26349
H	2.76189	-0.30198	-0.68349
H	2.05589	2.99902	1.10551
H	0.38789	1.50202	2.24751
H	3.25789	2.12102	-0.92849
C	0.39689	-1.61298	-1.28149
H	1.14889	-2.25598	-0.79849
H	0.57389	-1.69198	-2.36149
C	-1.01211	-0.59098	1.14951
C	-1.29711	-1.98598	0.56751
H	-0.65911	-2.69798	1.11151
H	-2.33211	-2.26298	0.80051
H	-1.74511	-1.54898	-1.50749
C	-1.00811	-2.12198	-0.93649
H	-1.11611	-3.17198	-1.23549
O	-2.11811	0.32202	1.03151
O	-2.38511	0.61302	-0.37749
H	-0.99011	-0.66898	2.24651
H	-2.37514	1.55190	-0.17748

JP-900-Hydroperoxide-O
(ZPE=712.50 kj/mol)

	Coordinates		
Atom	**x**	**y**	**z**
H	2.04597	0.81612	-2.45552
C	1.82597	0.90012	-1.38352
C	1.68197	2.50312	0.57748
C	0.04597	0.55712	0.39248
C	0.25797	2.00512	0.86548
C	0.39997	0.40012	-1.10252
C	2.03797	2.34512	-0.90852
H	2.39497	1.92612	1.18348
H	0.73697	-0.08888	0.95648
H	-0.46603	2.65612	0.35348
H	-0.29803	1.03812	-1.67152
H	1.40597	3.01912	-1.50452
H	2.54097	0.24012	-0.86952
H	1.78697	3.55012	0.88648
H	0.03397	2.08212	1.93748
H	3.07497	2.65612	-1.08452
C	0.19697	-1.05288	-1.56052
H	0.92097	-1.69588	-1.04552
H	0.41197	-1.13888	-2.63352
C	-1.38403	0.07012	0.67148
H	-1.61303	0.13312	1.74148
H	-2.10203	0.73012	0.16348
C	-1.63403	-1.36388	0.19148
H	-1.94603	-0.99888	-1.89052
C	-1.22703	-1.55488	-1.27552
H	-1.32803	-2.61288	-1.54152
O	-0.84503	-2.32488	0.91548
O	-1.34903	-2.36188	2.28248
H	-0.53994	-2.07465	2.71197
H	-2.69103	-1.62988	0.32448

JP-900-Hydroperoxide-P (ZPE=711.61 kj/mol)			
	Coordinates		
Atom	**x**	**y**	**z**
H	2.52998	0.80386	-2.08580
C	2.27698	0.82986	-1.01780
C	2.17798	2.29686	1.05020
C	0.40798	0.50586	0.66620
C	0.70898	1.89686	1.25120
C	0.80398	0.43486	-0.82380
C	2.58598	2.21386	-0.42780
H	2.81798	1.62586	1.64020
H	1.03398	-0.22414	1.20420
H	0.05898	2.63686	0.76220
H	0.18498	1.17286	-1.36180
H	2.03898	2.97986	-0.99680
H	2.91598	0.07686	-0.53180
H	2.34898	3.30786	1.43620
H	0.44898	1.91586	2.31720
H	3.65098	2.44686	-0.54080
C	0.48798	-0.95314	-1.40680
H	1.14498	-1.69814	-0.93280
H	0.72998	-0.97414	-2.47680
C	-1.06302	0.10686	0.87320
H	-1.31802	0.12286	1.93920
H	-1.71902	0.83586	0.37720
C	-1.35002	-1.27914	0.29020
H	-1.64102	-0.66614	-1.73980
C	-0.97902	-1.35014	-1.19080
H	-1.17402	-2.35814	-1.56780
H	-0.78302	-2.03914	0.85120
O	-2.74802	-1.49714	0.51620
O	-3.05302	-2.86814	0.12420
H	-3.22152	-3.25372	0.98707

JP-900-Hydroperoxide-R (ZPE=713.68 kj/mol)			
	Coordinates		
Atom	**x**	**y**	**z**
H	1.93591	0.90619	-2.06215
C	1.75791	1.05219	-0.99015
C	1.66591	2.77319	0.87185
C	0.05291	0.80019	0.87585
C	0.26291	2.27819	1.24785
C	0.35091	0.55719	-0.62215
C	1.96691	2.52619	-0.61315
H	2.40991	2.24519	1.48485
H	0.77691	0.20119	1.45385
H	-0.49109	2.88619	0.72585
H	-0.37409	1.15919	-1.19715
H	1.30291	3.15419	-1.22515
H	2.50091	0.43319	-0.46515
H	1.76691	3.83919	1.11185
H	0.08291	2.41919	2.32185
H	2.99191	2.83719	-0.85015
C	0.14591	-0.92081	-0.99715
H	0.88791	-1.53981	-0.47815
H	0.30091	-1.06881	-2.07215
C	-1.35509	0.30319	1.23585
H	-1.54309	0.44619	2.30785
H	-2.09709	0.92119	0.70985
C	-1.55909	-1.17281	0.86385
H	-0.88909	-1.80181	1.46385
H	-2.58609	-1.49281	1.07885
C	-1.25009	-1.41381	-0.61615
H	-1.99909	-0.89181	-1.23115
O	-1.48309	-2.77081	-1.02415
O	-0.52609	-3.63081	-0.33115
H	-1.10862	-4.14445	0.23314

JP-900-Hydroperoxide-S (ZPE=714.34 kj/mol)

	Coordinates		
Atom	**x**	**y**	**z**
H	2.02429	0.57633	-2.16987
C	1.95029	0.75133	-1.08887
C	1.95529	2.52933	0.71913
C	0.45529	0.48133	0.95013
C	0.62429	1.97933	1.25013
C	0.61429	0.20533	-0.56287
C	2.11929	2.24633	-0.78087
H	2.78529	2.06233	1.26813
H	1.26929	-0.05567	1.46713
H	-0.20771	2.53033	0.78813
H	-0.19571	0.74133	-1.08087
H	1.36329	2.81533	-1.33987
H	2.77629	0.18833	-0.62687
H	2.02429	3.60733	0.91213
H	0.54729	2.15433	2.33113
H	3.09729	2.59833	-1.13187
C	0.44929	-1.29267	-0.86787
H	1.28129	-1.85167	-0.41787
H	0.49329	-1.47167	-1.94787
C	-0.87871	-0.07367	1.47213
H	-0.96071	0.10033	2.55213
H	-1.70371	0.48133	1.00413
C	-1.03771	-1.57067	1.17213
H	-0.28771	-2.14467	1.73313
H	-2.01771	-1.93767	1.49513
C	-0.85371	-1.88267	-0.31687
H	-0.87571	-2.96667	-0.48387
O	-1.89071	-1.29367	-1.12187
O	-3.12771	-2.00467	-0.82587
H	-3.62957	-1.27922	-0.44711

APPENDIX C

THE CARTESIAN COORDINATES OF THE STRUCTURES CONSIDERED IN CHAPTER-4

TNAZ (1) (ZPE=281.09 kj/mol)			
	Coordinates		
Atom	x	y	z
H	0.00000	0.00000	0.00000
C	1.09233	0.00000	0.00000
H	1.48892	1.01463	0.00000
C	2.03145	-1.95081	0.05617
H	3.07098	-2.27284	0.09576
H	1.34986	-2.80442	0.07989
C	1.69597	-0.94260	-1.06101
N	1.66741	-0.89636	1.03012
N	0.70492	-1.44485	-2.10345
O	-0.30683	-1.95419	-1.64068
O	0.98577	-1.29754	-3.28003
N	2.89275	-0.39315	-1.80849
O	2.86238	0.79689	-2.08635
O	3.77225	-1.19650	-2.08254
N	0.87317	-1.24683	2.12497
O	0.10944	-0.37988	2.53093
O	1.06423	-2.36450	2.58791

2 (ZPE=265.33 kj/mol)			
	Coordinates		
Atom	x	y	z
C	0.35813	1.23495	-0.59841
C	-0.27287	0.09095	0.22659
C	0.27813	-0.93705	-0.78641
N	0.75613	0.21195	-1.58241
N	-1.77987	0.14895	0.35059
O	-2.25687	1.25295	0.57259
O	-2.38287	-0.90805	0.23459
N	0.28713	-0.06205	1.63559
O	1.50813	-0.02105	1.70559
O	-0.49987	-0.23005	2.55059
N	1.91813	0.24695	-2.26241
O	2.32513	-0.86305	-2.56841
H	1.21146	1.64606	-0.10070
H	-0.39289	1.88435	-0.99735
H	1.09618	-1.48871	-0.37245
H	-0.51548	-1.45162	-1.28672

3A (ZPE=263.59 kj/mol)			
	Coordinates		
Atom	x	y	z
H	0.00000	0.00000	0.00000
C	1.09303	0.00000	0.00000
H	1.48901	1.01471	0.00000
C	2.09616	-1.92337	0.07634
H	3.15865	-2.16537	0.10713
H	1.49515	-2.83551	0.12588
C	1.67682	-0.94736	-1.05397
N	1.66837	-0.88767	1.03981
N	2.80913	-0.43386	-1.88726
O	2.82244	0.76707	-2.13680
O	3.59277	-1.27923	-2.30128
N	0.86664	-1.26970	2.11644
O	0.07120	-0.42865	2.51963
O	1.07765	-2.38751	2.57381
N	0.72616	-1.60821	-2.06633
O	-0.41005	-1.60985	-1.68758

4A (ZPE=248.72 kj/mol)			
	Coordinates		
Atom	x	y	z
H	0.00000	0.00000	0.00000
C	1.09315	0.00000	0.00000
H	1.48042	1.02082	0.00000
C	2.28314	-1.82883	0.02704
H	3.37183	-1.90423	0.04404
H	1.82949	-2.82377	0.07409
C	1.72820	-0.90520	-1.08333
N	1.68888	-0.89676	1.00680
N	2.73313	-0.26277	-1.97932
O	2.48442	0.87765	-2.35424
O	3.66981	-0.96546	-2.34249
N	1.08871	-1.24591	2.15502
O	1.45497	-2.33471	2.57560
N	0.65470	-1.61796	-1.89746
O	0.79635	-1.56494	-3.08598

5 (ZPE=248.30 kj/mol)			
	Coordinates		
Atom	**x**	**y**	**z**
H	0.26529	-1.37712	-1.41876
C	0.44129	-0.54212	-0.74076
H	1.40629	-0.06612	-0.93576
C	-0.82771	0.33688	0.79224
H	-0.46871	1.22688	1.31824
H	-1.82971	0.07188	1.13524
C	0.20929	-0.83612	0.74624
N	-0.68471	0.41888	-0.67376
N	-0.54571	1.67788	-1.25576
O	0.11529	1.72588	-2.28576
O	-1.14171	2.59588	-0.70076
N	1.30729	-0.60312	1.75224
O	2.30629	-0.13012	1.27124
N	-0.45171	-2.12612	1.16624
O	-0.74071	-2.83912	0.23924

6 (ZPE=317.75 kj/mol)			
	Coordinates		
Atom	**x**	**y**	**z**
C	0.78610	0.87673	-0.99722
C	-0.02390	0.01573	-0.02222
C	-0.44990	1.32773	0.64478
N	-1.12190	-0.84227	-0.62722
O	-1.93990	-0.24027	-1.31122
O	-1.09890	-2.04327	-0.40422
N	0.80510	-0.89127	0.86778
O	1.79410	-1.40727	0.36678
O	0.40110	-1.04027	2.01278
N	0.70410	1.99173	-0.01722
N	0.30910	3.24573	-0.66122
H	1.78969	0.51606	-1.08454
H	0.21831	1.09699	-1.87699
H	-0.30976	1.28222	1.70459
H	-1.37697	1.67910	0.24231
H	0.30106	3.98062	0.01693
H	-0.60479	3.14505	-1.05449

7b **(ZPE=319.35 kj/mol)**			
	Coordinates		
Atom	**x**	**y**	**z**
C	0.58326	-0.17665	-0.89987
C	-0.90874	0.23435	0.62113
C	-0.20474	-1.05765	0.14613
N	0.00826	1.01035	-0.24187
N	-1.05074	-2.14065	-0.22587
N	0.80626	-1.59165	1.16513
O	1.15526	-2.75865	1.02313
O	1.24626	-0.80765	1.99513
N	-0.49674	2.04035	-1.02087
O	0.07626	2.24335	-2.08887
O	-1.43874	2.66935	-0.54687
H	1.63905	-0.23522	-0.73627
H	0.18694	-0.30135	-1.88592
H	-0.70960	0.42037	1.65584
H	-1.91221	0.28096	0.25263
H	-1.47449	-2.52893	0.59247
H	-0.50902	-2.84386	-0.68634

8 **(ZPE=357.67 kj/mol)**			
	Coordinates		
Atom	**x**	**y**	**z**
C	0.70932	-0.87674	-0.45803
C	-0.59068	-0.00274	1.04097
C	0.40232	-1.20774	1.04797
N	-0.44368	0.04226	-0.42803
N	-0.38968	1.25426	-1.09003
O	0.27332	1.28226	-2.12503
O	-1.04668	2.17226	-0.60303
N	1.55932	-0.99974	1.89297
N	-0.28868	-2.45574	1.34497
H	1.62918	-0.33887	-0.55524
H	0.51405	-1.72061	-1.08625
H	-0.15258	0.85973	1.49826
H	-1.57567	-0.31403	1.31989
H	1.33594	-1.25679	2.83320
H	1.82368	-0.03573	1.86480
H	-0.45244	-2.51999	2.32937
H	0.27492	-3.22724	1.04976

9 (ZPE=356.15 kj/mol)			
	Coordinates		
Atom	x	y	z
H	0.25431	0.33806	-1.71959
C	0.86631	0.52806	-0.83159
H	1.93531	0.45406	-1.05459
C	-0.43069	0.98606	0.75541
H	-0.40769	1.28106	1.80941
H	-1.45569	0.94206	0.37141
C	0.36431	-0.28394	0.38241
N	0.46431	1.77606	-0.13059
N	-0.57269	-1.47294	-0.04459
O	-1.48169	-1.23094	-0.83059
O	-0.32569	-2.57294	0.43941
N	-0.30069	2.66506	-1.01359
H	-0.57269	3.44106	-0.40359
H	0.41231	3.09006	-1.61159
N	1.35431	-0.68594	1.30641
H	0.93731	-1.05094	2.15741
H	1.93931	-1.42094	0.91941
H	-0.09702	-1.24429	0.28345

10a (ZPE=302.79 kj/mol)			
	Coordinates		
Atom	x	y	z
C	1.01077	-0.13511	-0.51070
C	-0.48723	0.15489	1.01730
C	0.42277	-1.04611	0.60930
N	0.29277	0.99989	0.09530
N	1.35077	-1.47611	1.59930
N	-0.35523	1.91589	-0.71670
O	0.16877	2.14189	-1.80470
O	-1.36223	2.44089	-0.24870
N	-0.45523	-2.11611	-0.04170
O	-0.24523	-3.22111	0.39730
H	2.06904	-0.02369	-0.39864
H	0.59726	-0.38519	-1.46536
H	-0.31652	0.43776	2.03501
H	-1.48666	0.01810	0.66047
H	0.88984	-2.08248	2.24727
H	1.71150	-0.68050	2.08600

11a (ZPE=304.80 kj/mol)			
	Coordinates		
Atom	x	y	z
C	0.24241	0.06086	-1.12626
C	-1.19959	0.46386	0.45874
C	-0.46159	-0.81314	-0.04826
N	-0.60659	1.17686	-0.68126
N	0.56941	-1.30614	1.02474
O	0.53241	-2.49314	1.32574
O	1.33541	-0.46914	1.48974
N	-1.28759	-1.84414	-0.54026
N	-0.28459	2.47486	-0.69626
O	0.60441	2.73986	-1.49726
H	1.26850	0.23185	-0.87566
H	-0.02155	-0.25593	-2.11361
H	-0.78839	0.80609	1.38540
H	-2.25940	0.36844	0.34650
H	0.10713	-1.42157	0.62352
H	-1.72032	-2.31894	0.22610
H	-0.73529	-2.49209	-1.06479

12b (ZPE=300.73 kj/mol)			
	Coordinates		
Atom	x	y	z
C	0.68876	0.62187	-1.11031
C	-0.57924	1.15187	0.50169
C	0.10376	-0.14513	0.09069
N	0.34076	1.88787	-0.41231
N	-0.73424	-1.33813	-0.22431
O	-1.79024	-1.45713	0.39169
O	-0.27024	-2.12813	-1.03931
N	1.22976	-0.69313	0.97869
O	1.52076	0.04987	1.87369
N	-0.40224	2.78787	-1.29931
H	1.74953	0.49406	-1.16791
H	0.08536	0.48628	-1.98349
H	-0.37052	1.38649	1.52457
H	-1.58558	1.18549	0.13968
H	-0.59115	3.64577	-0.82148
H	-1.26485	2.35717	-1.56464

APPENDIX D

THE CARTESIAN COORDINATES OF THE STRUCTURES CONSIDERED IN CHAPTER-5

TACOT (ZPE=499.61kj/mol)			
	Coordinates		
Atom	x	y	z
N	0.25097	-0.63503	0.00000
N	-0.25103	0.63597	0.00000
N	-0.66803	-1.60503	0.00000
N	0.66797	1.60597	0.00000
C	-1.61603	0.50797	0.00000
C	-4.20303	-0.41303	0.00000
C	-2.62203	1.46597	0.00000
C	-1.83203	-0.91303	0.00000
C	-3.18703	-1.34503	0.00000
C	-3.91303	0.96497	0.00000
H	-2.42803	2.53097	0.00000
H	-5.23203	-0.74803	0.00000
C	1.83197	0.91397	0.00000
C	3.91297	-0.96503	0.00000
C	4.20297	0.41297	0.00000
C	2.62197	-1.46603	0.00000
H	5.23197	0.74797	0.00000
H	2.42697	-2.53103	0.00000
N	3.54097	2.76997	0.00000
O	2.61297	3.57297	0.00000
O	4.73697	3.05497	0.00000
N	5.03397	-1.91903	0.00000
O	6.16997	-1.45303	0.00000
O	4.75197	-3.11503	0.00000
N	-5.03403	1.91797	0.00000
O	-4.75303	3.11497	0.00000
O	-6.17103	1.45297	0.00000
O	-2.61203	-3.57303	0.00000
O	-4.73603	-3.05603	0.00000

1 (ZPE=465.27 kj/mol)			
	Coordinates		
Atom	x	y	z
N	-0.96301	-0.92195	-1.11098
N	0.07299	-0.21195	-0.65098
N	-0.07301	0.21305	0.65002
C	-1.79601	-0.94395	-0.05198
C	1.28899	0.25005	-1.07798
C	1.79499	0.94405	0.05202
N	0.96299	0.92205	1.11102
C	-1.28901	-0.24895	1.07802
C	-3.07601	-1.53495	0.12302
C	-3.79201	-1.42795	1.36102
C	-3.18901	-0.69795	2.45802
C	-1.95501	-0.11795	2.31402
H	-1.51901	0.42305	3.14602
C	1.95499	0.11805	-2.31398
C	3.79199	1.42805	-1.36098
C	3.07599	1.53605	-0.12398
N	3.87299	0.55805	-3.74298
O	4.97399	1.09105	-3.84798
O	3.29799	-0.08195	-4.62498
N	-3.87201	-0.55995	3.74302
O	-3.29601	0.07805	4.62602
O	-4.97301	-1.09095	3.84802
N	4.95399	2.05205	-1.28598
O	5.02999	2.57505	-0.02598
N	3.82399	2.24605	0.72602
N	-3.82501	-2.24595	-0.72598
O	-5.03101	-2.57395	0.02602
O	3.70399	2.62605	1.87302
O	-3.70501	-2.62495	-1.87298

2 (ZPE=465.34 kj/mol)			
	Coordinates		
Atom	**x**	**y**	**z**
N	-1.04851	-0.92065	-0.95083
N	0.00149	-0.21965	-0.50583
N	-0.13151	0.22935	0.79017
C	-1.87551	-0.91265	0.11117
C	1.22149	0.21635	-0.94383
C	1.74349	0.92135	0.16717
N	0.91449	0.92835	1.22917
C	-1.35451	-0.20765	1.22917
C	-3.16451	-1.48065	0.30117
C	-3.87451	-1.34365	1.53917
C	-3.25751	-0.60565	2.62317
C	-2.01551	-0.04765	2.46517
H	-1.56751	0.50035	3.28517
C	1.86149	0.07035	-2.19783
H	1.39449	-0.45465	-3.02183
C	3.09149	0.65235	-2.35883
C	3.70849	1.34435	-1.25983
C	3.05149	1.49435	0.00917
N	3.67849	0.63635	-3.70083
O	4.38849	1.59235	-3.99983
O	3.38249	-0.30565	-4.43383
N	-3.93451	-0.43565	3.90617
O	-3.34751	0.20935	4.77617
O	-5.04351	-0.94965	4.02317
N	-3.92651	-2.19265	-0.53583
O	-5.13451	-2.49165	0.22417
N	-5.04651	-1.95165	1.47617
O	-3.81551	-2.59065	-1.67683
N	3.79449	2.12135	0.89217
O	4.96349	2.40335	0.26817
N	4.93849	1.87535	-1.11483
O	5.94149	1.98935	-1.77783

3 (ZPE=465.28 kj/mol)			
	Coordinates		
Atom	**x**	**y**	**z**
N	-0.94253	-0.85090	-1.26109
N	0.12447	-0.19990	-0.79809
N	0.02747	0.15410	0.52991
C	-1.74653	-0.90990	-0.18209
C	1.34247	0.25210	-1.23309
C	1.89847	0.86810	-0.08109
N	1.09747	0.81010	0.99891
C	-1.18653	-0.29790	0.96591
C	-3.04553	-1.50490	-0.02609
C	-3.68953	-1.40090	1.25391
C	-3.07453	-0.71990	2.36091
C	-1.81953	-0.18890	2.22691
H	-1.35153	0.32110	3.05991
C	1.97047	0.17410	-2.49309
H	1.49547	-0.30790	-3.34009
C	3.21647	0.72710	-2.64209
C	3.86947	1.37610	-1.52309
C	3.19047	1.43310	-0.26209
N	3.85647	0.64710	-3.95209
O	4.96247	1.16710	-4.06509
O	3.24247	0.06610	-4.84909
N	-3.79053	-0.46590	3.61391
O	-5.01153	-0.37590	3.53891
O	-3.11253	-0.32290	4.62991
N	5.05247	1.96210	-1.44609
O	5.17747	2.40910	-0.16109
N	3.98247	2.07310	0.60491
N	-3.74853	-2.19690	-0.89209
O	-4.86953	-2.58890	-0.23909
O	3.90547	2.39010	1.77391
N	-4.82953	-2.11290	1.16191
O	-5.73253	-2.44490	1.89291

4
(ZPE=465.22 kj/mol)

	Coordinates		
Atom	**x**	**y**	**z**
N	-0.97436	-0.86930	-1.13642
N	0.07864	-0.20730	-0.65142
N	-0.05236	0.15670	0.67158
C	-1.80236	-0.92530	-0.07542
C	1.30264	0.24870	-1.06142
C	1.82664	0.87870	0.09358
N	0.99964	0.82170	1.15458
C	-1.27436	-0.30230	1.08158
C	-3.10036	-1.52730	0.05358
C	-3.77536	-1.42230	1.31658
C	-3.19136	-0.73230	2.43458
C	-1.93636	-0.19130	2.32558
H	-1.49336	0.32370	3.16858
C	1.94164	0.18070	-2.32042
H	1.47464	-0.28830	-3.17742
C	3.17564	0.76370	-2.44542
C	3.79564	1.38270	-1.30442
C	3.13764	1.45470	-0.02942
N	3.75964	0.82970	-3.78642
O	4.49064	1.78770	-4.02042
O	3.44164	-0.05130	-4.58342
N	-3.93336	-0.47930	3.67158
O	-5.15436	-0.40230	3.57258
O	-3.27736	-0.32330	4.70058
N	-3.77936	-2.22730	-0.82642
O	-4.91336	-2.62330	-0.19842
N	-4.90936	-2.14130	1.20058
O	-5.82736	-2.47730	1.91258
N	5.02664	1.90170	-1.12442
N	3.88064	2.02470	0.89158
O	5.05064	2.34270	0.28658
O	6.03264	2.05270	-1.77742

APPENDIX E

THE CARTESIAN COORDINATES OF THE STRUCTURES CONSIDERED IN CHAPTER-6

TACOT (1) (ZPE=242.63kj/mol)			
	Coordinates		
Atom	**x**	**y**	**z**
C	1.37603	0.00000	0.00000
C	-0.05097	0.00000	0.00000
N	-0.80197	1.21600	-0.10300
O	-0.23297	2.28900	0.21900
O	-1.94597	1.18500	-0.53600
N	-0.80197	-1.21600	0.10300
O	-1.94597	-1.18500	0.53600
O	-0.23297	-2.28900	-0.21900
N	2.07203	1.13500	0.18300
H	3.04503	1.16700	-0.07600
H	1.52103	1.98400	0.29100
N	2.07203	-1.13500	-0.18300
H	1.52103	-1.98400	-0.29100
H	3.04503	-1.16700	0.07600

2 (ZPE=248.49kj/mol)			
	Coordinates		
Atom	**x**	**y**	**z**
C	0.00000	0.00000	0.00000
C	1.55302	0.00000	0.00000
O	2.09447	1.10303	0.00000
N	2.05527	-1.03788	1.19630
O	3.00544	-0.65412	1.84022
O	1.46840	-2.11893	1.34820
N	1.96885	-0.97969	-1.35125
O	2.89511	-0.53951	-1.99823
O	1.32624	-2.00162	-1.58392
N	-0.46642	1.21448	-0.21398
H	-1.44454	1.45499	-0.25699
H	0.27450	1.91780	-0.27607
N	-0.73517	-1.07339	0.17505
H	-0.22746	-1.93654	0.36259
H	-1.74579	-1.05973	0.15251

3
(ZPE=248.42kj/mol)

	Coordinates		
Atom	**x**	**y**	**z**
C	0.00000	0.00000	0.00000
C	1.38239	0.00000	0.00000
N	-0.66959	1.21056	0.00000
H	-0.07386	2.03414	-0.17457
N	-0.76246	-1.14231	0.10594
H	-1.76115	-1.00157	0.26103
N	-2.03492	1.43631	-0.22148
O	-2.82293	0.50146	-0.08077
O	-2.30730	2.58814	-0.49510
N	-0.57200	-2.29448	-0.73102
O	-1.47633	-3.09981	-0.63623
O	0.42692	-2.33830	-1.41877
N	2.18539	1.19291	-0.08989
O	3.37438	1.11085	0.16770
O	1.61784	2.26754	-0.39519
N	2.15081	-1.23667	0.22380
O	3.08751	-1.45394	-0.52474
O	1.76949	-1.94965	1.14926

4
(ZPE=254.30kj/mol)

	Coordinates		
Atom	**x**	**y**	**z**
O	0.00000	0.00000	0.00000
C	1.23116	0.00000	0.00000
C	1.91073	1.39471	0.00000
N	0.94986	2.32125	0.17164
H	-0.00612	1.93379	0.20713
N	3.18308	1.62196	-0.11659
H	3.54561	2.56968	-0.08123
H	3.76417	0.79806	-0.28071
N	1.10800	3.71616	0.23114
O	2.25524	4.14653	0.15343
O	0.07717	4.34082	0.35510
N	1.93326	-0.77689	1.37295
O	1.12184	-1.35944	2.05700
O	3.14294	-0.68458	1.56338
N	1.95031	-0.90350	-1.17230
O	3.16863	-0.78881	-1.35418
O	1.20522	-1.64655	-1.76937

5 **(ZPE=252.44kj/mol)**			
	Coordinates		
Atom	**x**	**y**	**z**
C	0.00000	0.00000	0.00000
C	1.38239	0.00000	0.00000
N	-0.66959	1.21056	0.00000
H	-0.07386	2.03414	-0.17457
N	-0.76246	-1.14231	0.10594
H	-1.76115	-1.00157	0.26103
N	-2.03492	1.43631	-0.22148
O	-2.82293	0.50146	-0.08077
O	-2.30730	2.58814	-0.49510
N	-0.57200	-2.29448	-0.73102
O	-1.47633	-3.09981	-0.63623
O	0.42692	-2.33830	-1.41877
N	2.18539	1.19291	-0.08989
O	3.37438	1.11085	0.16770
O	1.61784	2.26754	-0.39519
N	2.15081	-1.23667	0.22380
O	3.08751	-1.45394	-0.52474
O	1.76949	-1.94965	1.14926

6 **(ZPE=263.53kj/mol)**			
	Coordinates		
Atom	**x**	**y**	**z**
C	0.00000	0.00000	0.00000
C	1.47455	0.00000	0.00000
O	0.83583	1.20630	0.00000
N	-0.70647	-0.32131	-1.17864
H	-0.17869	-0.64560	-1.98620
N	-0.66792	-0.17613	1.24526
H	-1.49159	0.40993	1.36908
N	-1.78033	0.51462	-1.53675
O	-2.23275	1.23301	-0.65080
O	-2.16601	0.40372	-2.68373
N	-0.98005	-1.52184	1.56984
O	-1.91647	-1.66725	2.33202
O	-0.24379	-2.37251	1.09188
N	2.33479	-0.29342	-1.21699
O	3.46637	0.14464	-1.15535
O	1.81610	-0.88704	-2.15809
N	2.25872	-0.39801	1.24302
O	2.81566	-1.48038	1.15815
O	2.23214	0.37966	2.17549

APPENDIX F

THE CARTESIAN COORDINATES OF THE STRUCTURES CONSIDERED IN CHAPTER-7

Parabanic Acid (ZPE=162.80 kj/mol)			
	Coordinates		
Atom	x	y	z
C	0.00000	0.00000	0.00000
N	1.39980	0.00000	0.00000
C	1.94855	1.27471	0.00000
C	0.71038	2.21765	0.00013
N	-0.37257	1.35041	-0.00032
O	-0.73036	-0.95956	0.00019
O	3.11102	1.58778	0.00055
O	0.70411	3.42172	0.00071
H	-1.34235	1.63578	-0.00126
H	1.93404	-0.85907	0.00011

1 (ZPE=165.48 kj/mol)			
	Coordinates		
Atom	x	y	z
C	0.00000	0.00000	0.00000
N	1.39640	0.00000	0.00000
N	-0.35465	1.38533	0.00000
C	1.97008	1.26145	0.01926
C	0.76923	2.24613	0.00572
O	3.13747	1.55211	0.03815
O	0.80488	3.44051	-0.02916
O	-0.72877	-0.95051	0.03133
N	-1.73203	1.84099	-0.06270
O	-2.49033	1.12932	-0.68157
O	-1.94166	2.89061	0.50553
H	1.91745	-0.86633	0.03772

2 (ZPE=167.38 kj/mol)			
	Coordinates		
Atom	**x**	**y**	**z**
C	0.00000	0.00000	0.00000
N	1.42370	0.00000	0.00000
N	-0.33287	1.38380	0.00000
C	2.00205	1.28637	0.04135
C	0.78199	2.24662	0.04297
O	3.15553	1.59715	0.03517
O	0.81451	3.44149	0.03854
O	-0.73676	-0.93533	0.05567
N	-1.72844	1.84255	0.00004
O	-2.49156	1.16016	-0.64127
O	-1.91919	2.85549	0.63200
N	2.19739	-1.24910	-0.00590
O	1.70976	-2.15073	-0.64502
O	3.22860	-1.19821	0.62176

3 (ZPE=200.39 kj/mol)			
	Coordinates		
Atom	**x**	**y**	**z**
C	0.00000	0.00000	0.00000
N	1.44202	0.00000	0.00000
N	-0.31950	1.38124	0.00000
C	2.00217	1.30831	0.03339
C	0.77399	2.24631	0.00343
O	3.14783	1.64513	0.04975
O	0.79473	3.44399	-0.04255
N	-1.70190	1.86312	-0.15623
O	-2.35384	1.31090	-1.00916
O	-1.98695	2.77647	0.58138
N	2.21808	-1.20375	0.10104
O	1.59951	-2.24816	-0.03892
O	3.39861	-1.05514	0.30650
H	-0.43791	-1.83630	0.04331
N	-0.85862	-0.91013	0.04451

4 **(ZPE=204.31 kj/mol)**			
	Coordinates		
Atom	**x**	**y**	**z**
C	0.00000	0.00000	0.00000
N	1.40814	0.00000	0.00000
N	-0.37508	1.35621	0.00000
C	1.94818	1.31315	-0.06453
C	0.72027	2.23993	0.06748
O	3.08853	1.63376	-0.21249
O	0.71619	3.42697	0.20838
N	-1.74000	1.81399	0.39932
O	-2.27265	1.17336	1.26965
O	-2.10223	2.79250	-0.20193
N	2.21768	-1.12271	-0.55698
O	1.68991	-1.73252	-1.45896
O	3.30173	-1.23105	-0.05502
N	-0.88454	-0.91655	0.00141
N	-0.44127	-2.27681	0.13413
O	-1.01524	-3.06200	-0.58579
O	0.38996	-2.51478	1.00262

5 **(ZPE=237.42kj/mol)**			
	Coordinates		
Atom	**x**	**y**	**z**
C	0.00000	0.00000	0.00000
N	1.40122	0.00000	0.00000
N	-0.37674	1.35859	0.00000
C	1.92609	1.31621	-0.08423
C	0.72192	2.23354	0.02327
O	0.73270	3.42982	0.11820
N	-1.73849	1.82364	0.36936
O	-2.29293	1.18702	1.22932
O	-2.08603	2.80542	-0.23810
N	2.18781	-1.11600	-0.59647
O	1.64224	-1.69444	-1.51001
O	3.27247	-1.26560	-0.10604
N	-0.89095	-0.91355	-0.00199
N	-0.45764	-2.27272	0.12796
O	-1.05981	-3.05988	-0.56875
O	0.39755	-2.51808	0.97207
H	3.22386	2.64316	-0.27502
N	3.13645	1.62353	-0.23783

6
(ZPE=240.87 kj/mol)

	Coordinates		
Atom	**x**	**y**	**z**
C	0.00000	0.00000	0.00000
N	1.40125	0.00000	0.00000
N	-0.36939	1.36129	0.00000
C	1.93515	1.30629	-0.18060
C	0.71385	2.21632	-0.11689
O	3.07673	1.60698	-0.35847
N	-1.82255	1.75480	-0.12885
O	-2.54819	1.28359	0.69782
O	-2.03084	2.48709	-1.06417
N	2.22424	-1.15674	-0.48090
O	1.72213	-1.79713	-1.37471
O	3.28697	-1.25108	0.06514
N	-0.89369	-0.90700	0.02430
N	-0.46541	-2.26868	0.18386
O	-1.05068	-3.06469	-0.51388
O	0.36895	-2.49269	1.05352
N	0.88271	3.47911	-0.13019
N	-0.28565	4.31371	0.04177
O	-0.95191	4.11068	1.04894
O	-0.41677	5.18055	-0.78942

7
(ZPE=273.93 kj/mol)

	Coordinates		
Atom	**x**	**y**	**z**
C	0.00000	0.00000	0.00000
N	1.39381	0.00000	0.00000
N	-0.37294	1.36374	0.00000
C	1.91331	1.30682	-0.20551
C	0.70844	2.20917	-0.14620
N	-1.82319	1.75236	-0.14608
O	-2.54912	1.31304	0.69743
O	-2.03267	2.44855	-1.10993
N	2.18746	-1.15451	-0.53403
O	1.67162	-1.73748	-1.46002
O	3.24123	-1.31382	0.01305
N	-0.90285	-0.90140	0.01976
N	-0.48469	-2.26432	0.16790
O	-1.10770	-3.05621	-0.50291
O	0.38223	-2.50208	1.00210
N	0.88091	3.47467	-0.20239
N	-0.26740	4.32688	-0.02889
O	-0.97412	4.10517	0.94722
O	-0.35300	5.23152	-0.82750
H	3.24236	2.58597	-0.54152
N	3.12441	1.57903	-0.40603

8 (ZPE=277.21 kj/mol)			
	Coordinates		
Atom	**x**	**y**	**z**
C	0.00000	0.00000	0.00000
N	1.39842	0.00000	0.00000
N	-0.36886	1.35903	0.00000
C	1.91199	1.29782	-0.19181
C	0.71672	2.20939	-0.13320
N	-1.81931	1.75722	-0.17953
O	-2.56911	1.29278	0.62833
O	-1.99527	2.48093	-1.12774
N	2.20090	-1.16748	-0.55134
O	1.68282	-1.72758	-1.48509
O	3.24511	-1.33566	0.00633
N	-0.89529	-0.90924	0.02068
N	-0.46430	-2.27061	0.16315
O	-1.08926	-3.06549	-0.49991
O	0.41651	-2.49964	0.98515
N	0.87616	3.47574	-0.15279
N	3.14827	1.51216	-0.37394
N	-0.28749	4.31127	0.03660
O	-0.96911	4.07334	1.02448
O	-0.40177	5.20856	-0.76334
N	3.55335	2.89483	-0.59945
O	3.55544	3.24373	-1.75954
O	3.94837	3.47299	0.38757

CURRICULUM VITAE

Serhat VARIŞ
serhat.varis@tubitak.gov.tr

EDUCATION

Ph.D.: Middle East Technical University, Faculty of Arts and Sciences,
Department of Chemistry 2007 – 2013.
Thesis: Molecular Modelling of Some Explosives and Propellants
Supervisor: Prof. Dr. Lemi TÜRKER

M.Sc.: Middle East Technical University, Faculty of Arts and Sciences,
Department of Chemistry, 2005 – 2007.
Thesis: Synthesis and Electrochromic Properties of Conducting Polymers of 1-(4-nitrophenyl)-2,5-di(2-thienyl)-1H-pyrrole and Their Use in Electrochromic Devices
Supervisor: Prof. Dr. Levent TOPPARE

B.Sc.: Middle East Technical University, Faculty of Arts and Sciences,
Department of Chemistry, 2000 – 2005.

WORK EXPERIENCE

February 2007- Present,	*Researcher,*	TÜBİTAK-SAGE
September 2006- February 2007,	*Research Assistant,*	Department of Chemistry, METU

PUBLICATIONS

1. S. Varis, M. Ak, I.M. Akhmedov, C. Tanyeli, L. Toppare, A novel multielectrochromic copolymer based on 1-(4-nitrophenyl)-2, 5-di (2-thienyl)-1H-pyrrole and EDOT, *Journal of Electroanalytical Chemistry*, 2007, 603 (1), 8-14.

2. L. Türker, S. Variş, A review of polycyclic aromatic energetic materials, *Polycyclic Aromatic Compounds*, 2009, 29(4), 228-266.

3. L. Türker, S. Variş, Prediction of Explosive Performance Properties of z-DBBD and Its Isomers by Quantum Chemical Computations, *Journal of Energetic Materials*, 2012, 31 (3), 203-216.

4. L. Türker, S. Variş, Ç. Çelik Bayar, A theoretical study of JP-10 hydroperoxidation, *Fuel*, 2013, 104, 128-132.

5. L. Türker, S. Variş, Desensitization of TNAZ via Molecular Structure Modification and Explosive Properties-A DFT Study, *Acta Chimica Slovenica*, 2012, 59(4), 749-759.

6. L. Türker, S. Variş, Effects of Epoxidation and Nitration on Ballistic Properties of FOX-7 A DFT Study, *Zeitschrift Fur Anorganische und Allgemeine Chemie*, 2013, 639, 982-987.

7. L. Türker, S. Variş, Nitro Derivatives of Parabanic Acid as Potential Explosives: A Theoretical Study, *Zeitschrift Fur Anorganische und Allgemeine Chemie*, 2013, *Accepted*